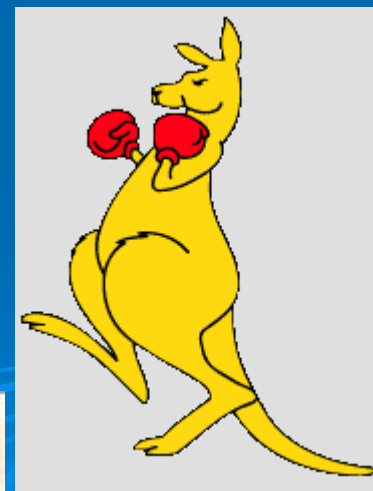


Correlation between small scale velocity and scalar fields in a turbulent channel flow

- H Abe * R A Antonia** and H Kawamura***
- * JAXA Japan
- ** University of Newcastle Australia
- *** Tokyo University of Science Japan





Ability to mix scalar contaminants is one of the major characteristics of turbulence

The large scales play a major part in transporting the scalar

...but the small scales are instrumental

for implementing the mixing at the molecular level

Why is it important to study how the small scale scalar mixing is affected by the strain and rotation imposed by the velocity field?

- In turbulent wall shear flows, the small scales are not only stretched by the mean shear, but also distorted by the organized motion (e.g. the near-wall vortical structures).
- Such scalar mixing occurs in a reactive flow with a wall, e.g. in a combustion chamber.

- For a turbulent channel flow DNS was first performed by Kim and Moin (1989) for $Re_\tau = 180$, $Pr = 0.1 ,0.71$ and 2 with uniform internal heating. The focus was mainly on large scale transport.
- Antonia and Kim (1994) examined the isotropy of the small scales for $Re_\tau =180 ,392$ and $Pr=0.71$
- However there was no attempt to investigate the spatial structures associated with these scales especially near the wall

Here we perform DNSs for $\text{Re}_\tau = 180, 395$ and 640 at $\text{Pr} = 0.71$

The main objective is to study the structure of the vorticity and scalar dissipation fields

...in particular the manner in which these fields are correlated...in the context of the flow organization...

The high correlation between u and θ in the near-wall region

(e.g. Iritani Kasagi and Hirata 1985, Antonia Krishnamoorthy Fulachier 1988, Kim and Moin 1989, Kasagi Tomita Kuroda 1992) and its association with low and high speed streaks ...

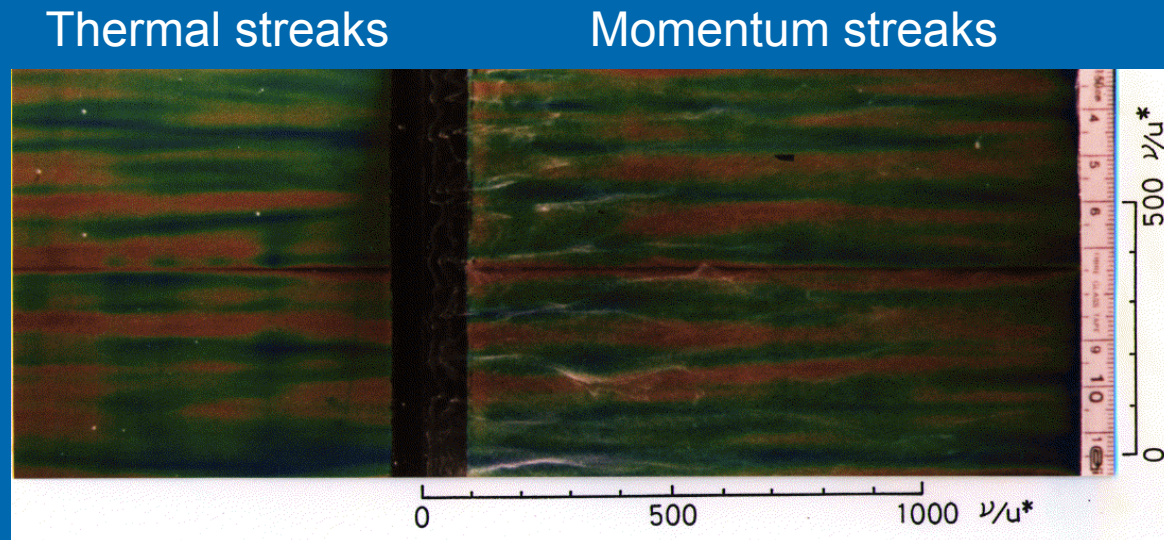
...implies a high correlation between ...

$\partial u / \partial y$ and $\partial \theta / \partial y$ (i.e. between $-\omega_3$ and $\theta_{,2}$)

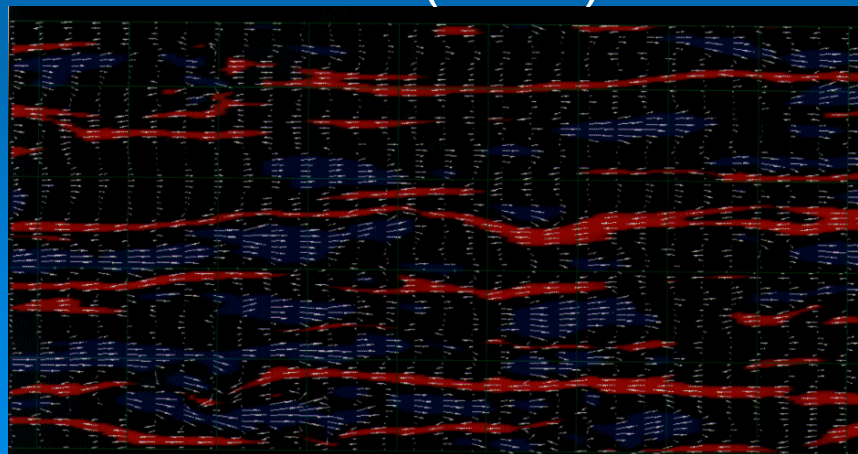
...as well as between $\partial u / \partial z$ and $\partial \theta / \partial z$
(i.e. between ω_2 and $\theta_{,3}$)

Visualization of momentum and thermal streaks

1. Experiment in a turbulent boundary layer by Iritani, Kasagi and Hirata (1992)



2. DNS in a turbulent channel flow for $Re_\tau=150$ at $Pr=0.71$ by Kasagi and Ohtsubo (1993)



Thermal streaks (blue, $T'^+ < -1.0$; red, $T'^+ > 1.0$)
and velocity vectors in
the x-z plane
(1600*600 wall units).

Approach

The focus is on the relationship between the three components of the fluctuating vorticity vector ω_i ($i=1,2,3$ represent the streamwise, wall-normal and spanwise directions, respectively) and those of the fluctuating scalar derivative vector $\theta_{,i} (\equiv \partial \theta / \partial x_i)$

In particular, we compare mean-square values, correlation coefficients and instantaneous fields associated with those two vector fields.

Enstrophy

$$\omega_i \omega_i$$

Scalar enstrophy

$$\theta_{,i} \theta_{,i}$$

The summation rule is applied to the suffix i.

Outline

1. Numerical methodology
2. Validation checks for small scales
3. Statistics of vorticity and scalar dissipation fields
 - a) Mean-square values
 - b) Anisotropy invariant maps (AIMs)
 - c) Budgets
4. Correlation coefficients between $\overline{\omega_i \omega_i}$ and $\overline{\theta_{,i} \theta_{,i}}$
 - a) Relationship to organized motions
 - e.g. streaks, quasi-streamwise vortices,
internal shear layers, backs or fronts, etc
 - b) Relationship with the strain rates
5. Near-wall similarity between velocity and scalar fields
6. Transport and destruction of momentum and scalar fluxes as a result of near-wall organizations
7. Conclusions

Numerical methodology

Time Advancement

- 1) 3rd-order Runge-Kutta
- 2) 2nd-order Crank Nicolson

Spatial discretization

- Finite Difference Method
 - 1) 4th-order central difference (x, z dir.)
 - 2) 2nd-order central difference (y dir.)

Boundary condition

- 1) Periodic (x, z dir.)
- 2) Non-slip (y dir.)

Averaging

- Spatially (x, z dir.) and temporally (t)

Energy equation

The instantaneous temperature is converted as

$$T^+(x^\#, y^\#, z^\#) = \frac{d \left\langle \bar{T}_m^+ \right\rangle}{dx^\#} x^\# - \Theta^+(x^\#, y^\#, z^\#).$$

The “*averaged*” wall heat flux is *constant* since

$$\frac{d \left\langle \bar{T}_m^+ \right\rangle}{dx^\#} x^\# = 2 / \left\langle \bar{U}_1^+ \right\rangle. \quad \left. \begin{array}{l} \left\langle \bar{T}_m^+ \right\rangle \text{ bulk mean temperature} \\ \left\langle \bar{U}_1^+ \right\rangle \text{ velocity averaged over} \\ \text{the channel section} \end{array} \right\}$$

The energy equation is expressed as

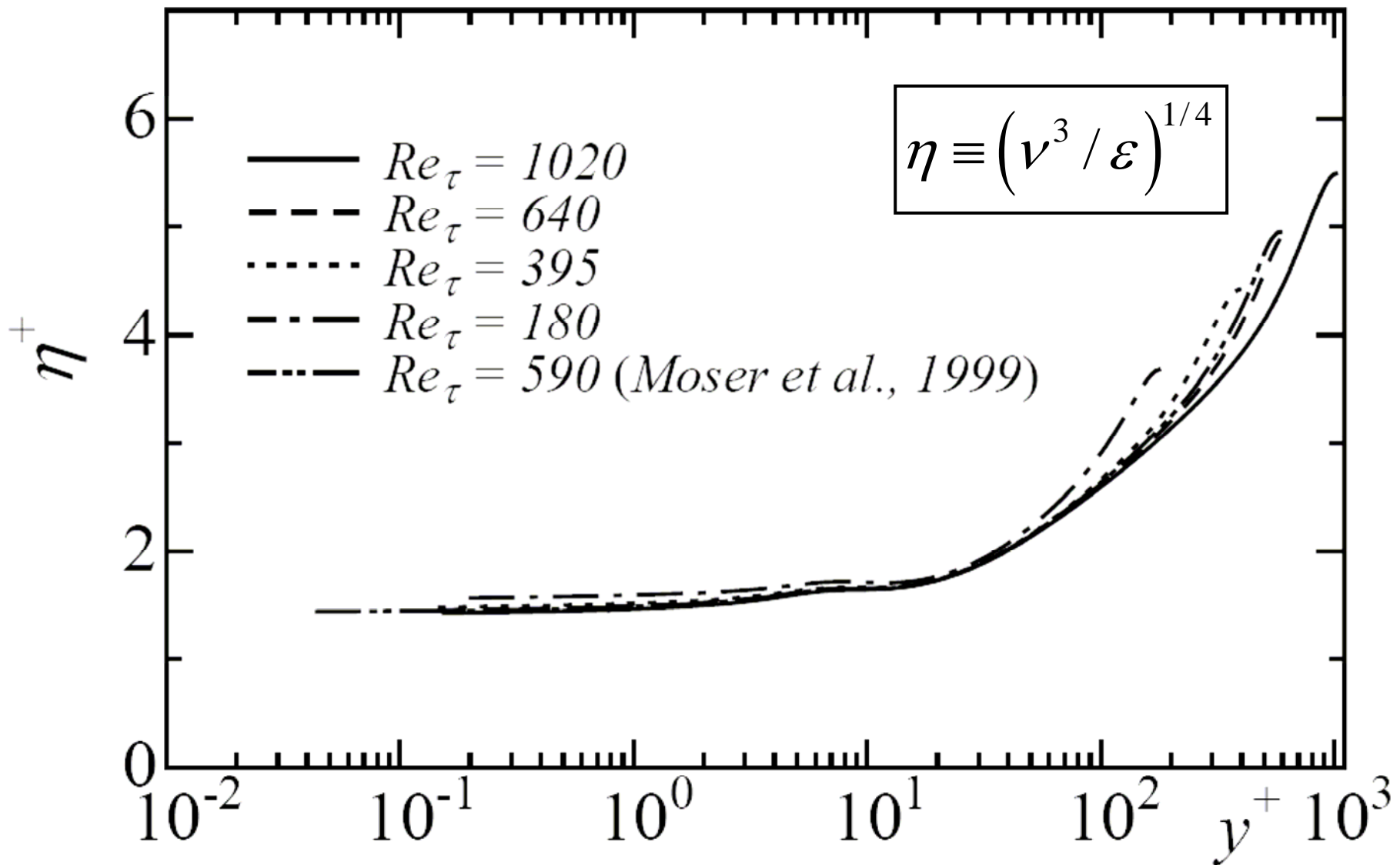
$$\frac{\partial \Theta^+}{\partial t^\#} + U_j^+ \frac{\partial \Theta^+}{\partial x_j^\#} = \frac{1}{Re_\tau \cdot \text{Pr}} \frac{\partial^2 \Theta^+}{\partial x_j^{\#2}} + \frac{2U_1^+}{\left\langle \bar{U}_1^+ \right\rangle}.$$

Superscripts + and # denote normalization by wall units and δ , respectively.

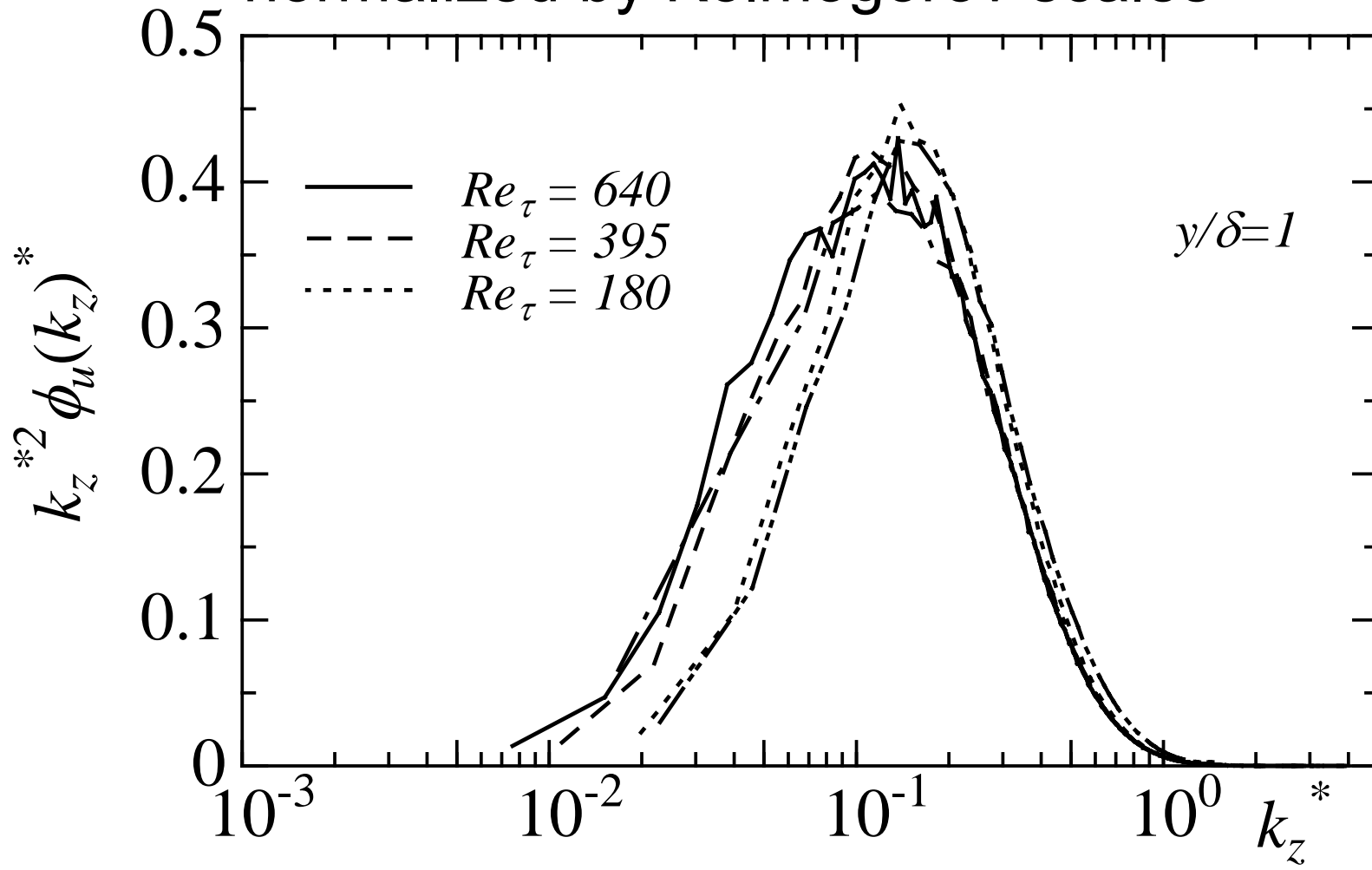
Domain size Grid points Spatial resolution Sampling time period

Re_τ	180	395	640
Pr	0.71	0.71	0.71
$L_x \times L_y \times L_z$	$12.8\delta \times 2\delta \times 6.4\delta$	$12.8\delta \times 2\delta \times 6.4\delta$	$12.8\delta \times 2\delta \times 6.4\delta$
$L_x^+ \times L_y^+ \times L_z^+$	$2304 \times 360 \times 1152$	$5056 \times 790 \times 2528$	$8192 \times 1280 \times 4096$
$N_x \times N_y \times N_z$	$768 \times 128 \times 384$	$1536 \times 192 \times 768$	$2048 \times 256 \times 1024$
$\Delta x^+, \Delta y^+, \Delta z^+$	$3.00, 0.20\text{--}5.90,$ 3.00	$3.29, 0.15\text{--}6.52,$ 3.29	$4.00, 0.15\text{--}8.02,$ 4.00
$\Delta x_c^*, \Delta y_c^*,$ Δz_c^*	$0.81, 1.61, 0.81$	$0.75, 1.48, 0.75$	$0.81, 1.62, 0.81$
t^+	3960	5008	2228

Kolmogorov microscale normalized by wall units

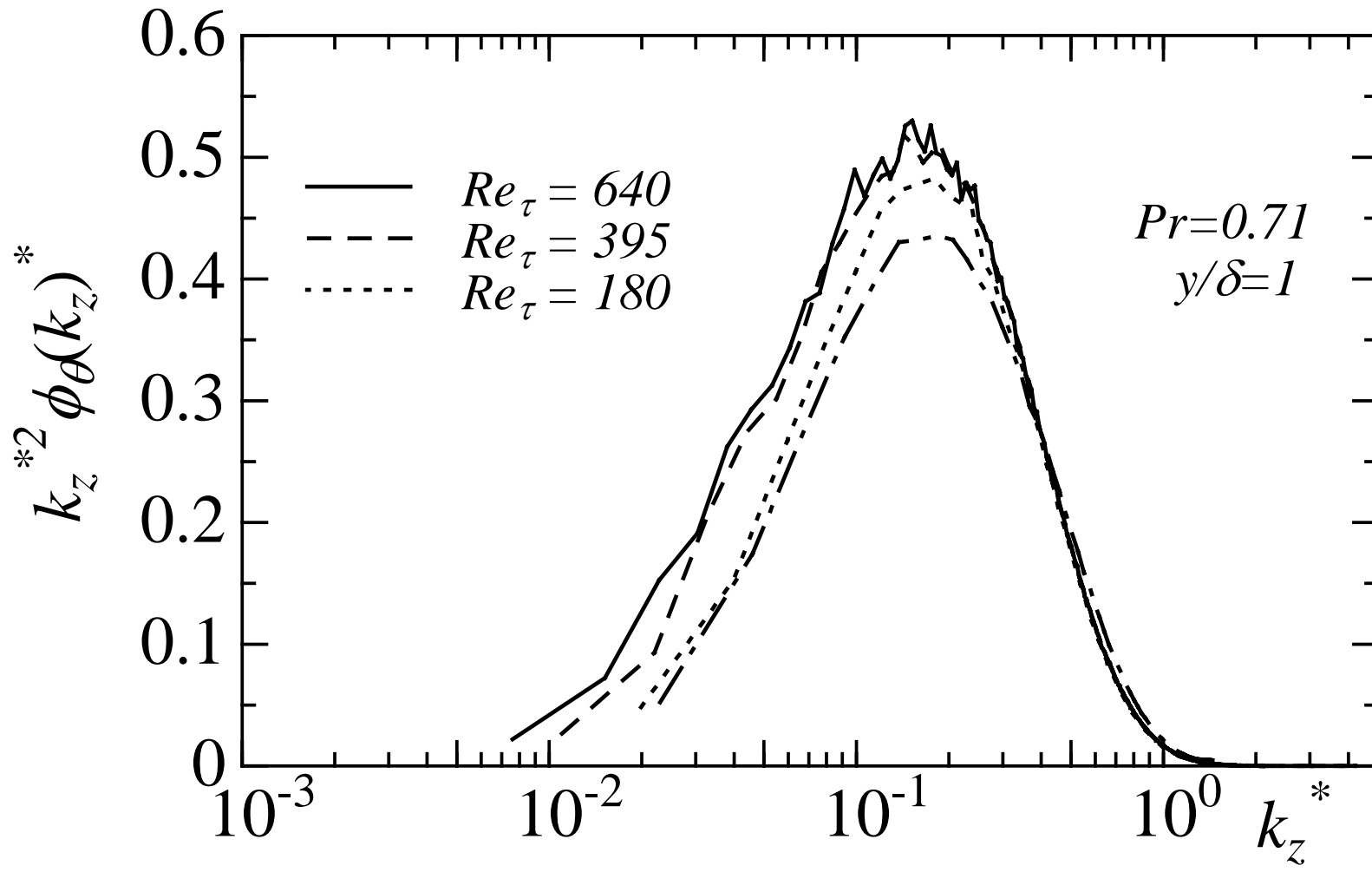


Spanwise spectra of u_1 multiplied by k_z^2
normalized by Kolmogorov scales



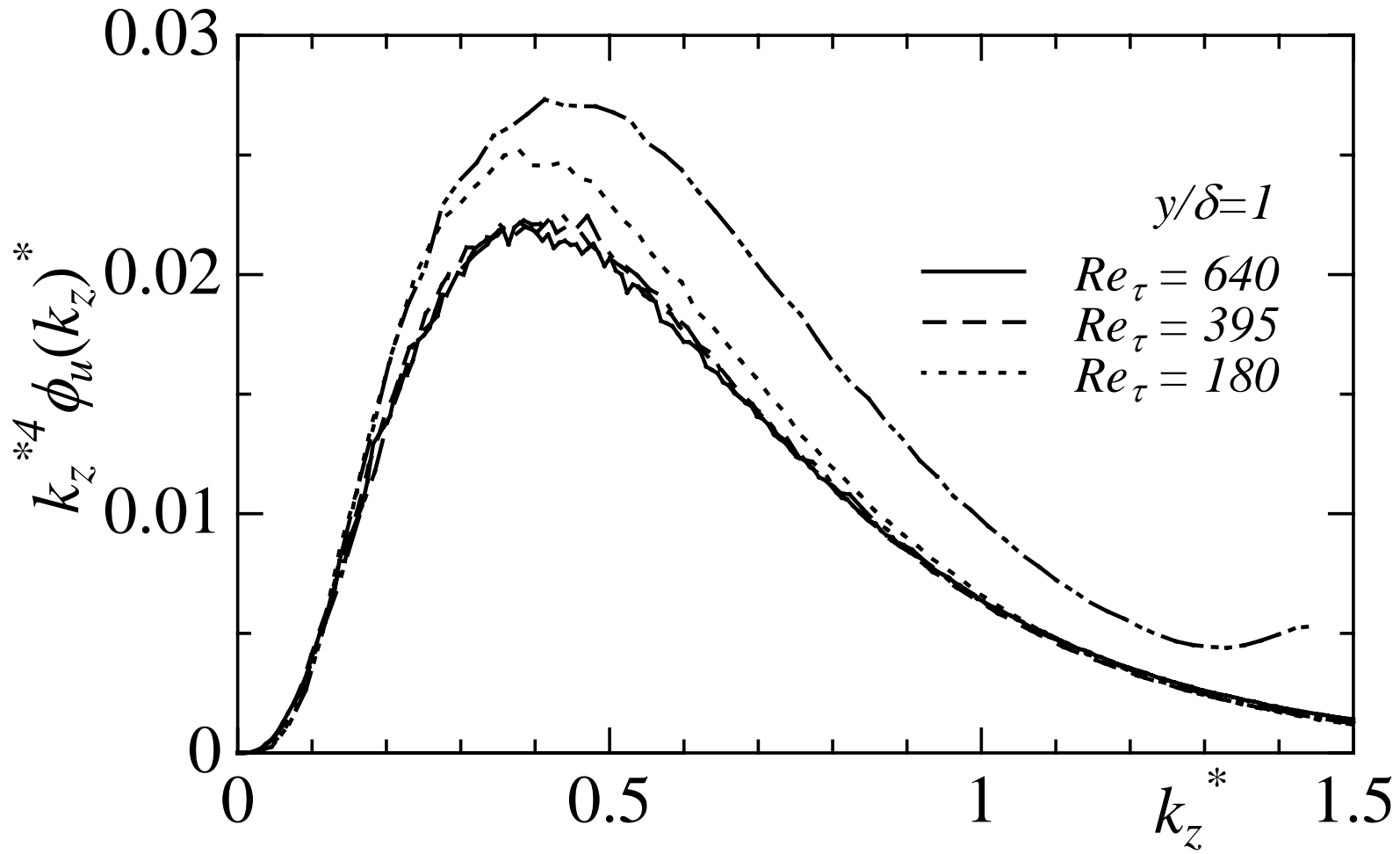
----- Moser et al. (1999) at $Re_\tau = 590$
----- Kasagi et al. (1992) at $Re_\tau = 150$

Spanwise spectra of θ multiplied by k_z^2
normalized by Kolmogorov scales



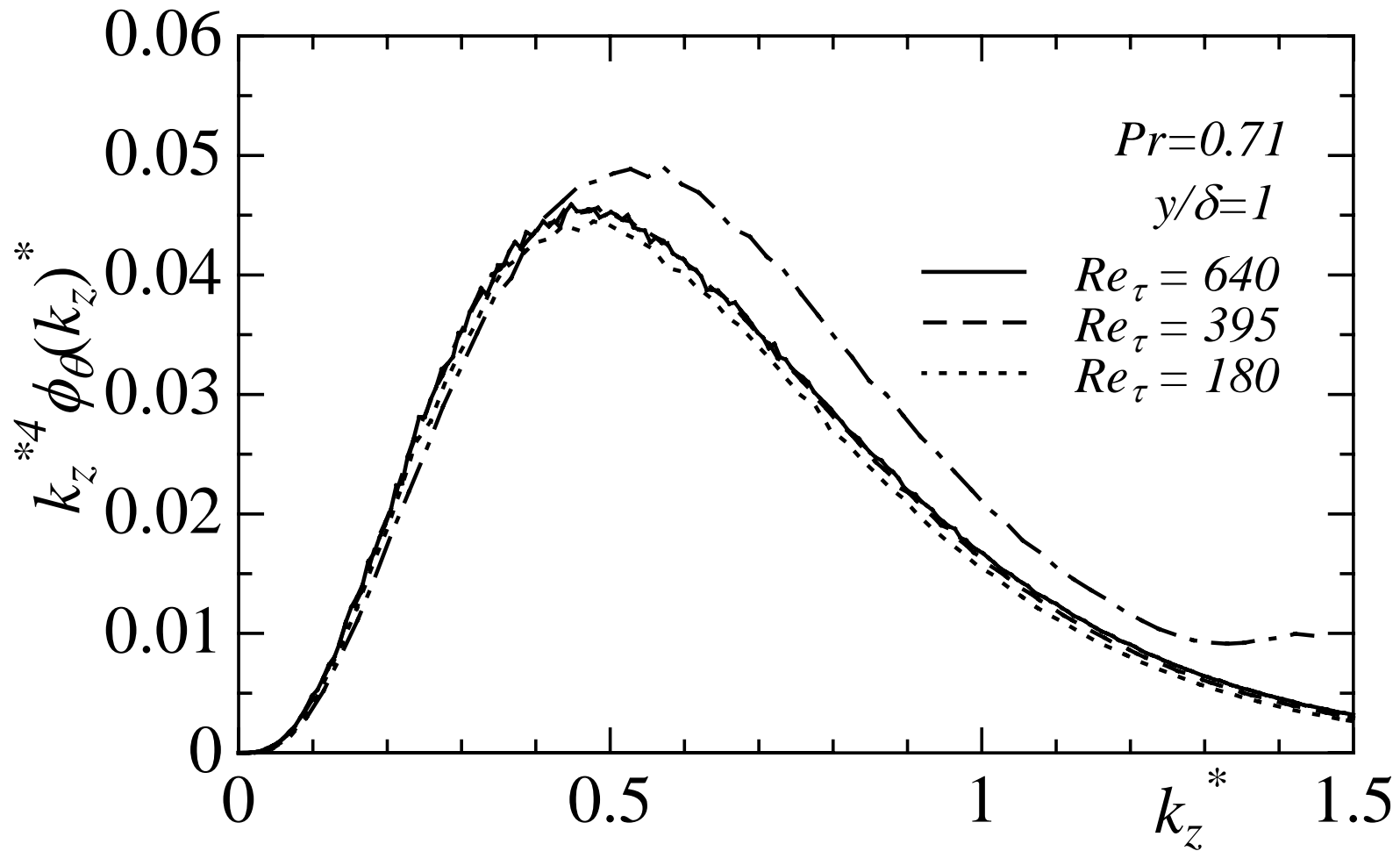
----- Kasagi et al. (1992) at $Re_\tau=150$

Spanwise spectra of u_1 multiplied by k_z^4 normalized by Kolmogorov scales

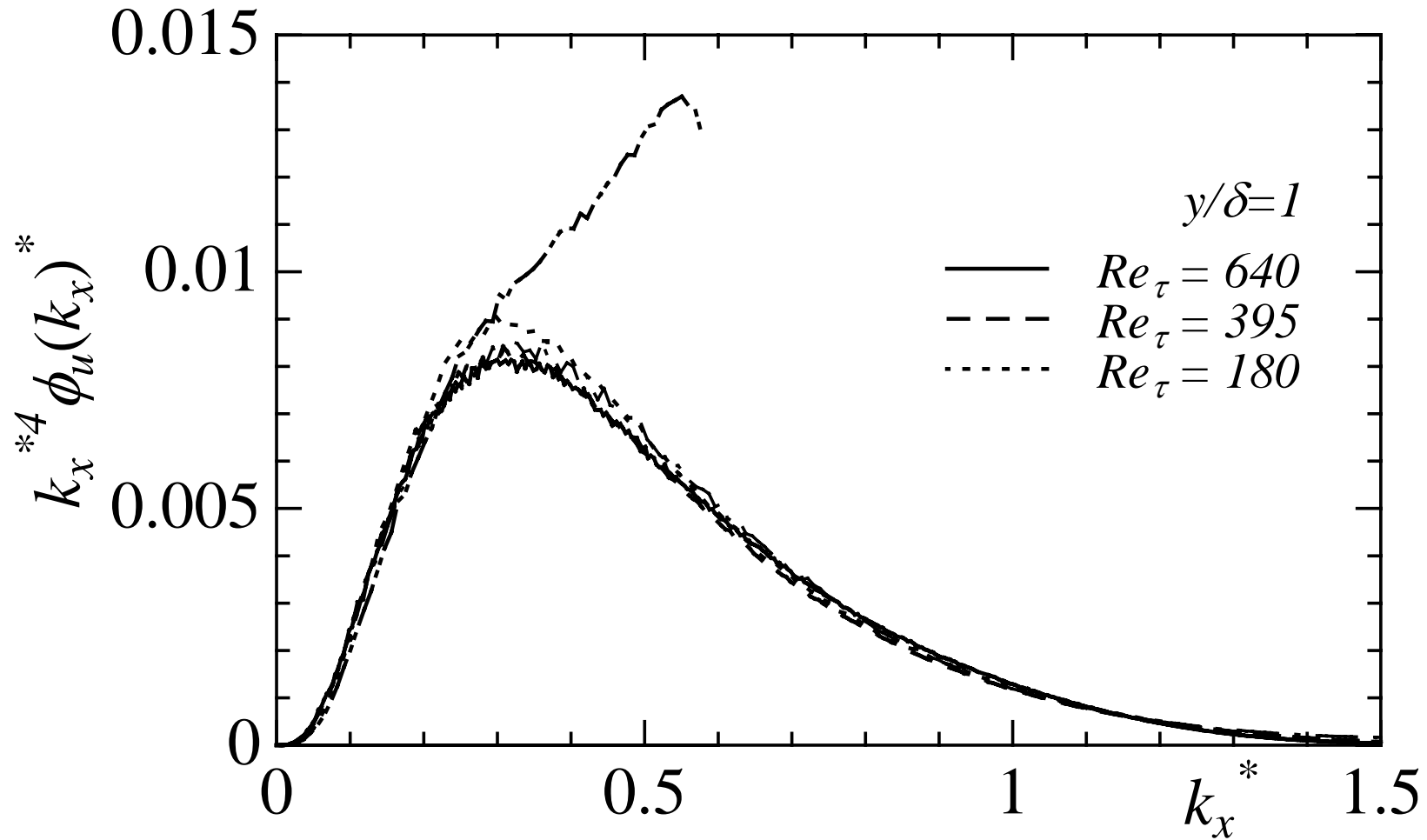


— Moser et al. (1999) at $Re_\tau = 590$
- - - Kasagi et al. (1992) at $Re_\tau = 150$

Spanwise spectra of θ multiplied by k_z^4 normalized by Kolmogorov scales

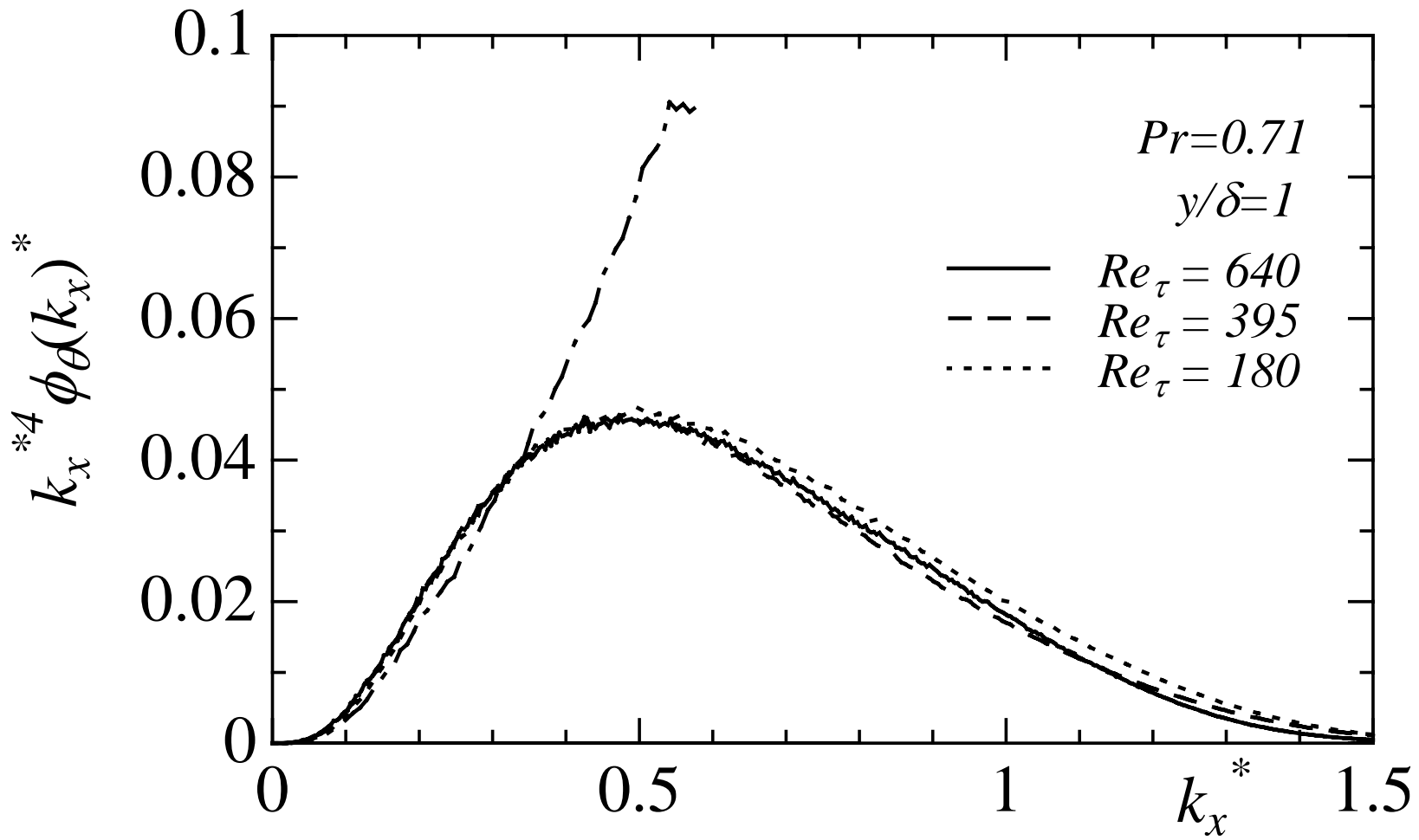


Spanwise spectra of u_1 multiplied by k_x^4 normalized by Kolmogorov scales

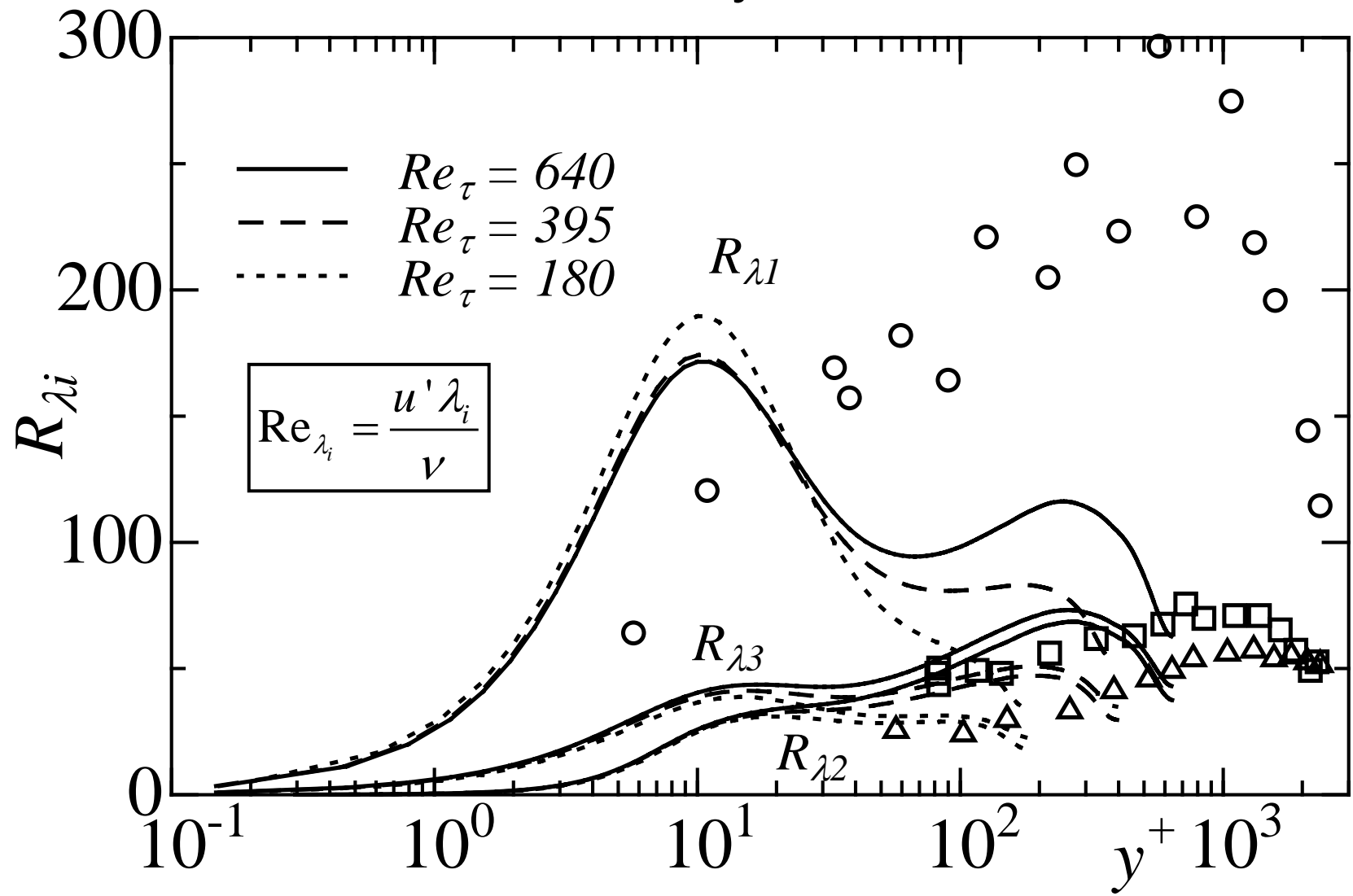


— Moser et al. (1999) at $Re_\tau=590$
- Kasagi et al. (1992) at $Re_\tau=150$

Spanwise spectra of θ multiplied by k_x^4 normalized by Kolmogorov scales

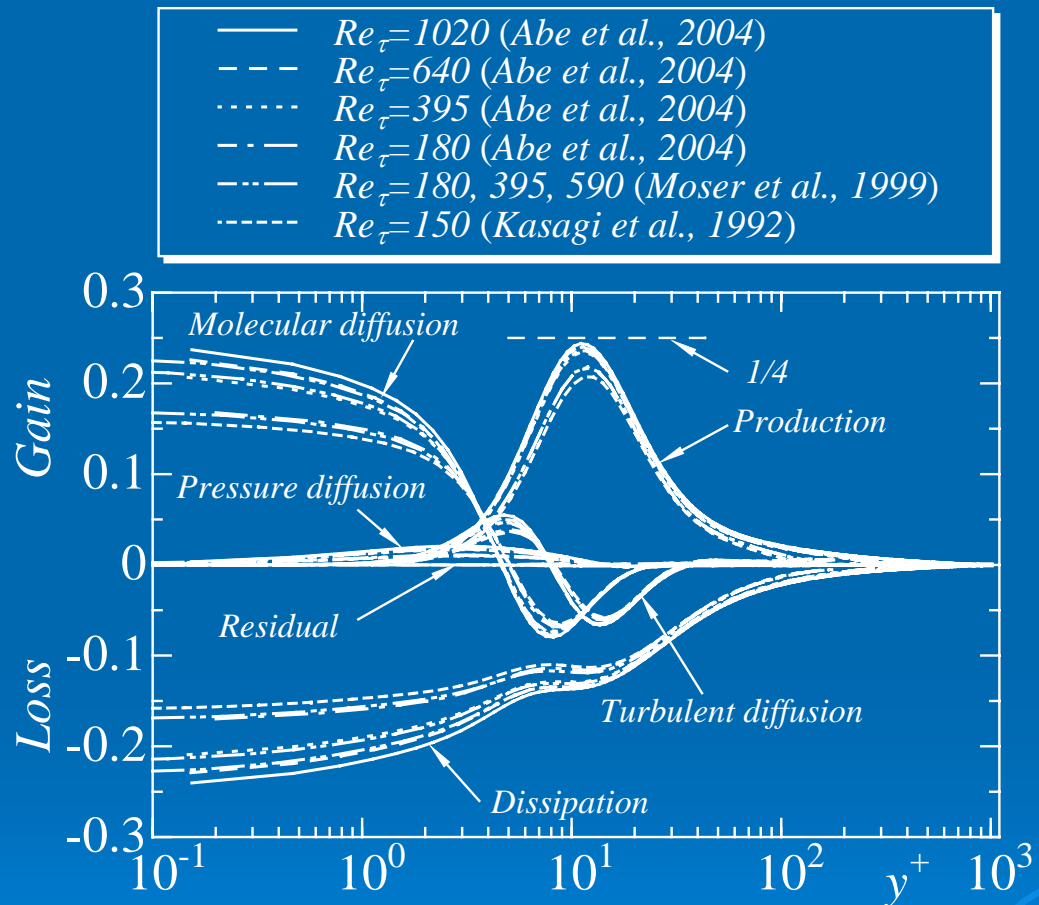


Turbulence Reynolds number



Comte-Bellot (1963) at $Re_\tau = 2340$

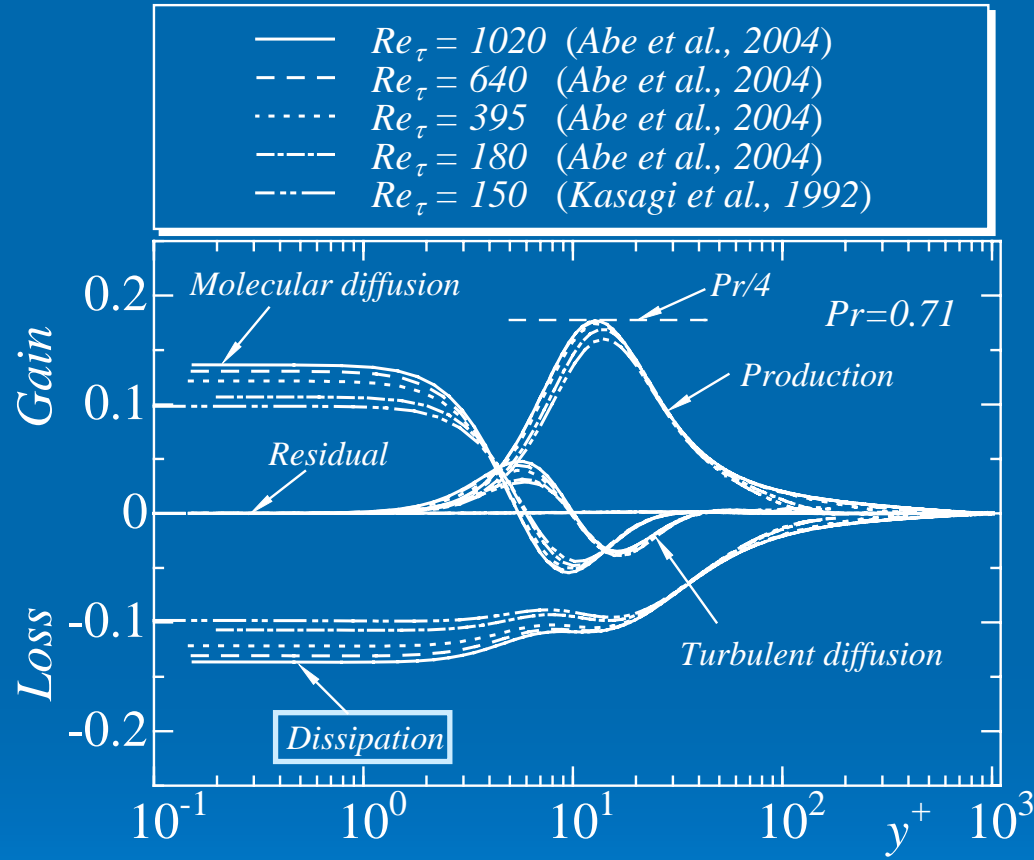
Budget of the turbulent kinetic energy k



$$k = \frac{\overline{u_i u_i}}{2}$$

$$\frac{Dk}{Dt} = \underbrace{-\overline{u_i u_j} \frac{\partial U}{\partial x_j}}_{\text{Production}} - \underbrace{\frac{1}{2} \frac{\partial}{\partial x_j} (\overline{u_i^2 u_j})}_{\text{Turbulent Diffusion}} - \underbrace{\frac{\partial}{\partial x_j} (\overline{u_j p})}_{\text{Pressure Diff.}} + v \underbrace{\frac{\partial^2 k}{\partial x_j^2}}_{\text{Molecular Diff.}} - v \underbrace{\left(\frac{\partial u_i}{\partial x_j} \right) \left(\frac{\partial u_i}{\partial x_j} \right)}_{\text{Dissipation}}$$

Budget of the temperature variance k_θ

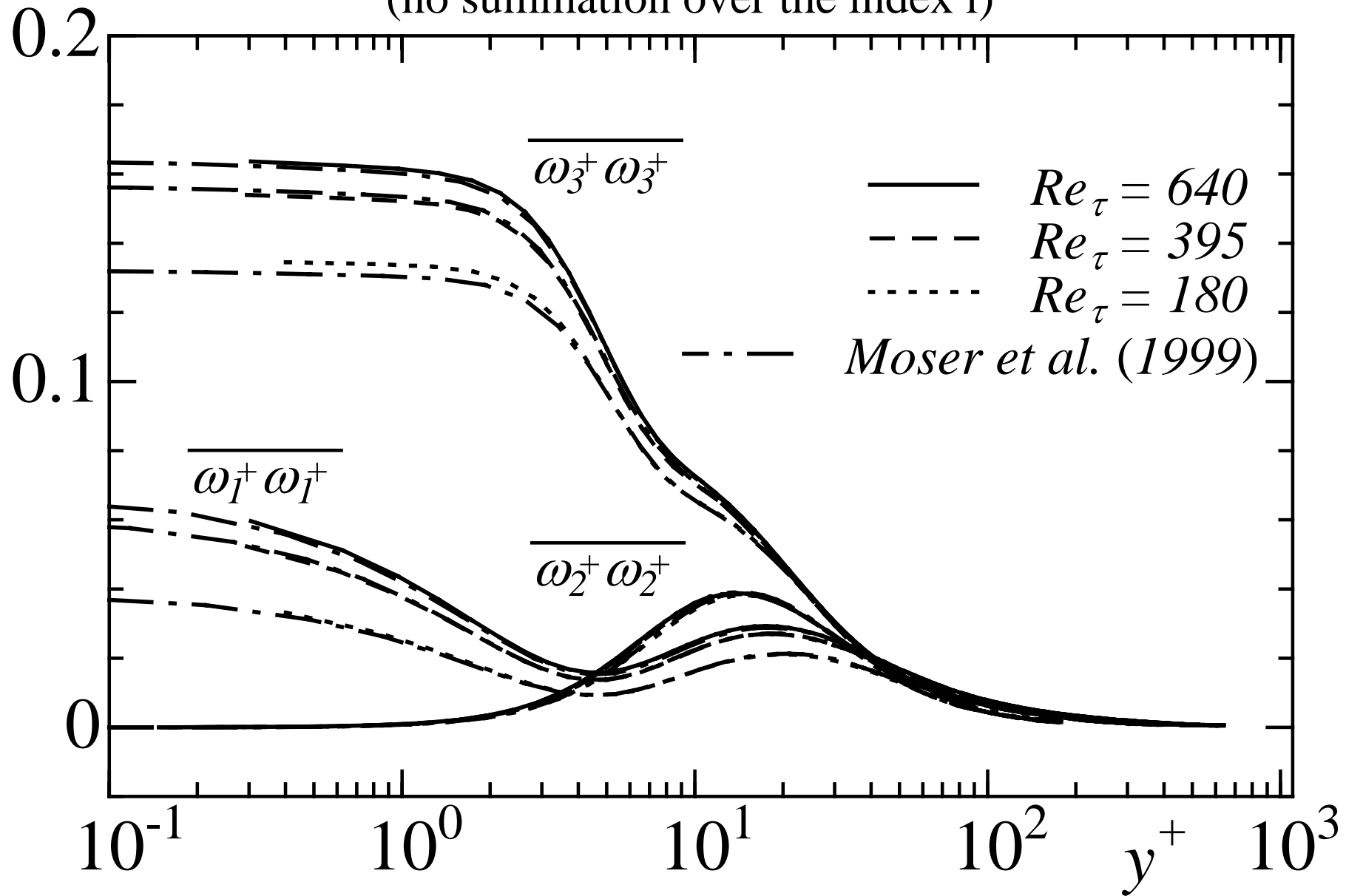


$$k_\theta = \frac{\overline{\theta\theta}}{2}$$

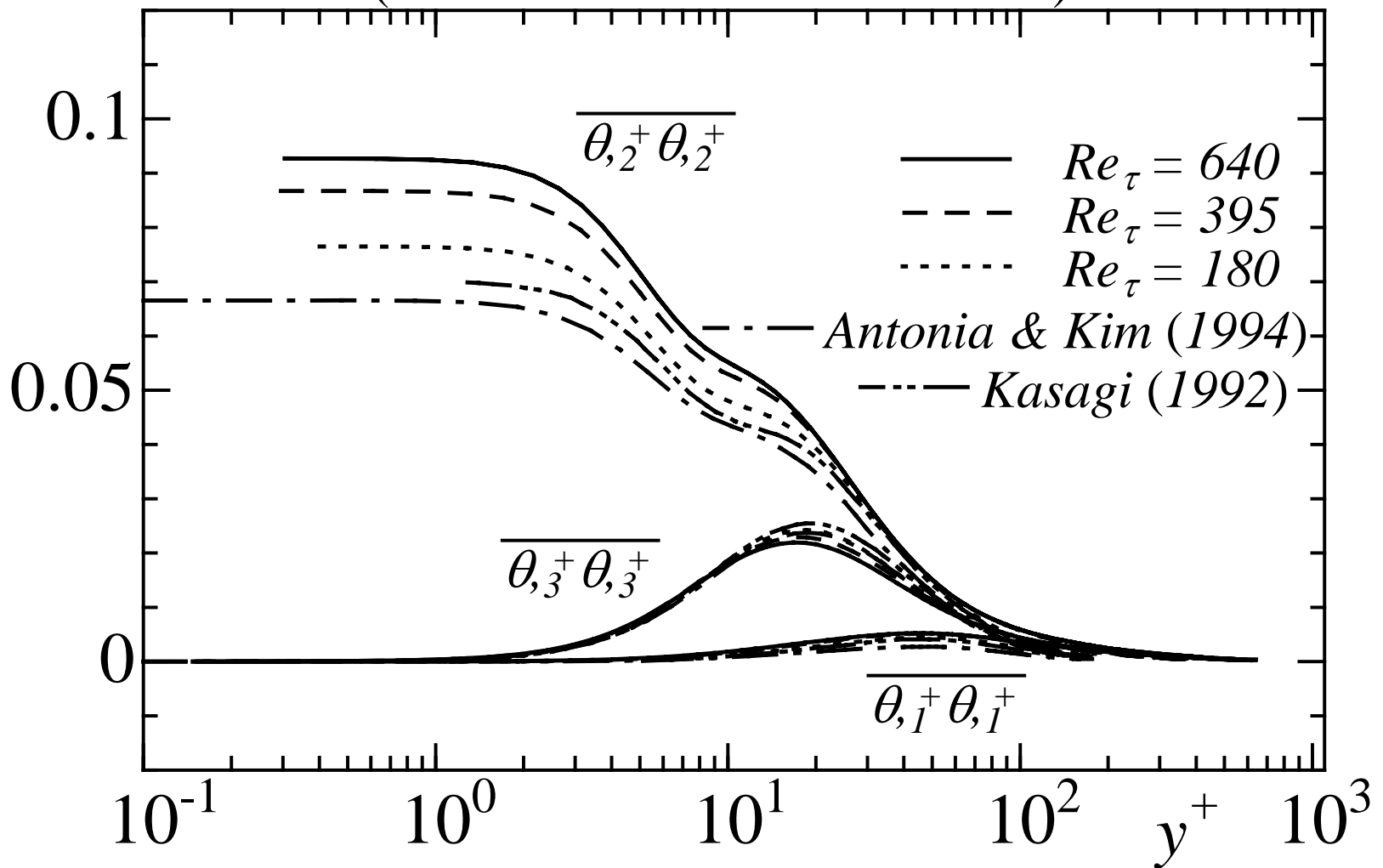
$$\frac{Dk_\theta}{Dt} = \underbrace{-\overline{u_j}\overline{\theta}\frac{\partial\Theta}{\partial x_j}}_{Production} - \underbrace{\frac{1}{2}\frac{\partial}{\partial x_j}\left(\overline{u_j\theta^2}\right)}_{Turbulent Diff.} + \underbrace{a\frac{\partial^2 k_\theta}{\partial x_j^2}}_{Molecular Diff.} - \boxed{a\left(\frac{\partial\theta}{\partial x_j}\right)\left(\frac{\partial\theta}{\partial x_j}\right)}$$

Dissipation

$\overline{\omega_i \omega_i}$ normalized by wall units
(no summation over the index i)

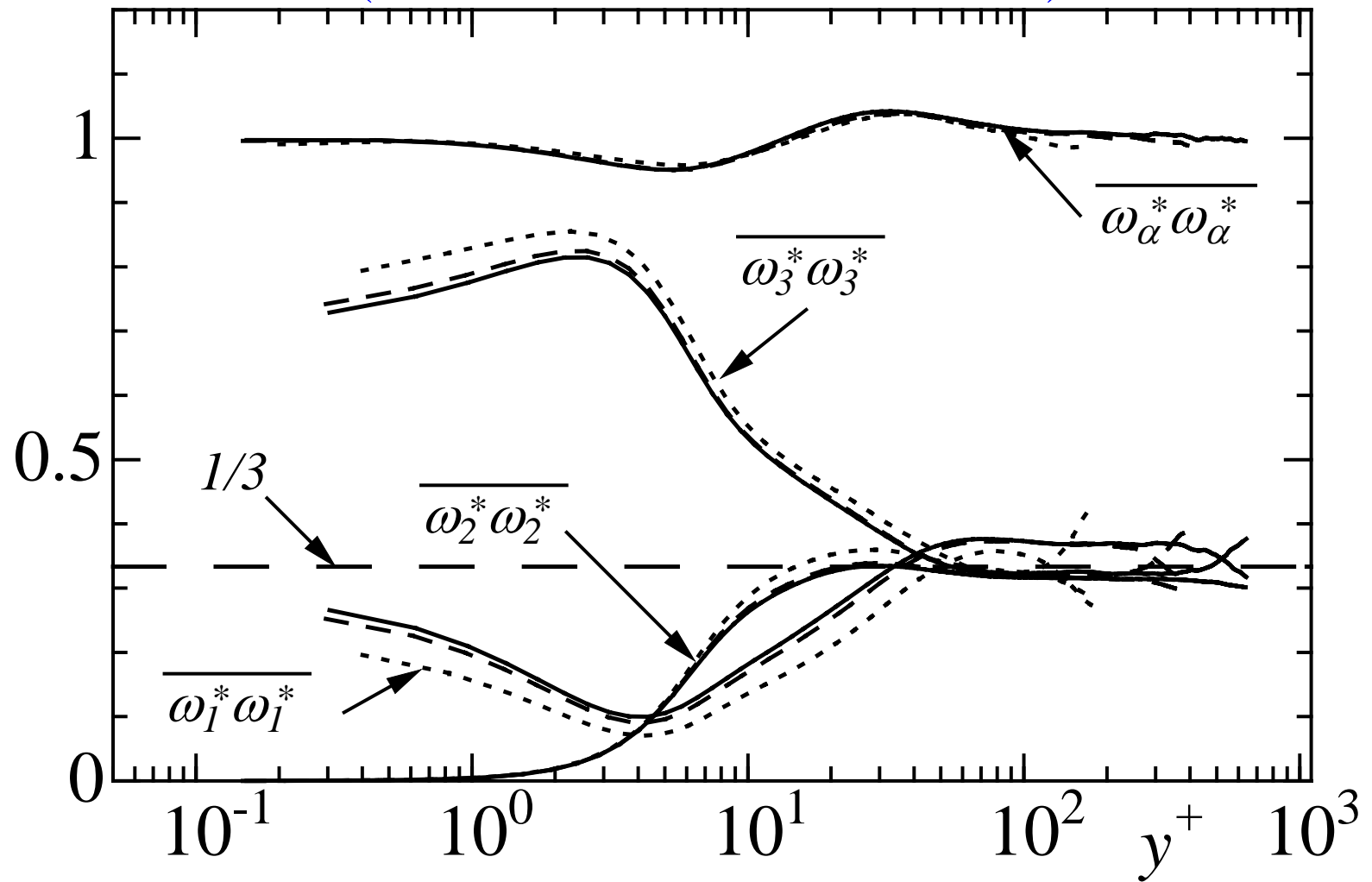


$\overline{\theta_{,i} \theta_{,i}}$ normalized by wall units
(no summation over the index i)



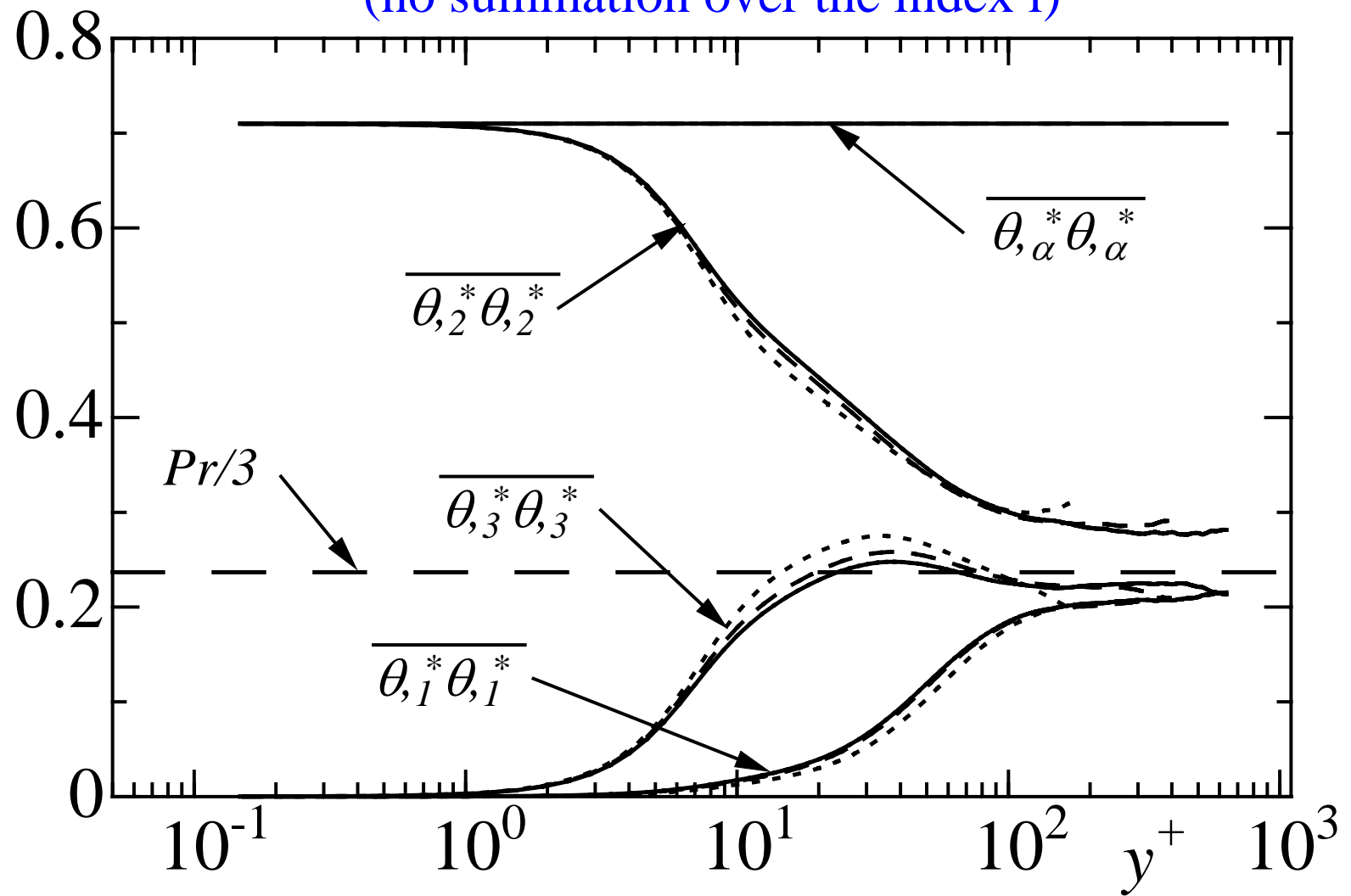
— Antonia and Kim (1994) at $Re_\tau=392$
— Kasagi (1992) at $Re_\tau=150$

$\overline{\omega_i \omega_i}$ normalized by Kolmogorov scales
 (no summation over the index i)



—	$Re_\tau = 640$	- - -	$Re_\tau = 395$	· · ·	$Re_\tau = 180$
---	-----------------	-------	-----------------	-------	-----------------

$\overline{\theta_{,i} \theta_{,i}}$ normalized by Kolmogorov scales
 (no summation over the index i)



— $Re_\tau = 640$ - - - $Re_\tau = 395$ - · - - $Re_\tau = 180$

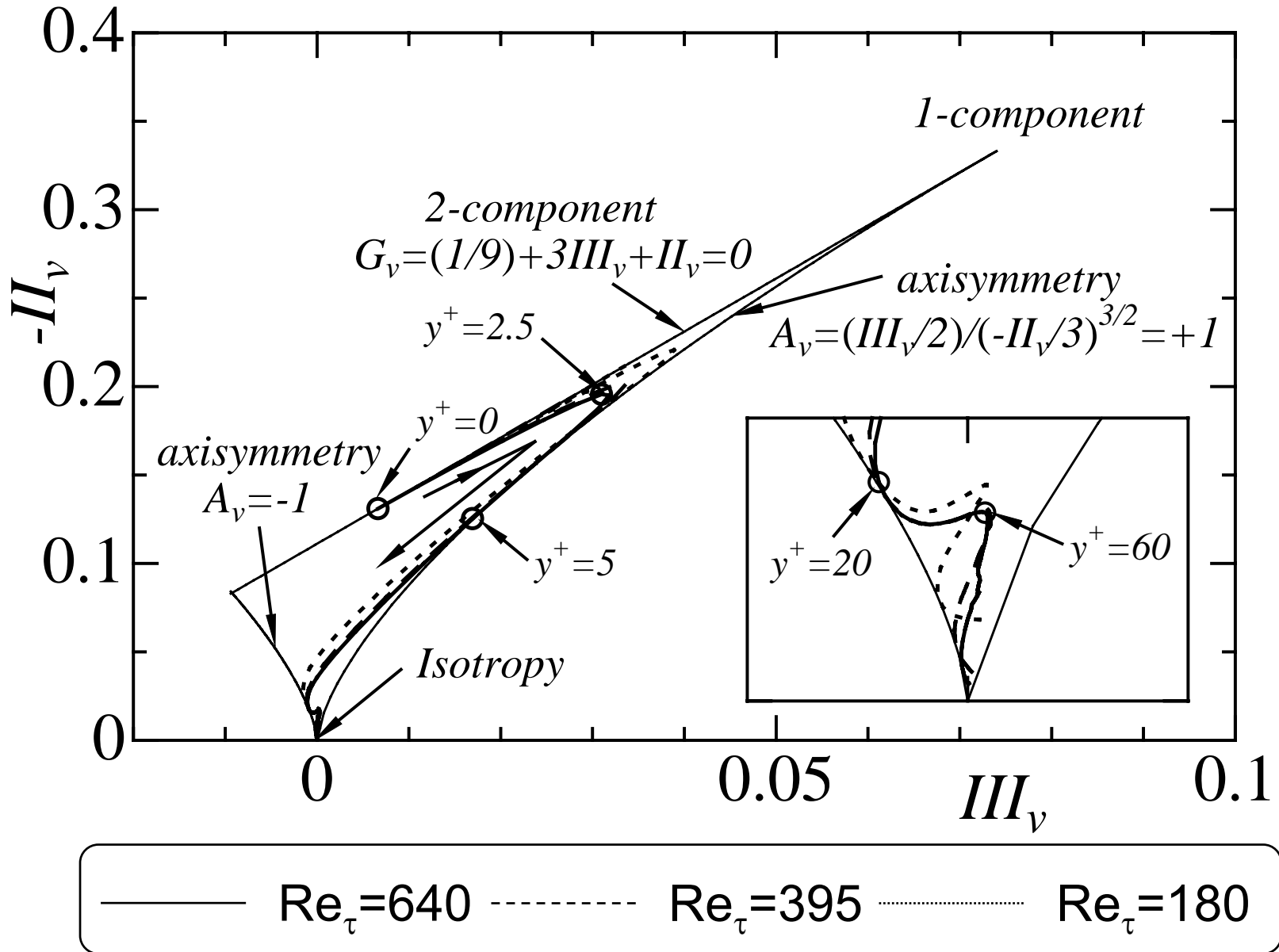
Vorticity and scalar derivative anisotropy tensors

$$\nu_{ij} = \frac{\overline{\omega_i \omega_j}}{\omega_\alpha \omega_\alpha} - \frac{1}{3} \delta_{ij} \quad t_{ij} = \frac{\overline{\theta, i \theta, j}}{\theta, \alpha \theta, \alpha} - \frac{1}{3} \delta_{ij}$$

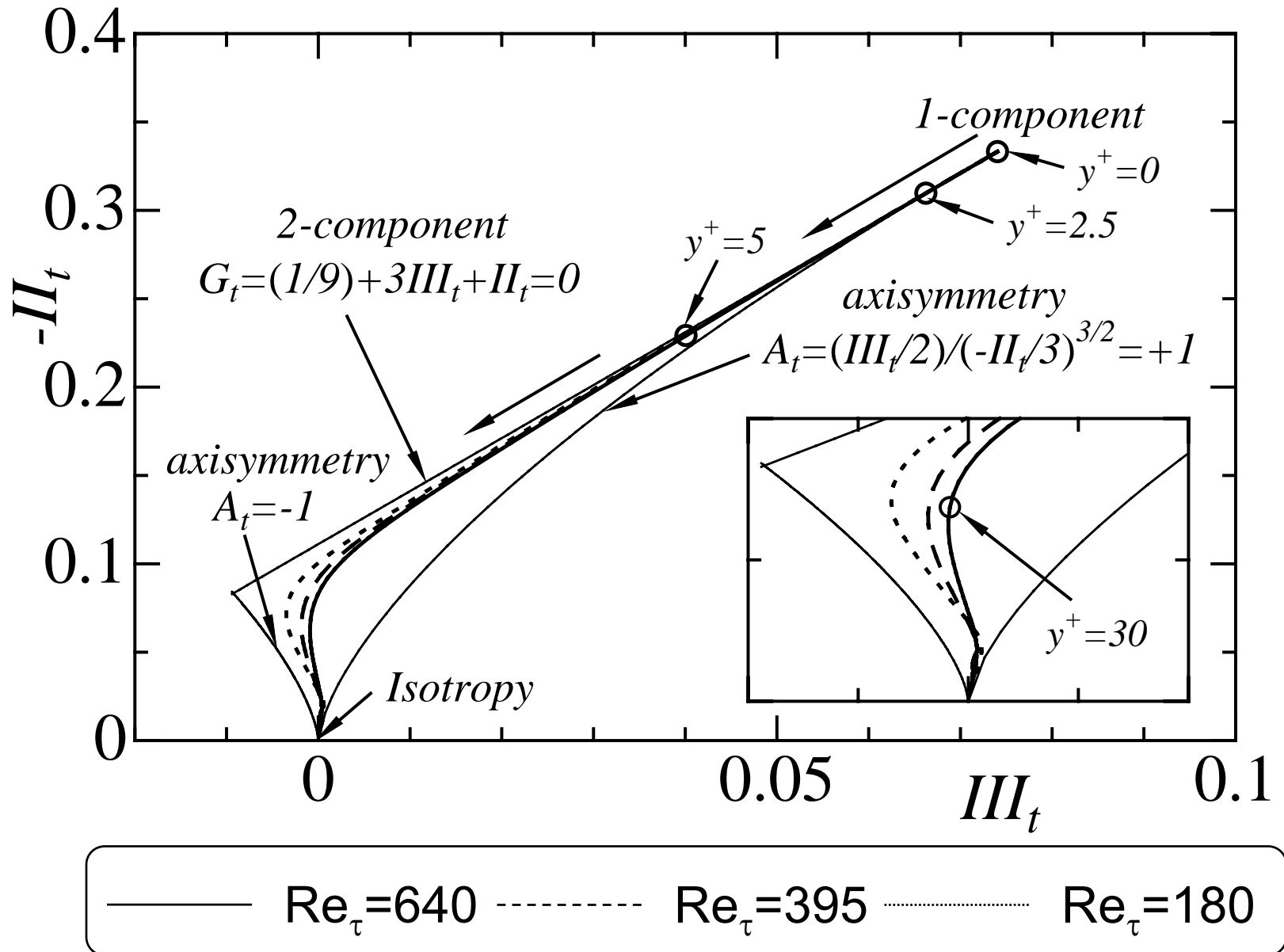
$$II = -\frac{1}{2} \nu_{ij} \nu_{ji} \quad or \quad -\frac{1}{2} t_{ij} t_{ji}$$

$$III = \frac{1}{3} \nu_{ij} \nu_{jk} \nu_{ki} \quad or \quad \frac{1}{3} t_{ij} t_{jk} t_{ki}$$

AIMs of the vorticity anisotropy tensor



AIMs of the scalar derivative anisotropy tensor



Corrsin (1953)

- Temperature derivative

$$\Theta_{,i} = \bar{\Theta}_{,i} + \theta_{,i} \quad \left(\Theta_{,i} \equiv \frac{\partial \Theta}{\partial x_i} \right)$$

- Vorticity

$$\Omega_i = \bar{\Omega}_i + \omega_i$$

$\Theta_{,i}$ is lamellar $(\nabla \times \Theta_{,i} \equiv 0)$

Ω_i is solenoidal $(\nabla \cdot \Omega_i \equiv 0)$

Transport equations of $\overline{\theta}_{,i} \theta_{,i}$ and $\overline{\omega_i} \omega_i$

- Budget of $\overline{\theta_{,i}^+ \theta_{,i}^+}$

$$0 = -2\overline{\theta_{,i}^+ u_j^+} \frac{\partial \overline{\theta_{,i}^+}}{\partial x_j^+} + 2 \underbrace{\left(\frac{\partial \langle \bar{T}_w \rangle^+}{\partial x_1^+} \right) \left(\frac{\partial u_1^+}{\partial x_i^+} \right) \left(\frac{\partial \theta^+}{\partial x_i^+} \right)}_{gradient production} - \underbrace{\frac{\partial}{\partial x_j^+} \left(\overline{\theta_{,i}^+ \theta_{,i}^+ u_j^+} \right)}_{turbulent diffusion} - 2\overline{\theta_{,j}^+} \cdot \overline{\theta_{,i}^+} \underbrace{\frac{\partial u_j^+}{\partial x_i^+}}_{mean gradient production (1)} - 2\overline{\theta_{,i}^+ \theta_{,j}^+} \underbrace{\frac{\partial \bar{U}_j^+}{\partial x_i^+}}_{mean gradient production (2)}$$

$$-2\overline{\theta_{,i}^+ \theta_{,j}^+} \frac{\partial u_j^+}{\partial x_i^+} + \underbrace{\frac{1}{Pr} \frac{\partial^2}{\partial x_j^+ \partial x_i^+} \left(\overline{\theta_{,i}^+ \theta_{,i}^+} \right)}_{molecular diffusion} - \underbrace{\frac{2}{Pr} \left(\frac{\partial \theta_{,i}^+}{\partial x_j^+} \right) \left(\frac{\partial \theta_{,i}^+}{\partial x_j^+} \right)}_{dissipation} \quad \left[2 \left(\frac{\partial \langle T_w \rangle^+}{\partial x_1^+} \right) \left(\frac{\partial u_1^+}{\partial x_i^+} \right) \left(\frac{\partial \theta^+}{\partial x_i^+} \right) = \frac{4}{Re_\tau \bar{U}_b} \left(\frac{\partial u^+}{\partial x_i^+} \right) \left(\frac{\partial \theta^+}{\partial x_i^+} \right) \approx 0 \right]$$

turbulent production *molecular diffusion* *dissipation*

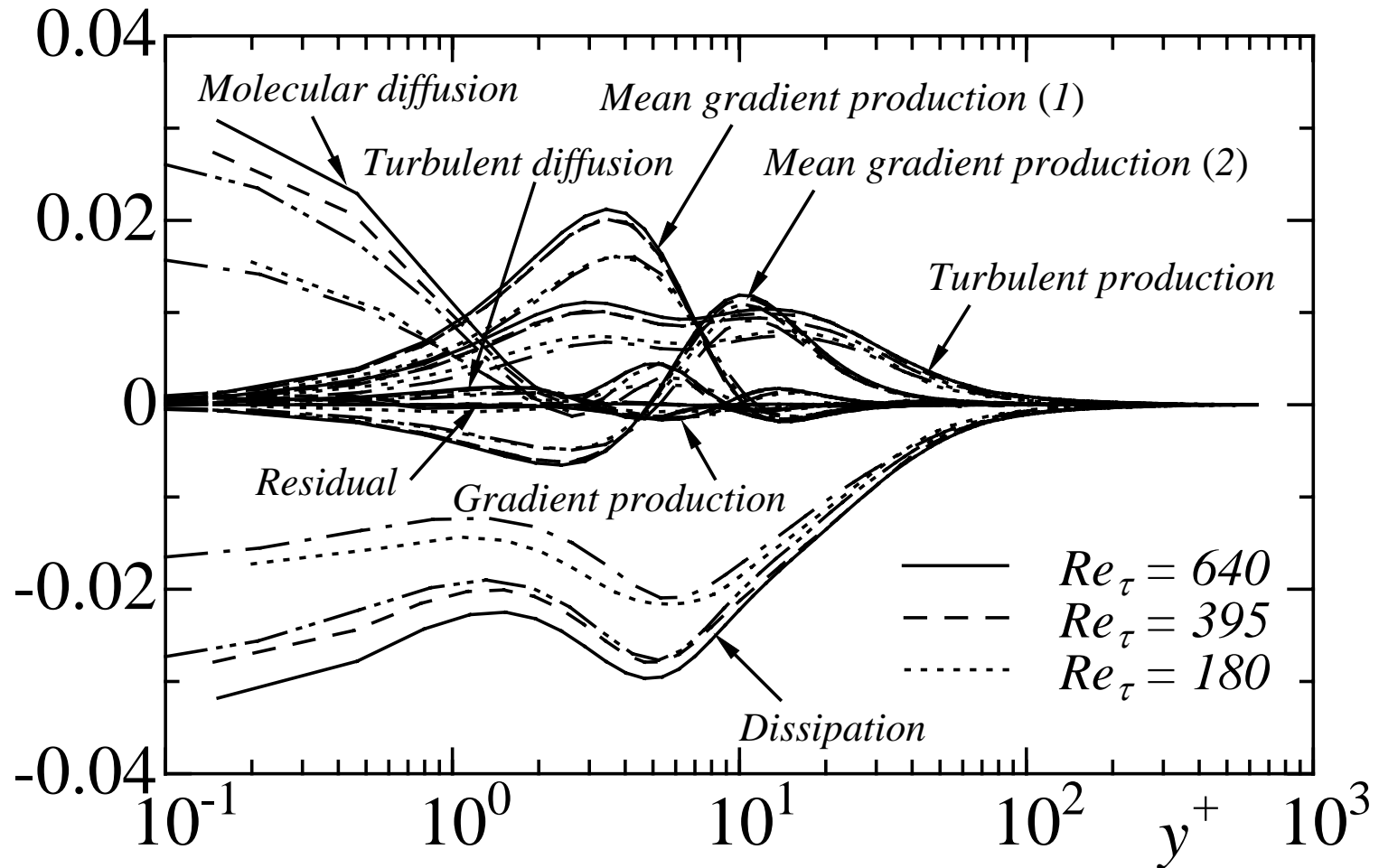
- Budget of $\overline{\omega_i^+ \omega_i^+}$

$$0 = -2\overline{\omega_i^+ u_j^+} \frac{\partial \overline{\Omega_i^+}}{\partial x_j^+} - \underbrace{\frac{\partial}{\partial x_j^+} \left(\overline{\omega_i^+ \omega_i^+ u_j^+} \right)}_{turbulent diffusion} + \overline{\Omega_j^+} \cdot \overline{\omega_i^+} \underbrace{\left(\frac{\partial u_j^+}{\partial x_i^+} + \frac{\partial u_i^+}{\partial x_j^+} \right)}_{mean gradient production (1)} + \overline{\omega_i^+ \omega_j^+} \cdot \underbrace{\left(\frac{\partial \bar{U}_i^+}{\partial x_j^+} + \frac{\partial \bar{U}_j^+}{\partial x_i^+} \right)}_{mean gradient production (2)}$$

$$+ \overline{\omega_i^+ \omega_j^+} \underbrace{\left(\frac{\partial u_i^+}{\partial x_j^+} + \frac{\partial u_j^+}{\partial x_i^+} \right)}_{turbulent production} + \underbrace{\frac{\partial^2}{\partial x_j^+ \partial x_i^+} \left(\overline{\omega_i^+ \omega_i^+} \right)}_{molecular diffusion} - 2 \underbrace{\left(\frac{\partial \omega_i^+}{\partial x_j^+} \right) \left(\frac{\partial \omega_i^+}{\partial x_j^+} \right)}_{dissipation}$$

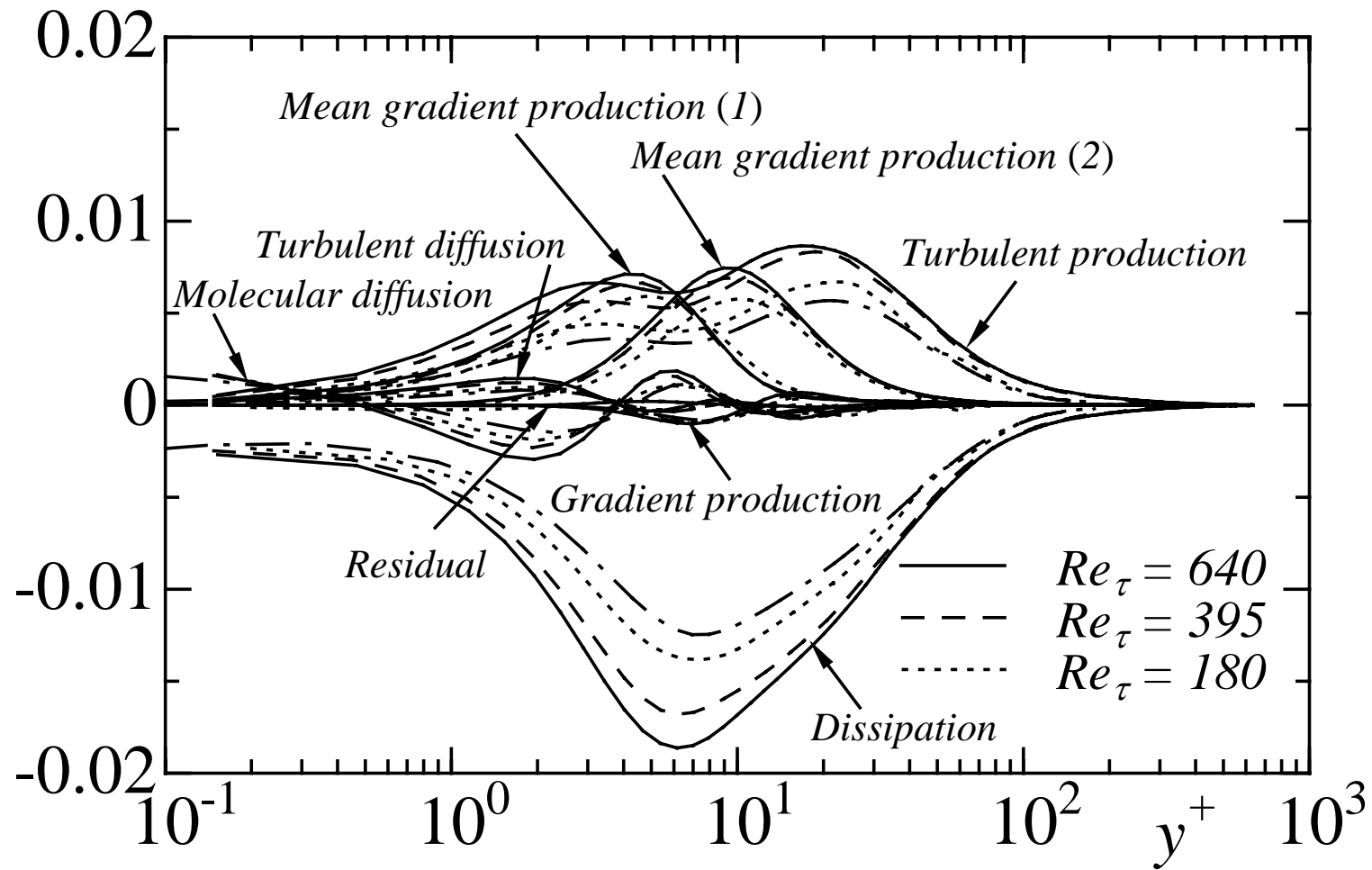
gradient production *turbulent diffusion* *mean gradient production (1)* *mean gradient production (2)*

Transport equation of $\overline{\omega_i \omega_i}$



— Antonia and Kim (1994) at $Re_\tau=180$
- - - Antonia and Kim (1994) at $Re_\tau=395$

Transport equation of $\overline{\theta_i \theta_i}$

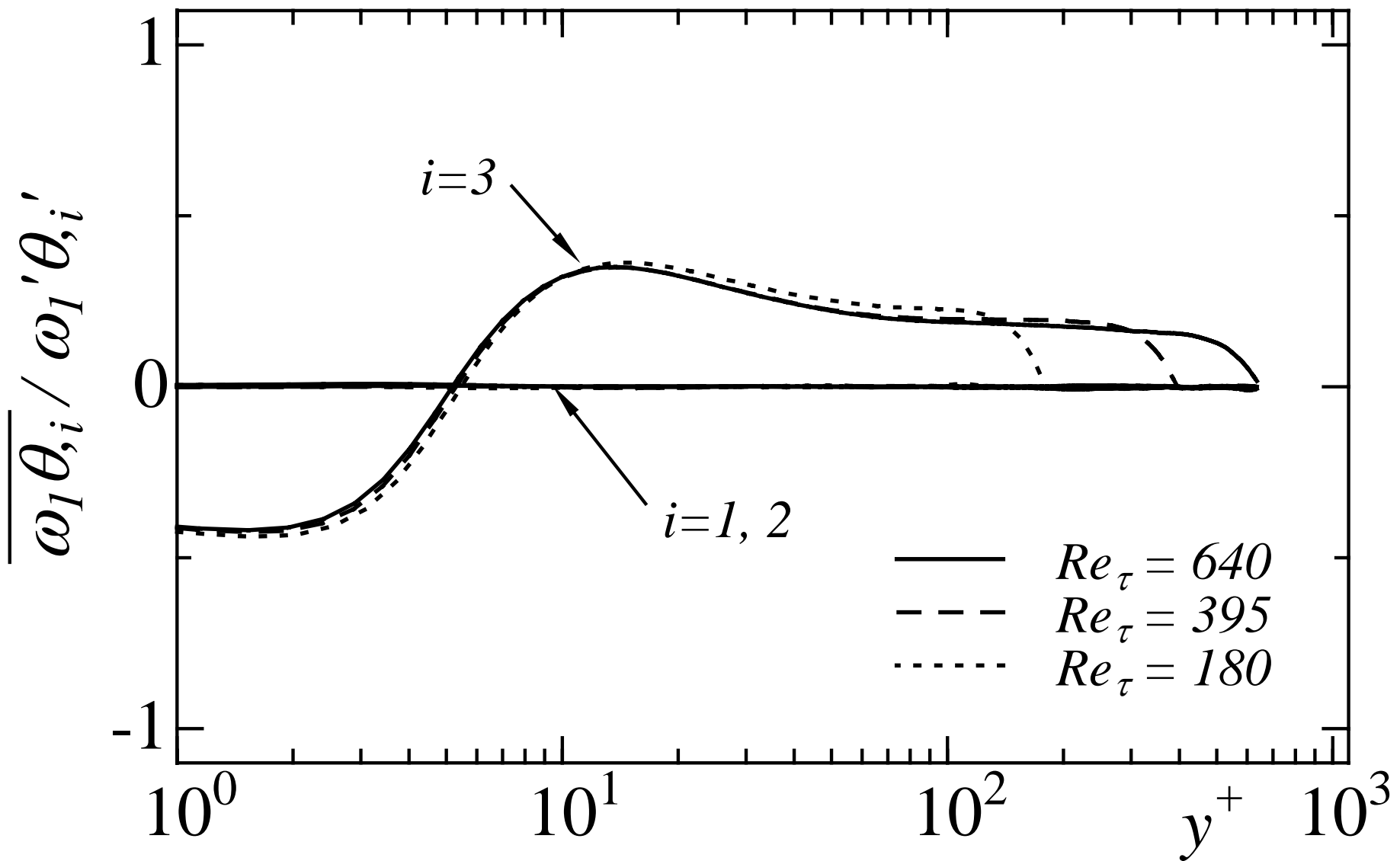


— Kasagi et al. (1992) at $Re_\tau=150$

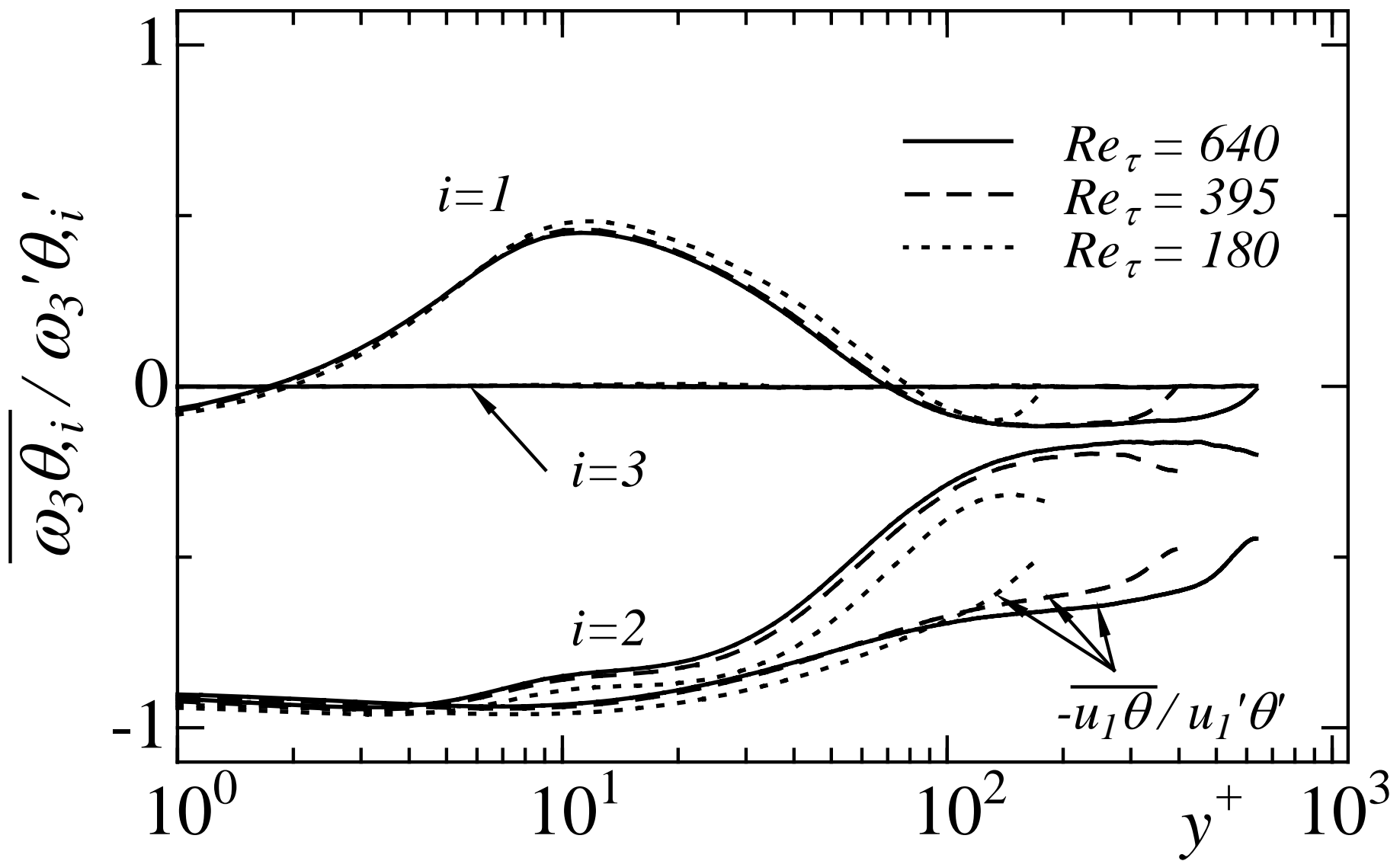
The correlation tensor $\overline{\omega_i \theta_j}$ has
only four non-zero terms

the other five are zero due to symmetry

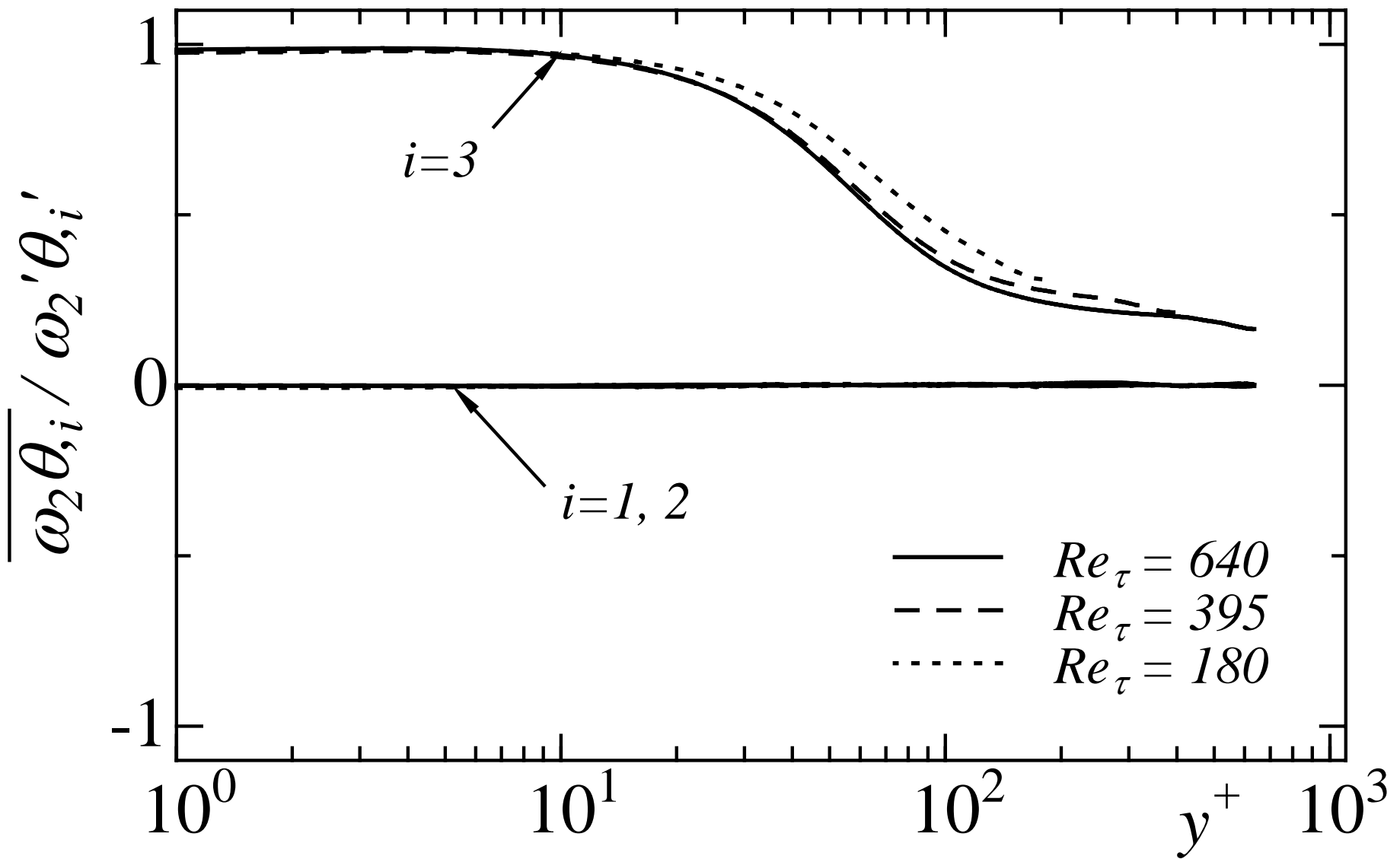
Correlation coefficients of $\overline{\omega_1 \theta_{,i}}$



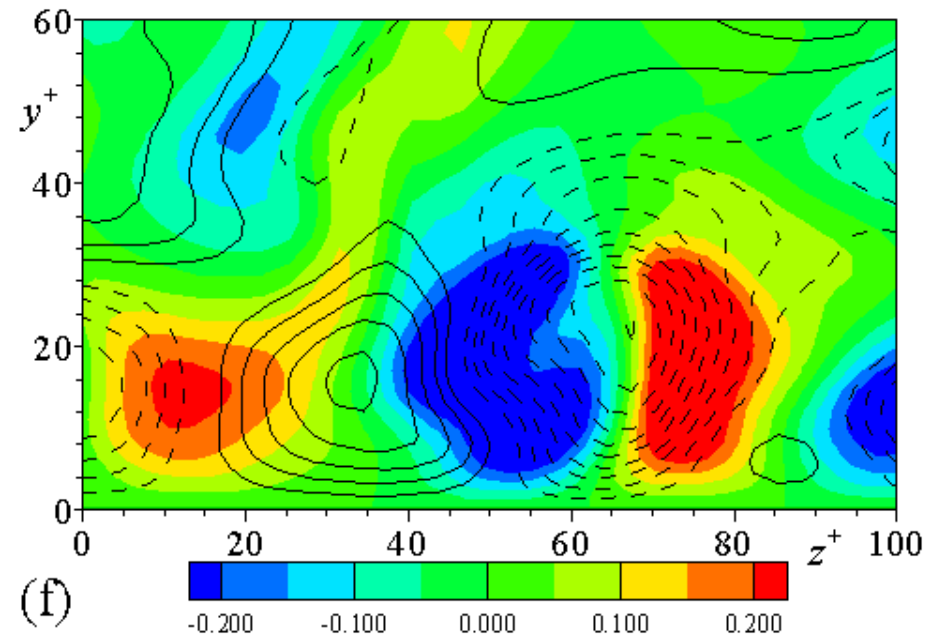
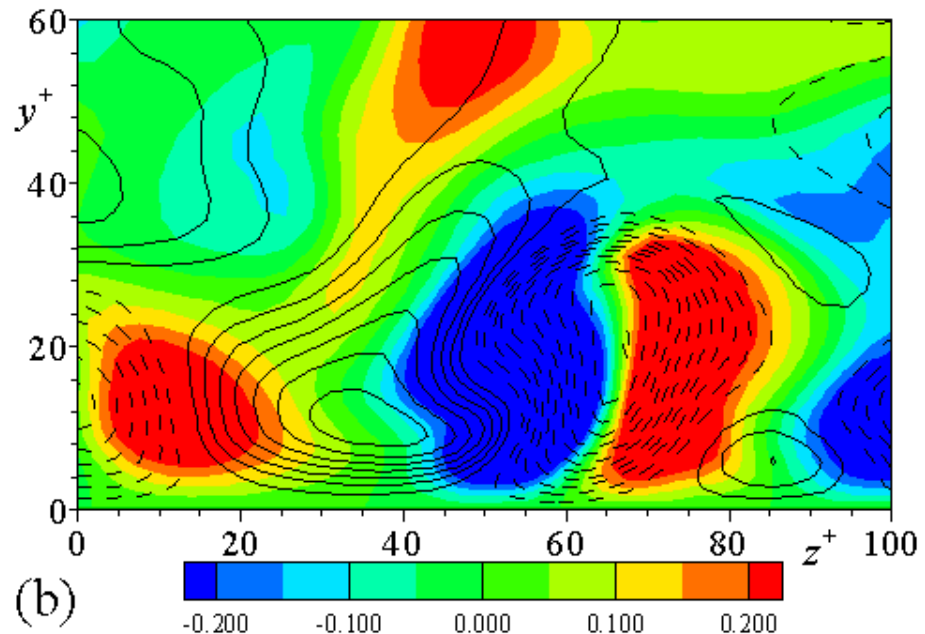
Correlation coefficients of $\overline{\omega_2 \theta}_{,i}$



Correlation coefficients of $\overline{\omega_3 \theta_{,i}}$



Contours of ω_2 and $\theta_{,3}$ in y-z plane at $Re_\tau = 180$

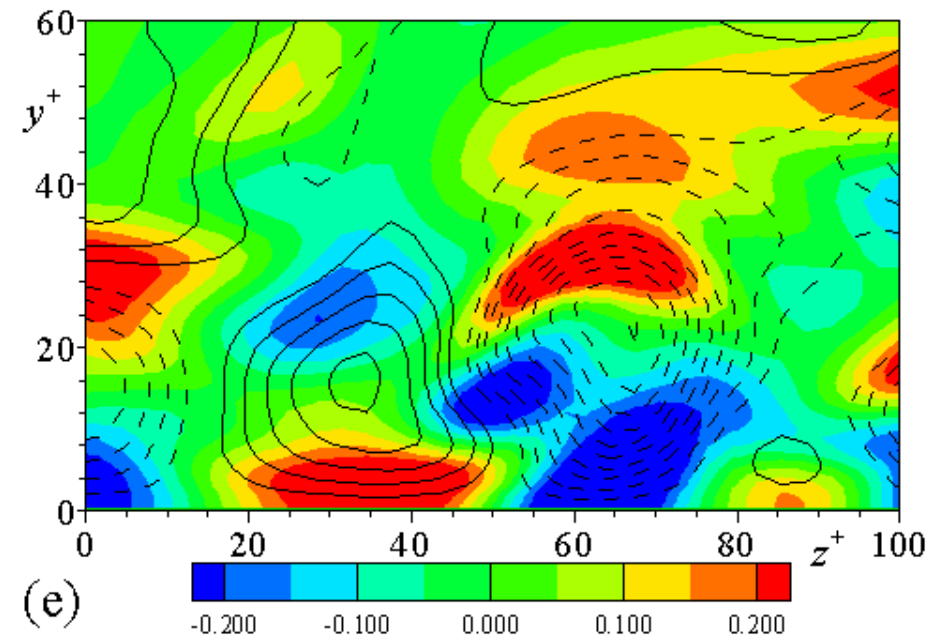
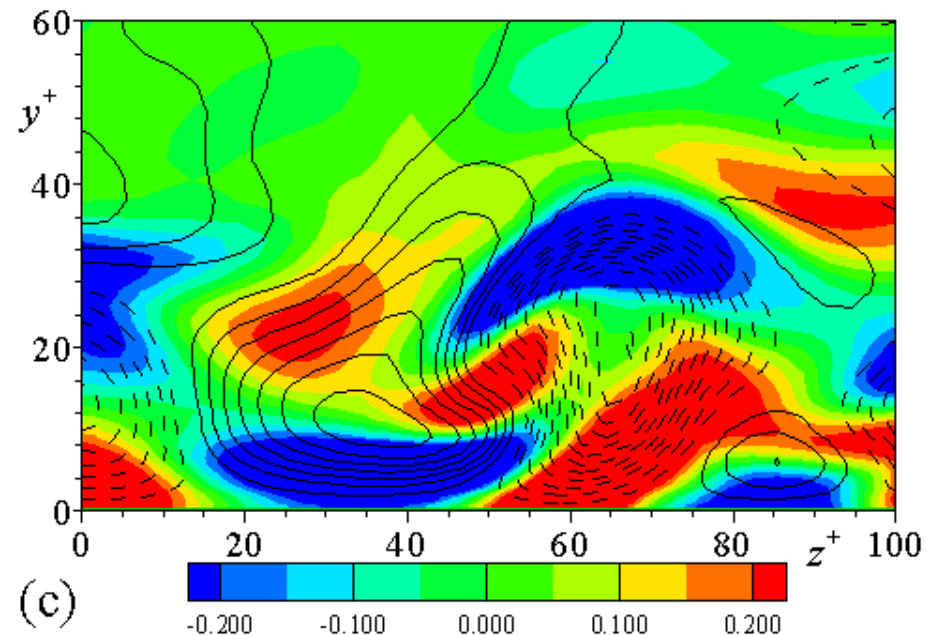


ω_2 (contour) with u_1 (lines)

$\theta_{,3}$ (contour) with θ (lines)

Solid and dashed lines are positive and negative values.

Contours of ω_3 and $\theta_{,2}$ in y-z plane at $Re_\tau = 180$

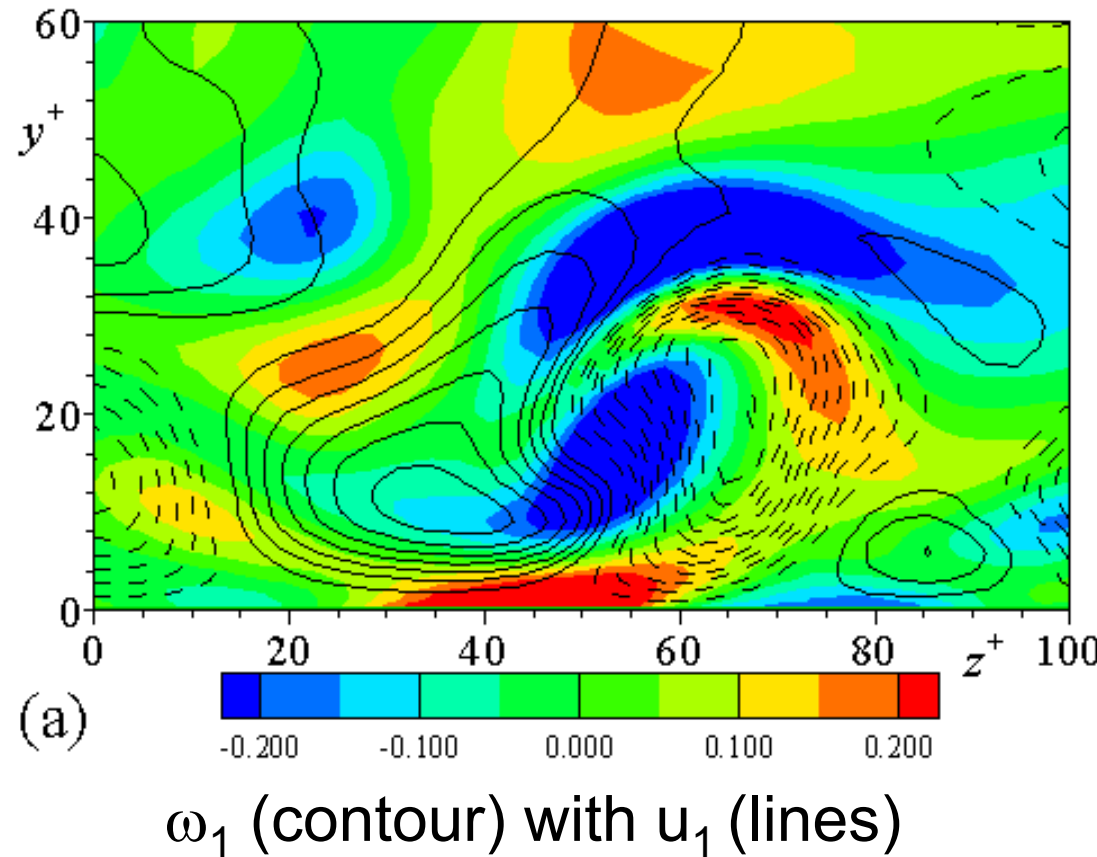


ω_3 (contour) with u_1 (lines)

$\theta_{,2}$ (contour) with θ (lines)

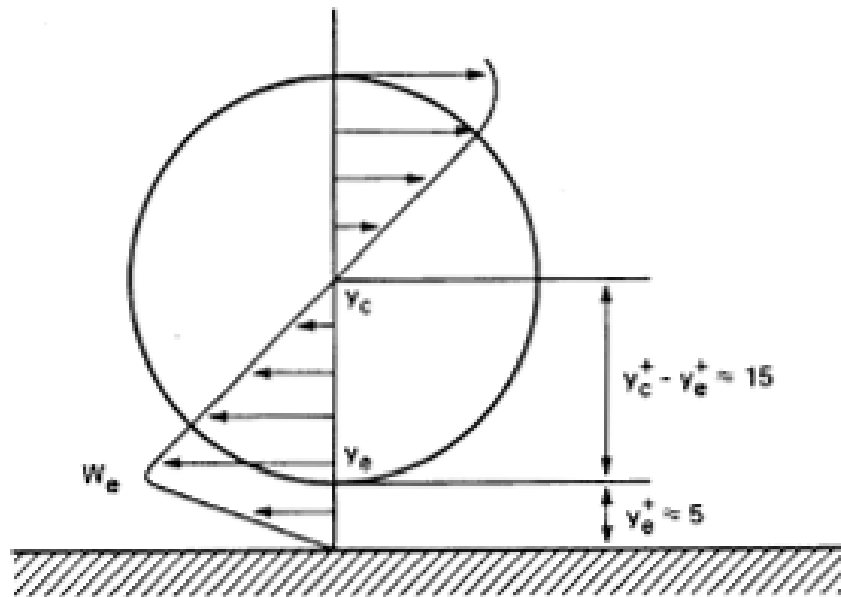
Solid and dashed lines are positive and negative values.

Contours of ω_1 in y-z plane at $Re_\tau = 180$



Solid and dashed lines are positive and negative values.

Schematic of near-wall streamwise vortex with resulting high streamwise vorticity at the wall



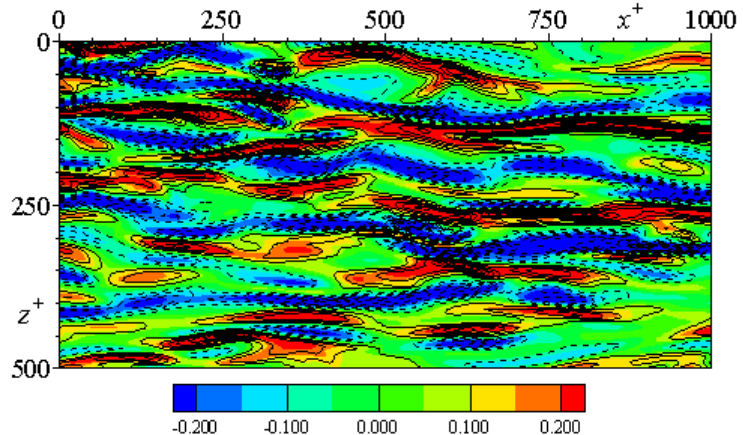
Kim, Moin and Moser (1987)

Two types of ω_x

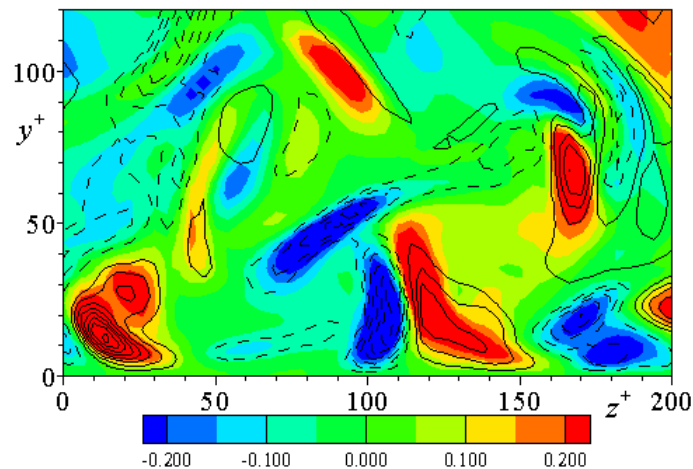
- 1) quasi-streamwise vortices
- 2) thin $\partial w / \partial y$ layers

Contours of instantaneous fields for ω_2 and $\theta_{,3}$ for $Re_\tau=640$ and $Pr=0.71$

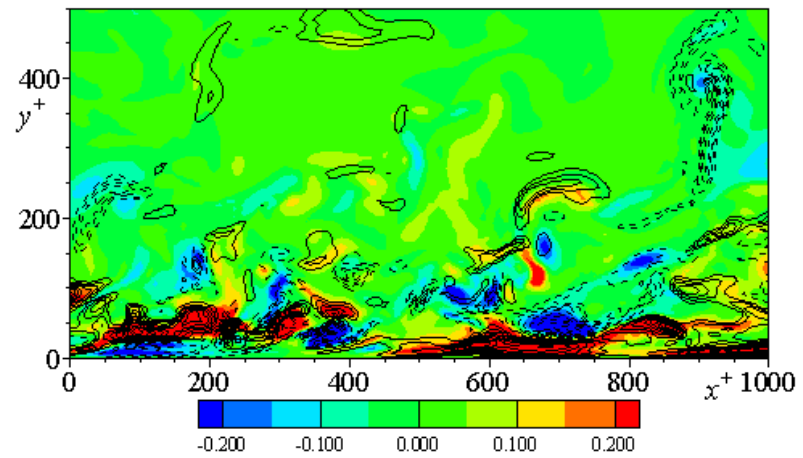
ω_2 (contour) with $\theta_{,3}$ (lines)



x-z plane at $y^+ = 10$



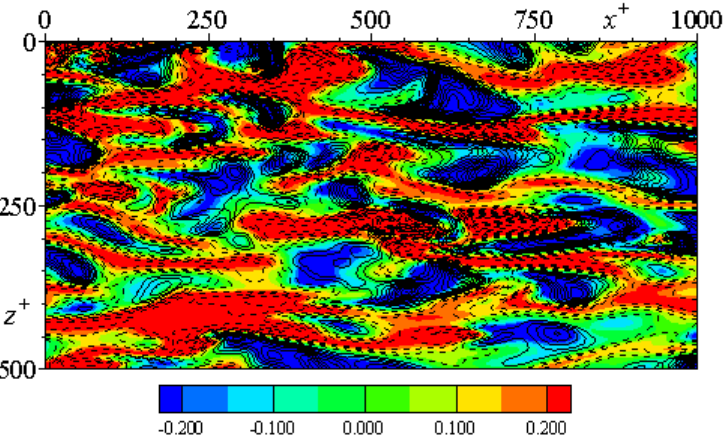
y-z plane



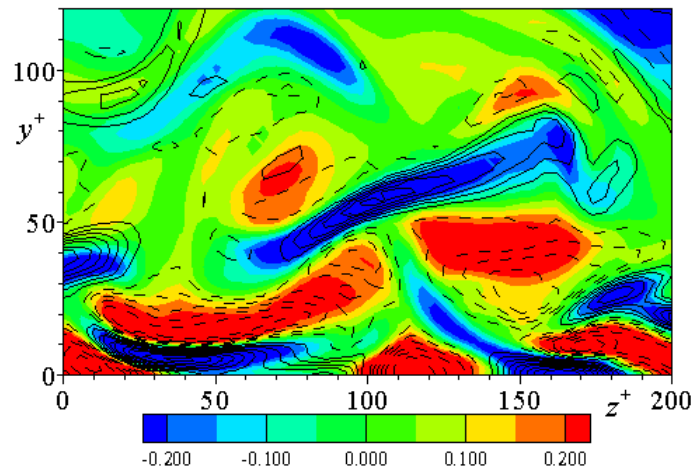
x-y plane

Contours of instantaneous fields for ω_3 and $\theta_{,2}$ for $Re_\tau=640$ and $Pr=0.71$

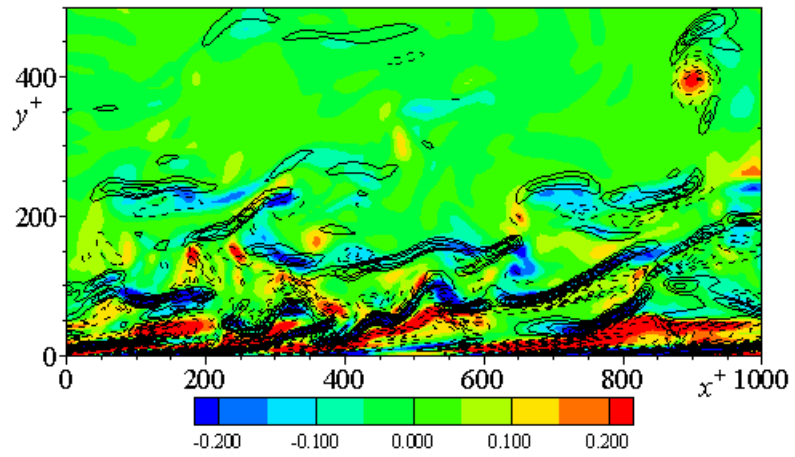
ω_3 (contour) with $\theta_{,2}$ (lines)



x-z plane at $y^+ = 10$



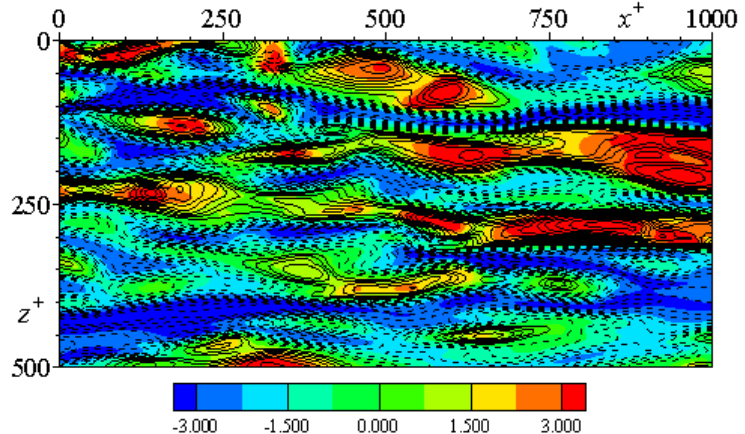
y-z plane



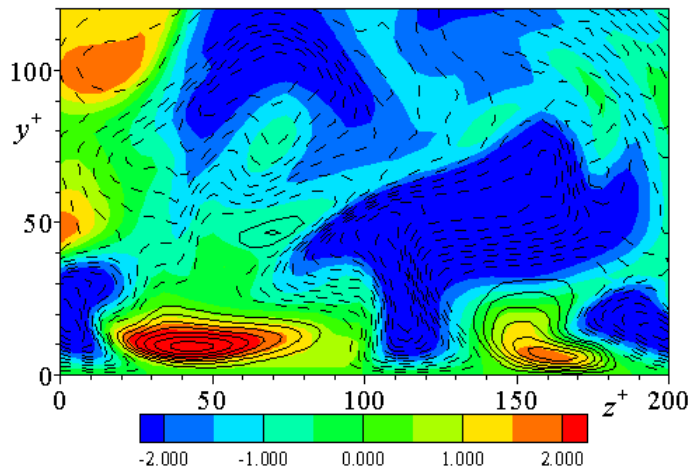
x-y plane

Contours of instantaneous fields for u_1 and θ for $Re_\tau=640$ and $Pr=0.71$

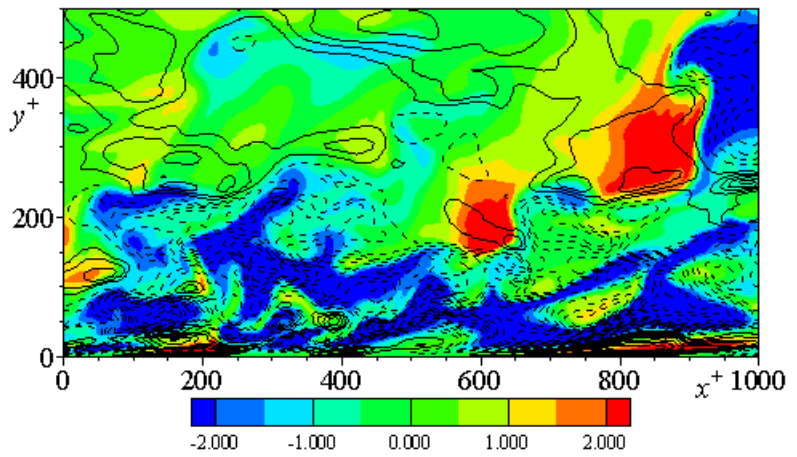
u_1 (contour) with θ (lines)



x - z plane at $y^+=10$

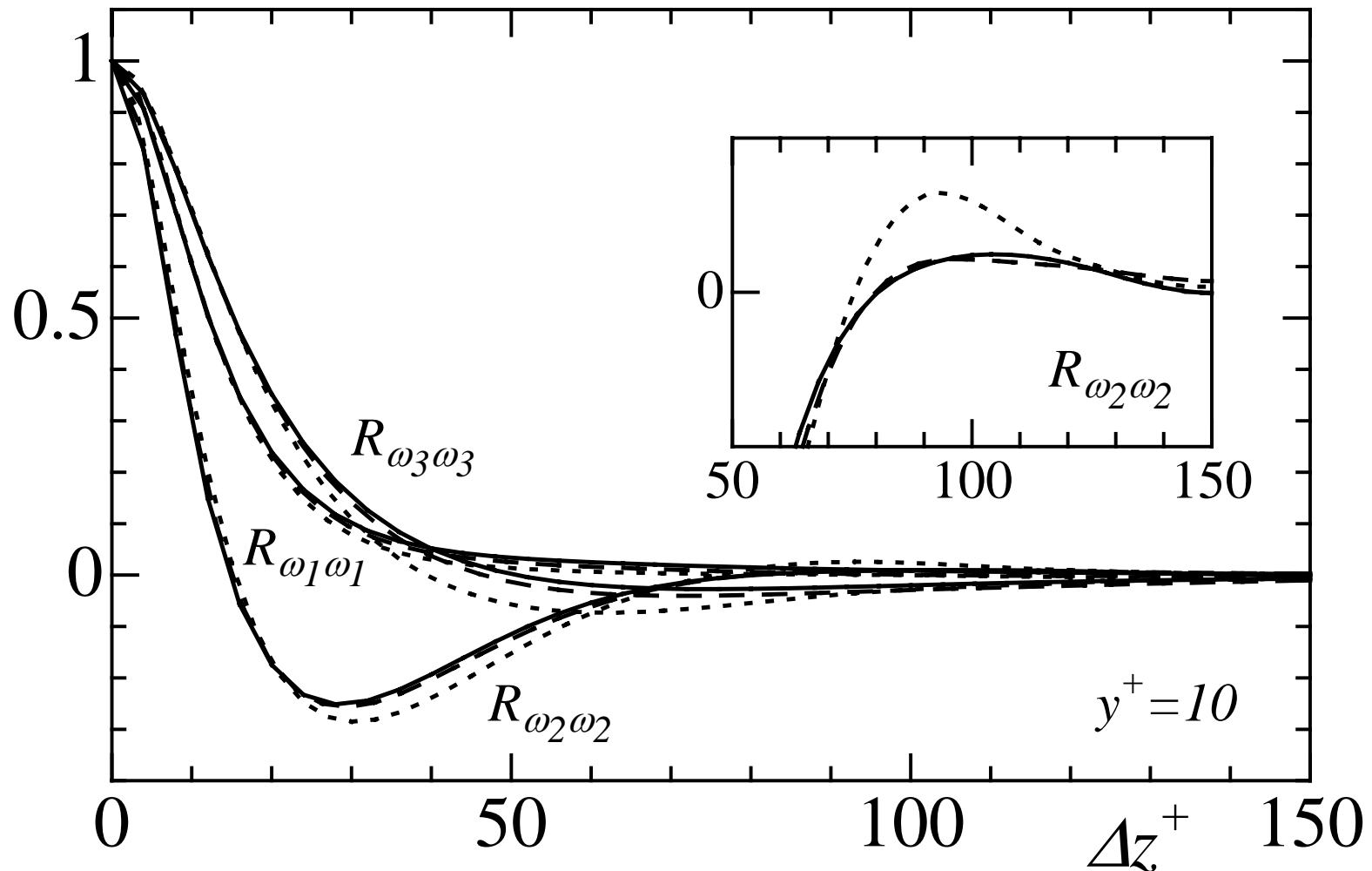


y - z plane



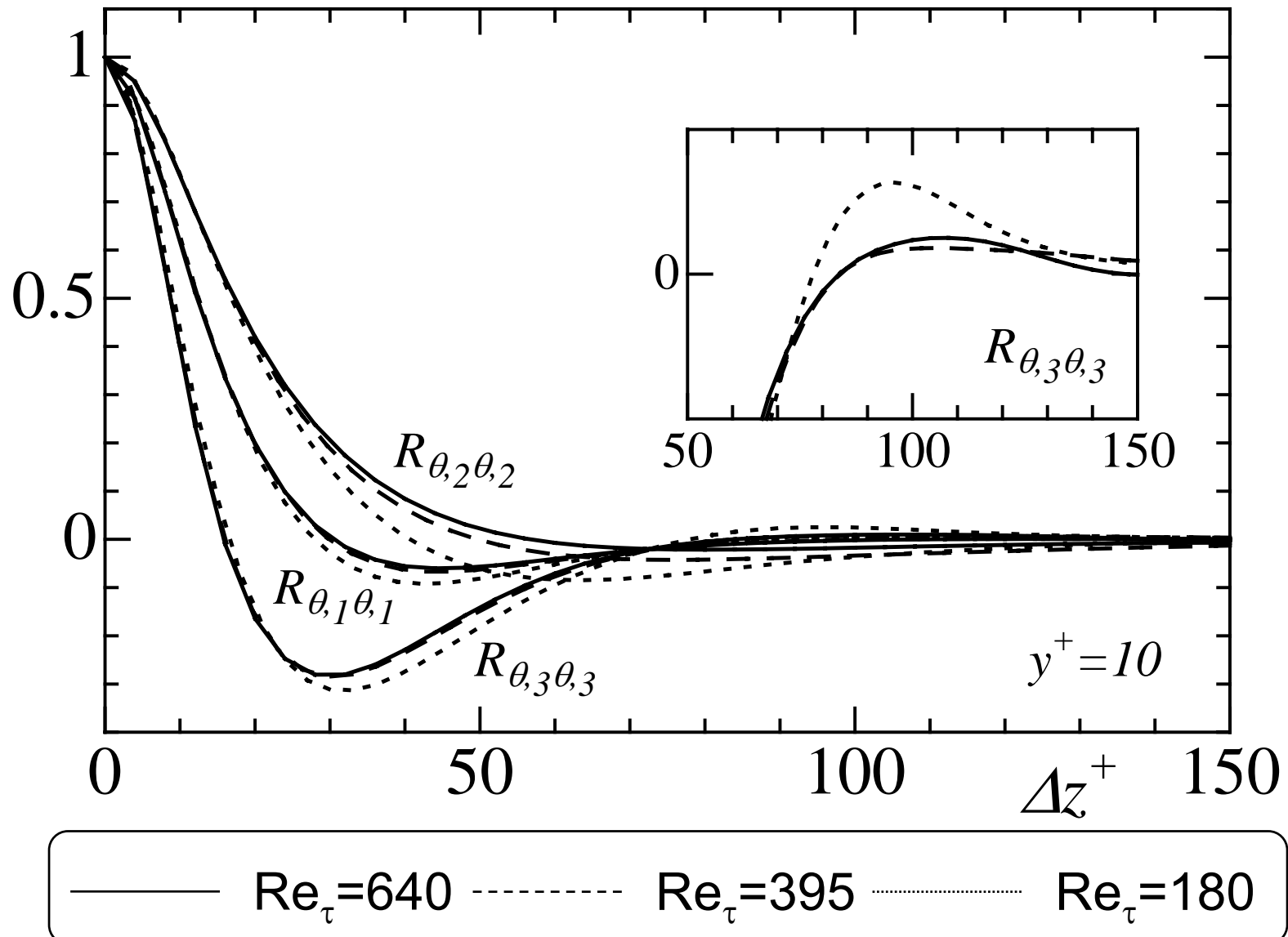
x - y plane

Spanwise two-point correlations of $\overline{\omega_i \omega_i}$ (no summation over the index i)



— $Re_\tau = 640$ - - - $Re_\tau = 395$ - · - · - $Re_\tau = 180$

Spanwise two-point correlations of $\overline{\theta_{,i} \theta_{,i}}$ (no summation over the index i)



The positive peak at $100\Delta z^+$ may correspond to the width of both low and high velocity streaks.

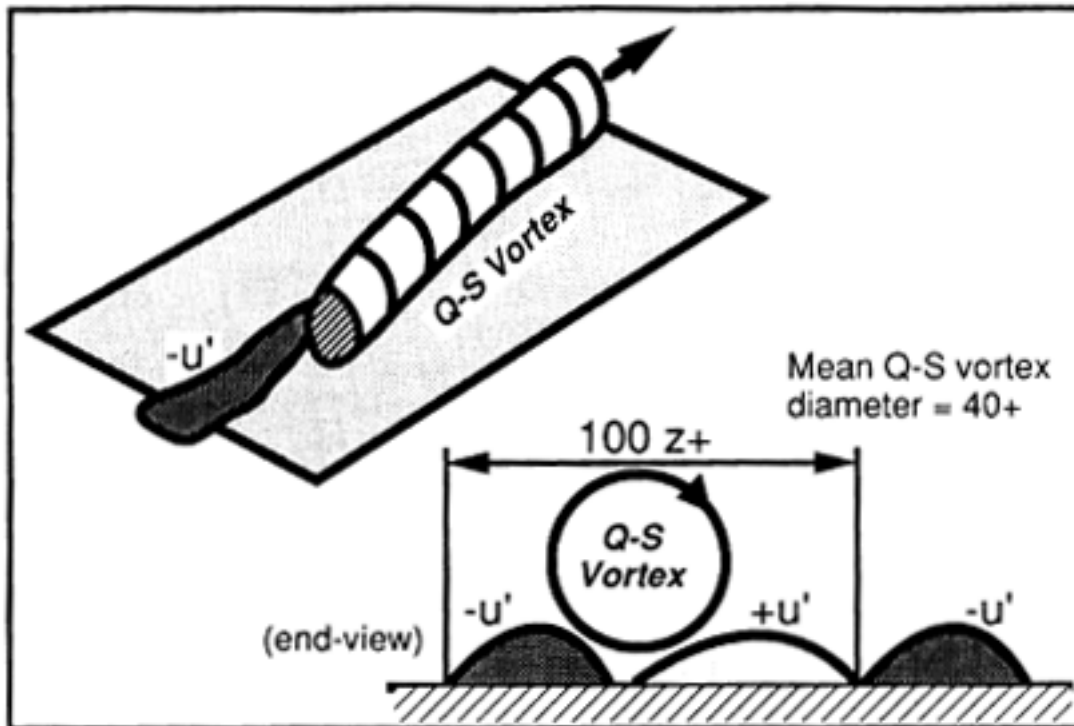
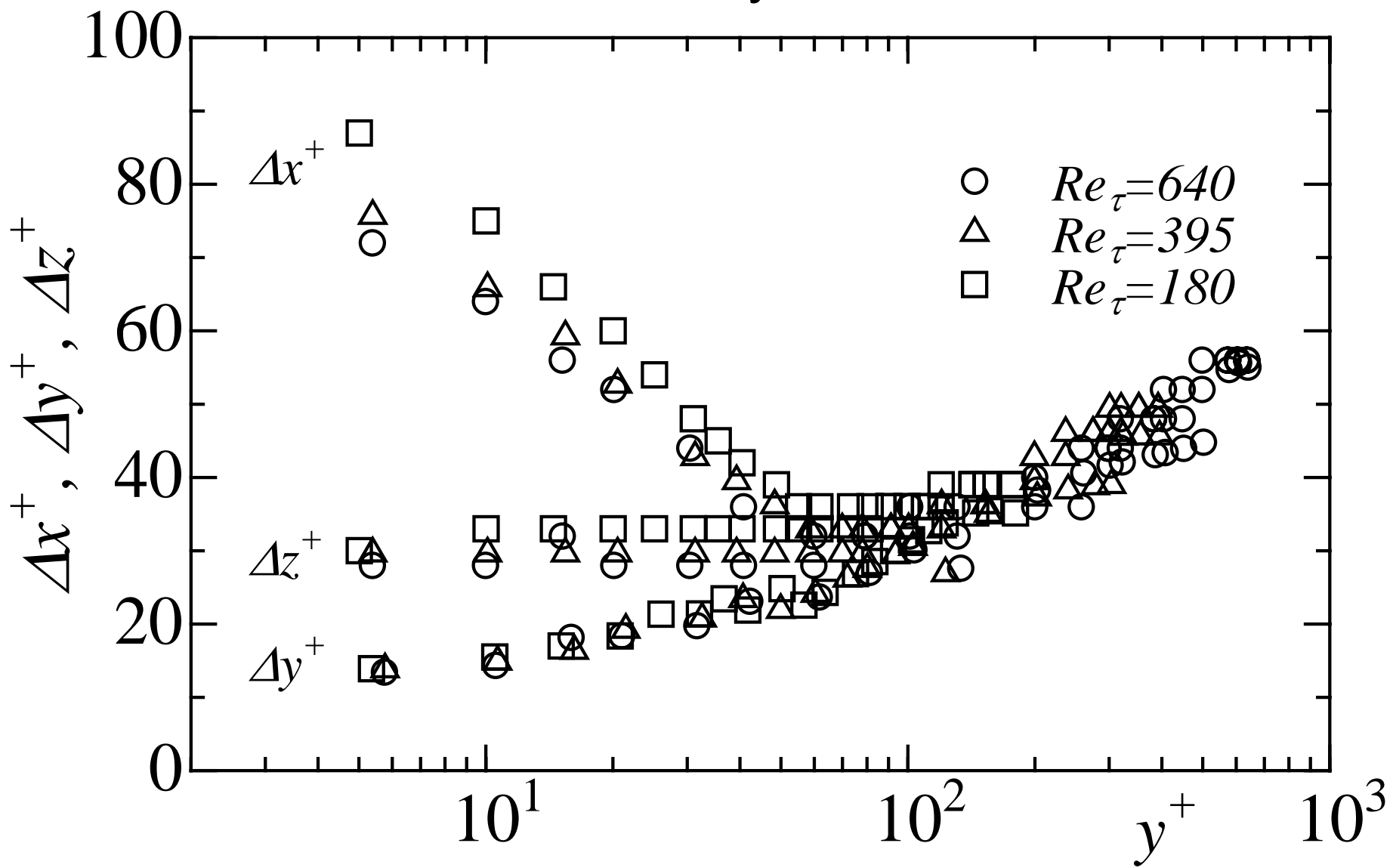


Fig. 12.1 Relationship between near-wall quasi-streamwise vortices and low-speed streaks in the sublayer and buffer layer.

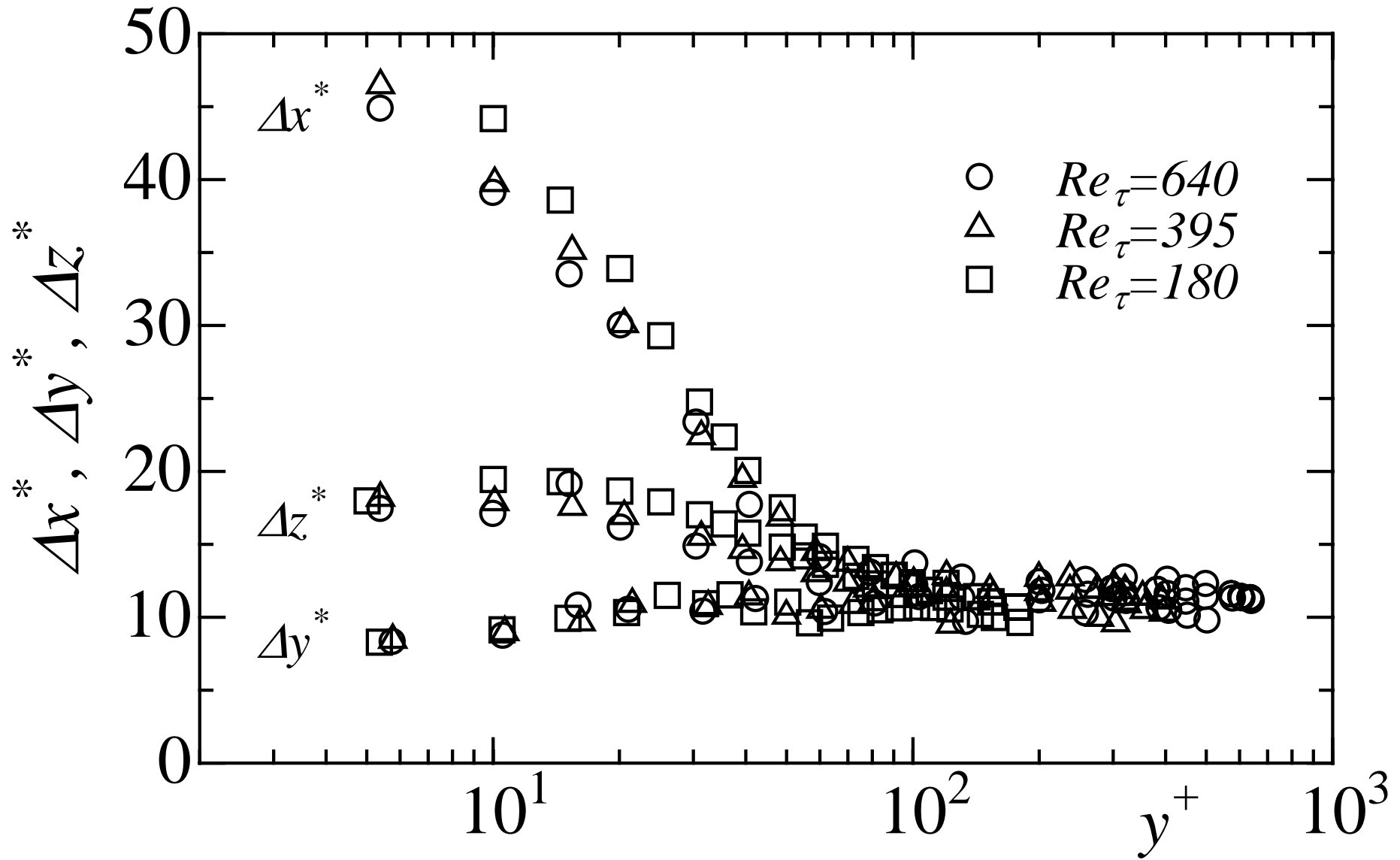
Robinson (1991, NASA TM 103859)

- 1) Widths of low u streaks: $20-80\Delta z^+$
- 2) Widths of high u streaks: $40-110\Delta z^+$

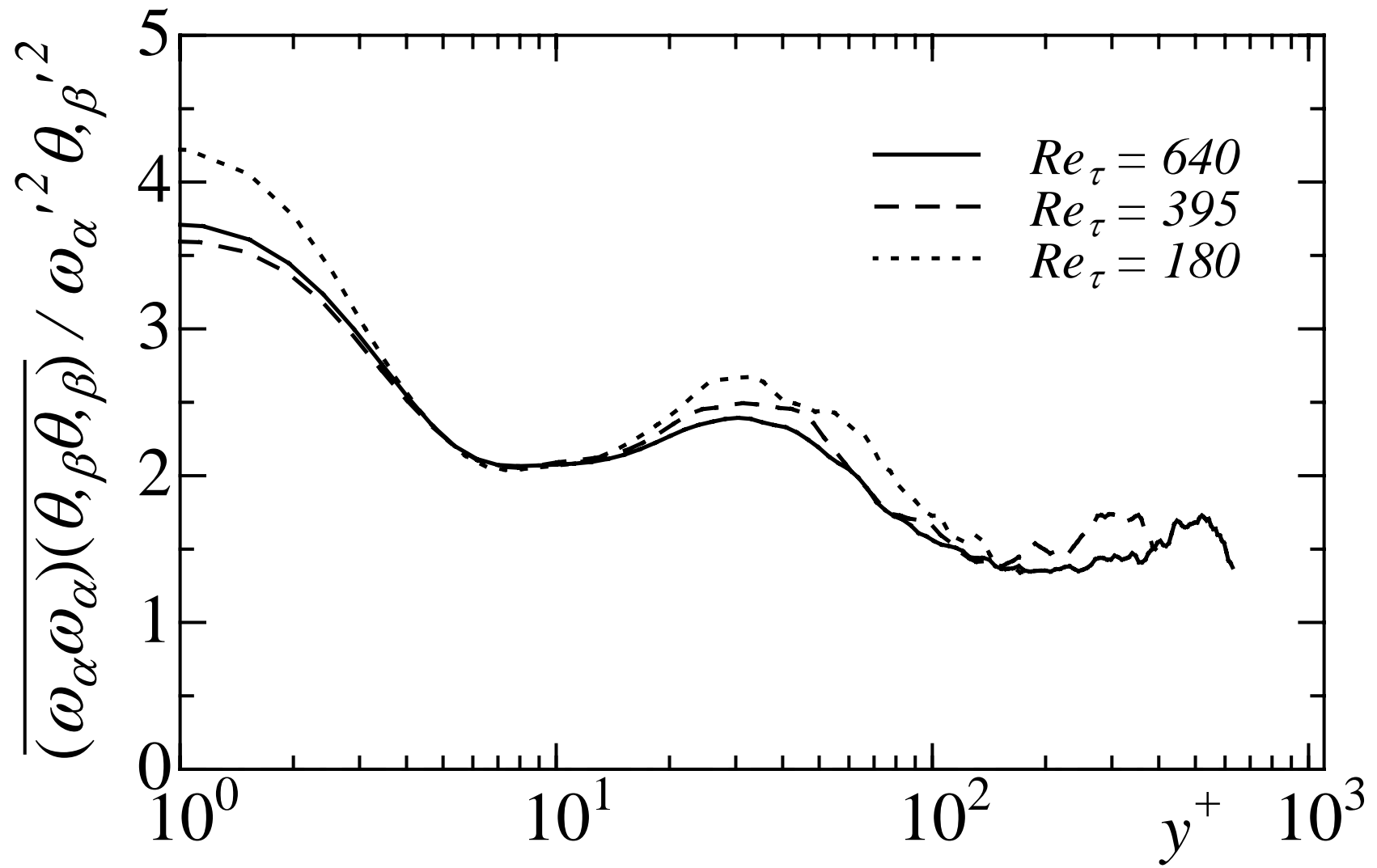
Minimum separations of $R_{\theta_{,1}\theta_{,1}}(\Delta x)$, $R_{\theta_{,2}\theta_{,2}}(\Delta y)$, $R_{\theta_{,3}\theta_{,3}}(\Delta z)$ normalized by wall units



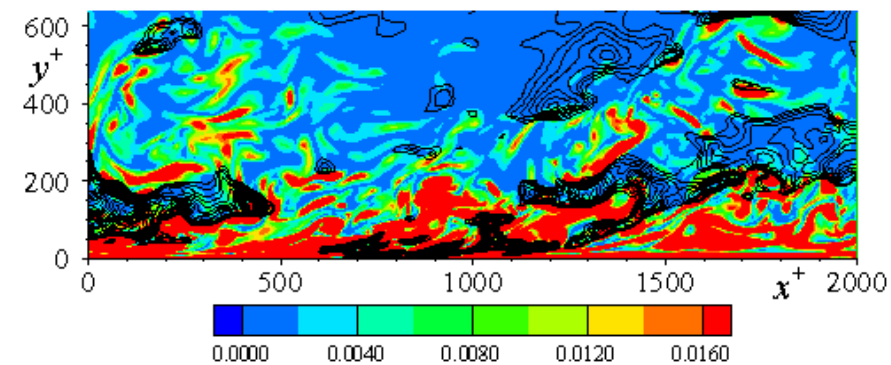
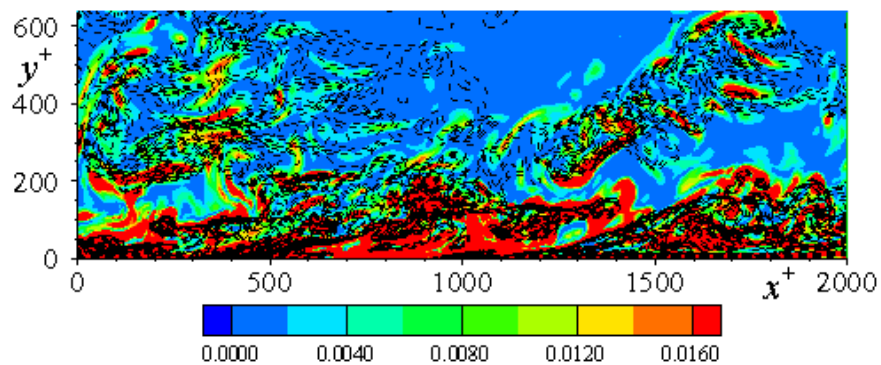
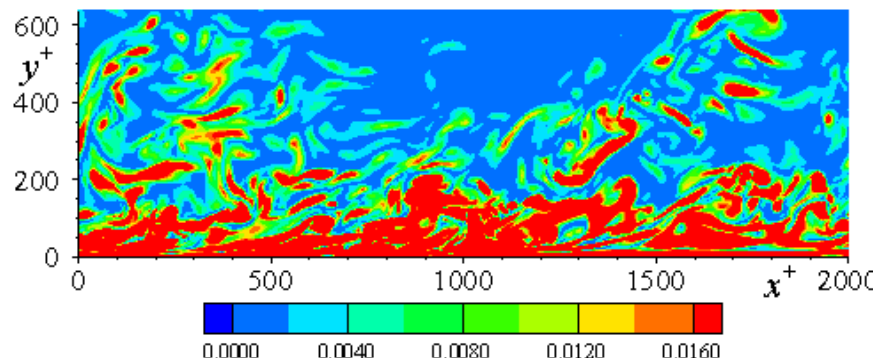
Minimum separations of $R_{\theta_{,1}\theta_{,1}}(\Delta x)$, $R_{\theta_{,2}\theta_{,2}}(\Delta y)$, $R_{\theta_{,3}\theta_{,3}}(\Delta z)$
normalized by Kolmogorov scale



Correlation coefficients of $\overline{(\omega_\alpha \omega_\alpha)(\theta_\beta \theta_\beta)}$

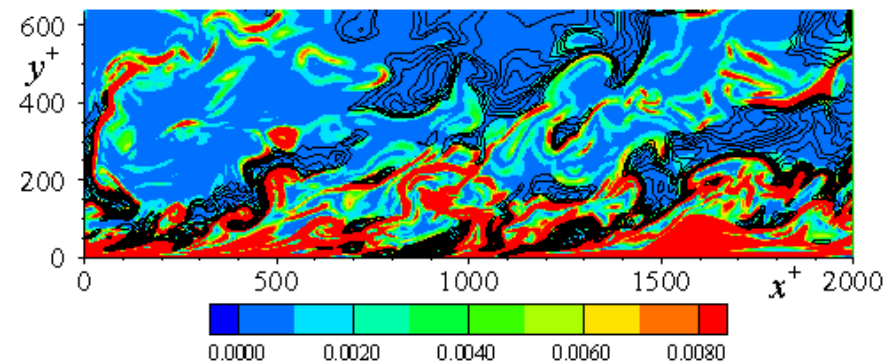
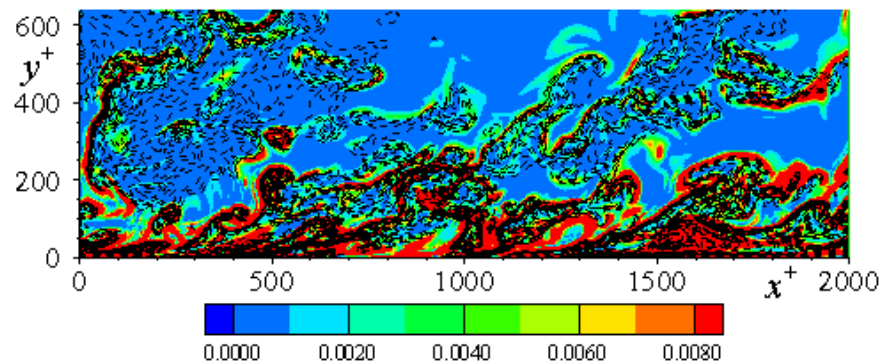
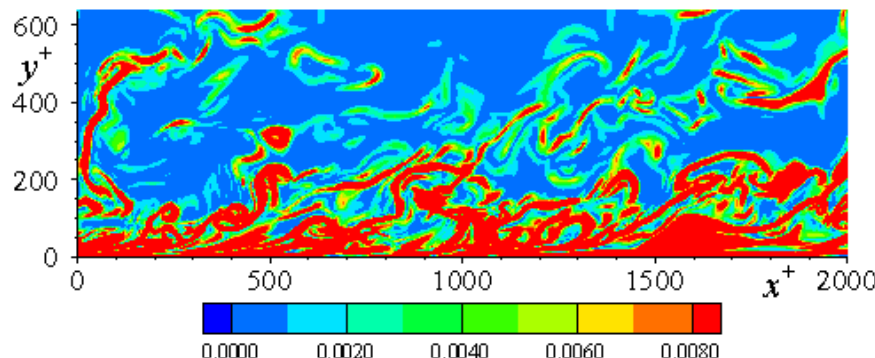


Instantaneous enstrophy for $\text{Re}_\tau=640$



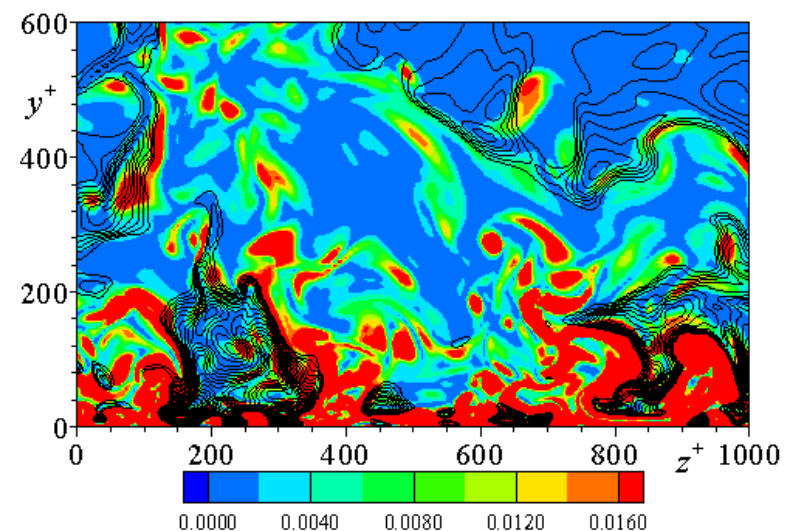
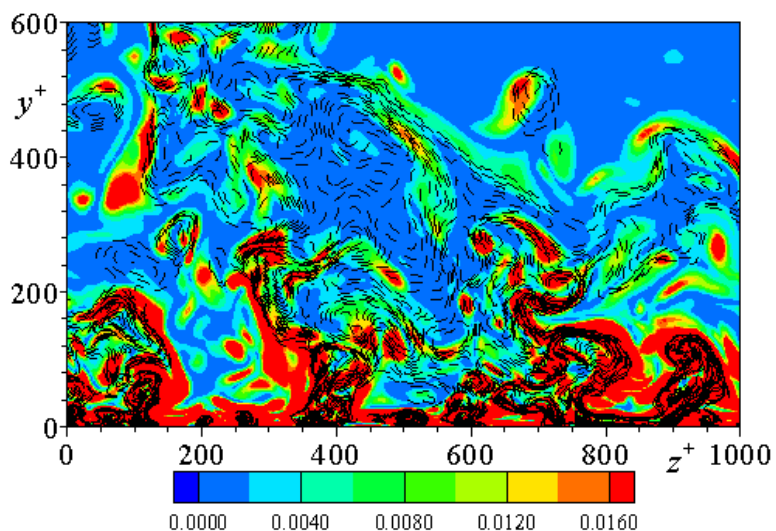
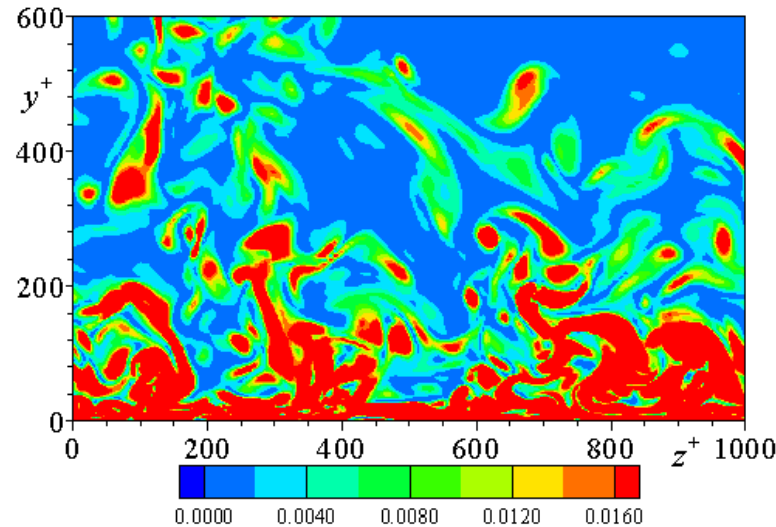
Lines are the instantaneous u_1 .
(solid lines: positive u_1 ; dashed lines: negative u_1)

Instantaneous scalar enstrophy for $\text{Re}_\tau=640$ and $\text{Pr}=0.71$



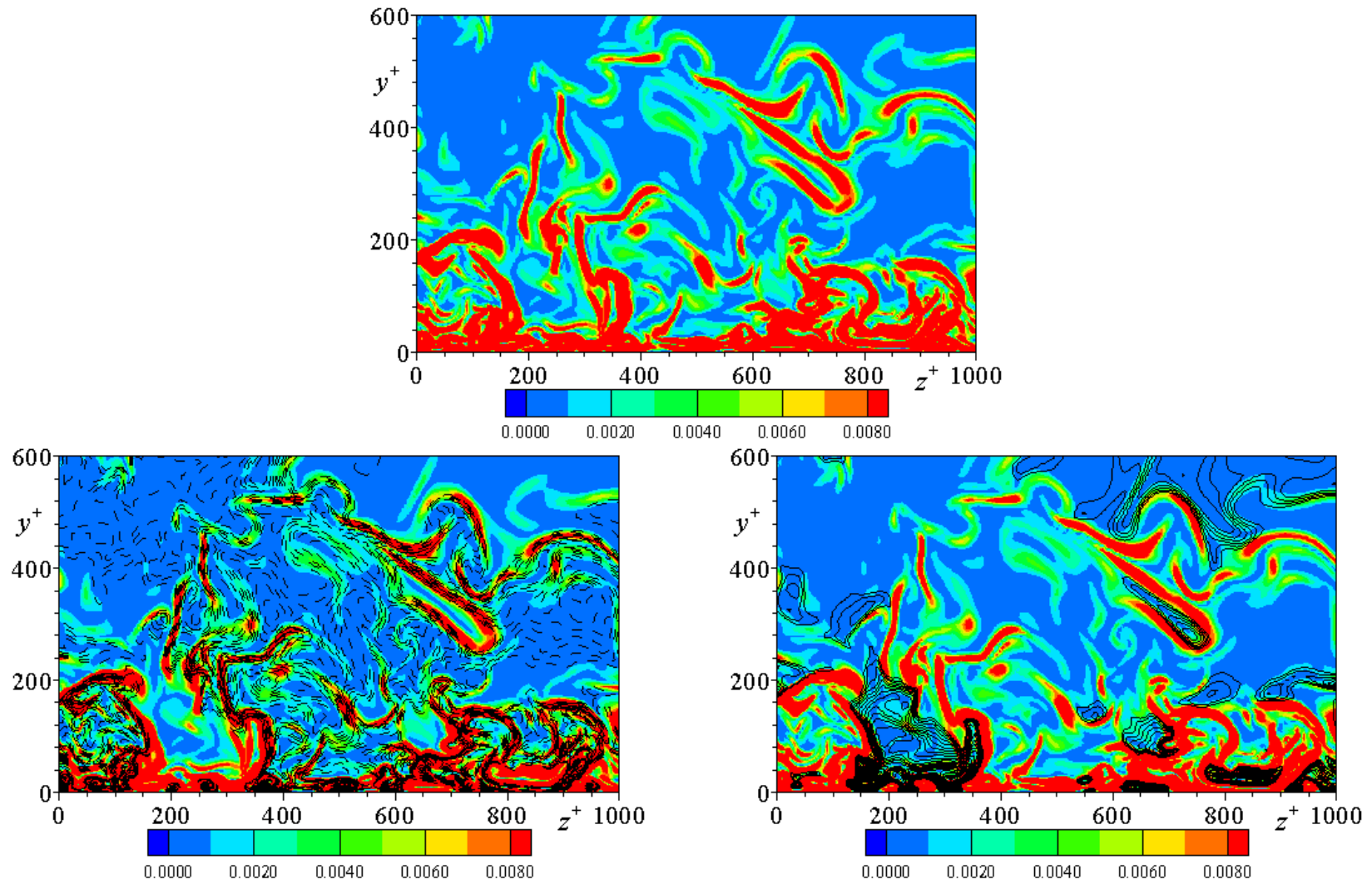
Lines are the instantaneous θ .
(solid lines: positive θ ; dashed lines: negative θ)

Instantaneous enstrophy for $\text{Re}_\tau=640$



Lines are the instantaneous u_1 .
(solid lines: positive u_1 ; dashed lines: negative u_1)

Instantaneous scalar enstrophy for $\text{Re}_\tau=640$ and $\text{Pr}=0.71$



Lines are the instantaneous θ .
(solid lines: positive θ ; dashed lines: negative θ)

The scalar enstrophy tends to exhibit
sheet-like structures away from the wall.

possibly because the scalar gradient is
aligned with the most compressive strain
rate in this flow region.

Eigenvalues and eigenvectors of the strain rate tensor S_{ij}

$$S_{ij} = \frac{1}{2} \left(\frac{\partial u_i}{\partial x_j} + \frac{\partial u_j}{\partial x_i} \right)$$

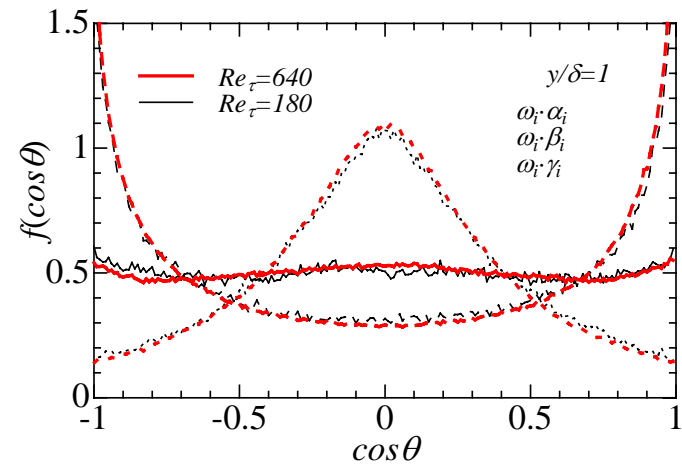
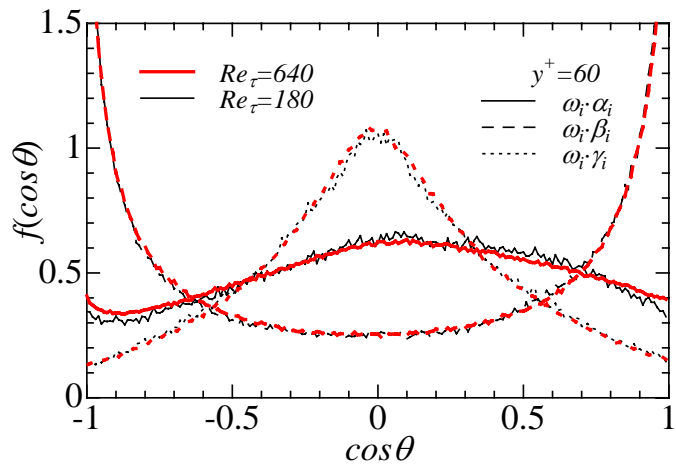
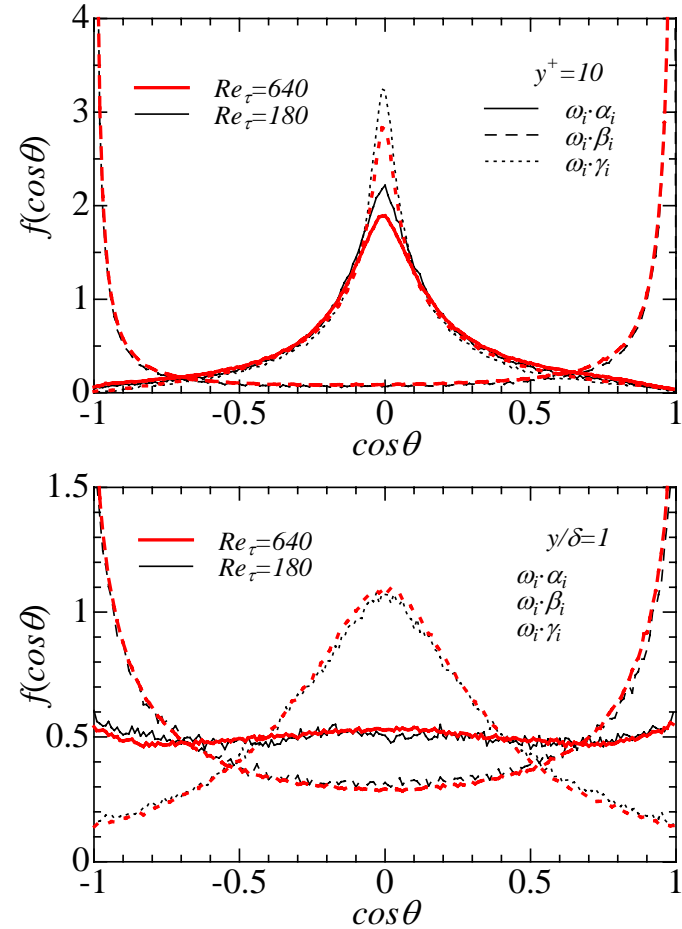
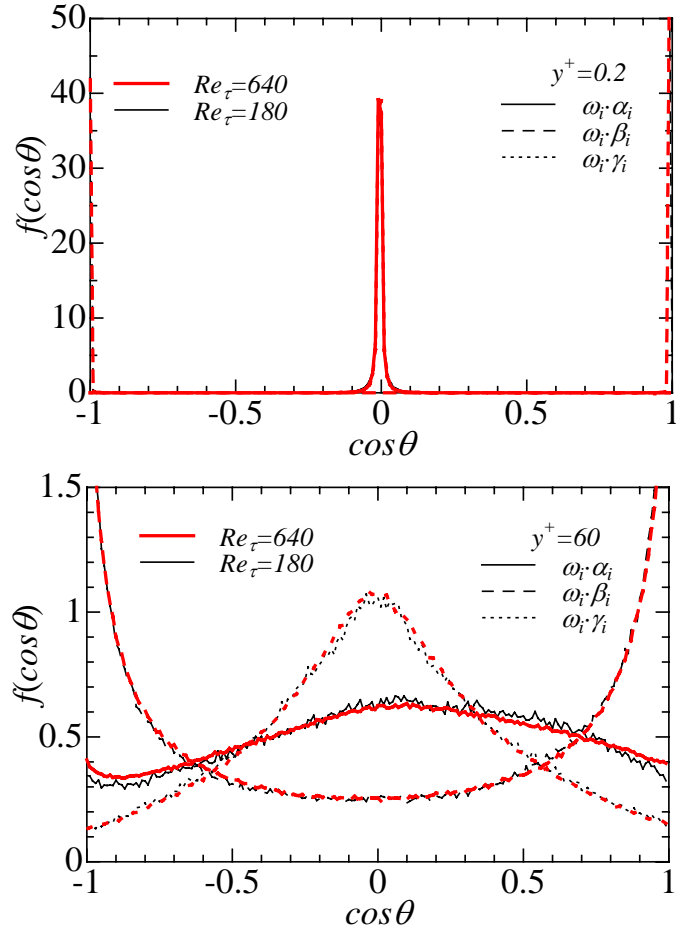
Since S_{ij} is symmetric, its three eigenvalues, α, β, γ , are real and satisfy the following relations

- 1) $\alpha + \beta + \gamma = 0$ (Continuity)
- 2) $\alpha \geq \beta \geq \gamma, \quad \alpha \geq 0 \geq \gamma$

Also, the eigenvectors, $\alpha_i, \beta_i, \gamma_i$, are expressed as follows:

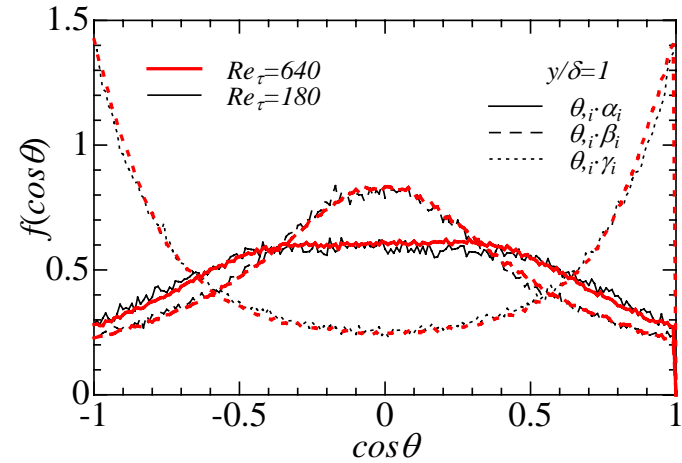
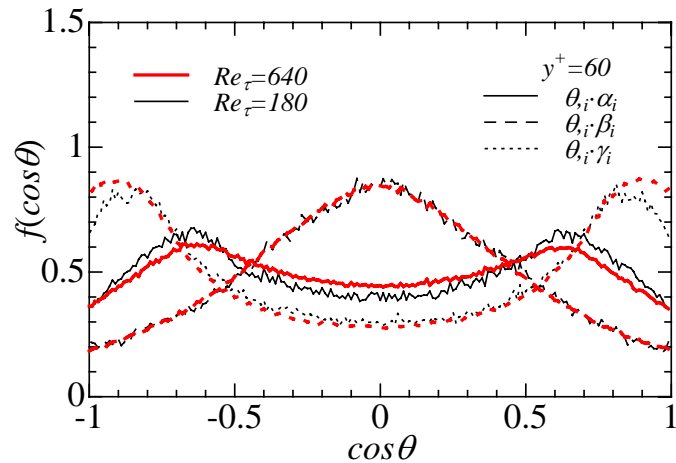
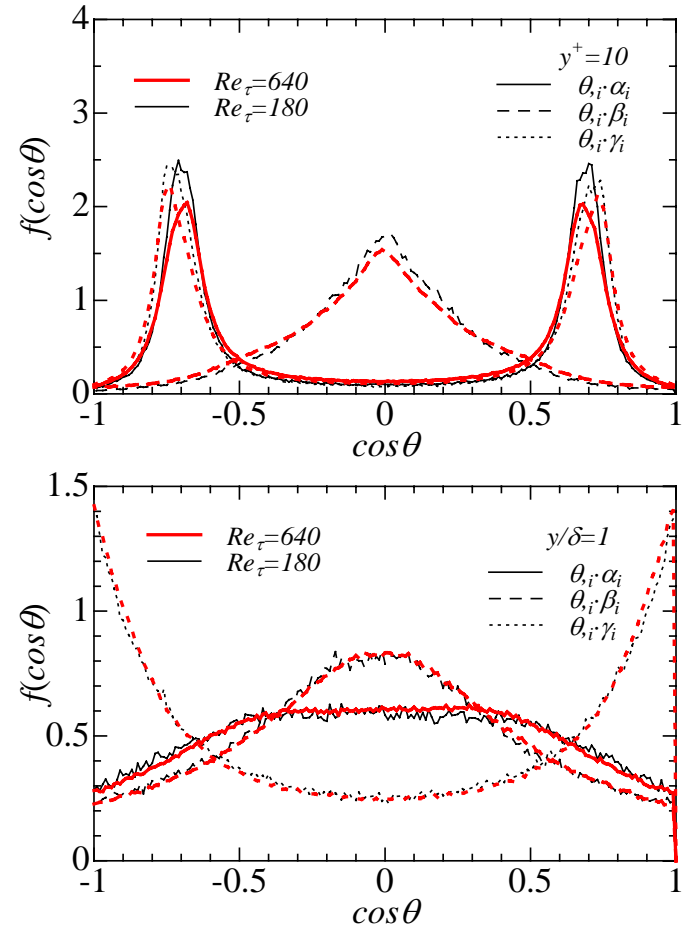
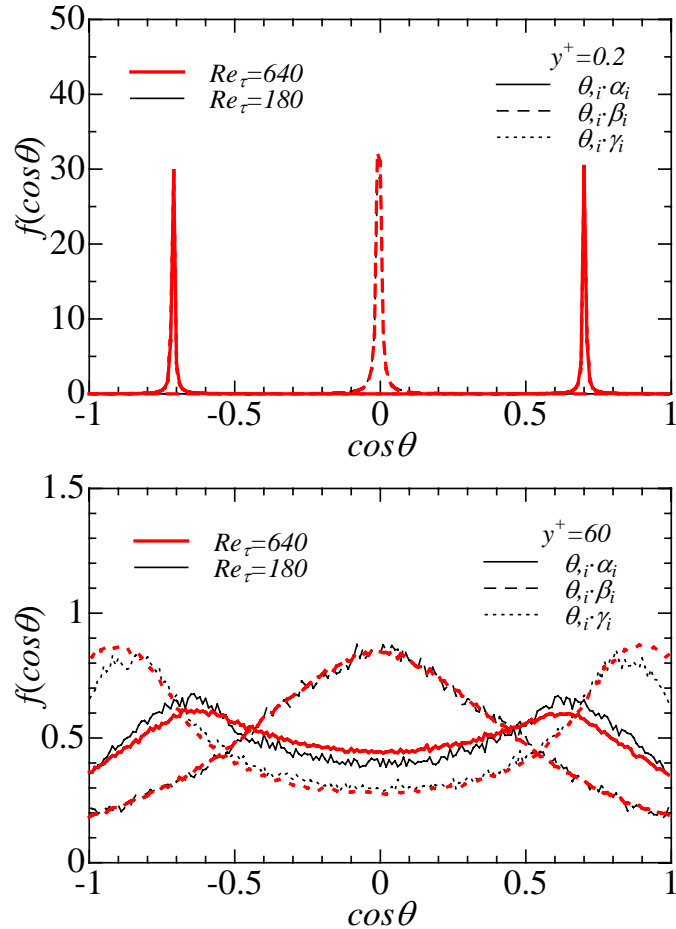
$$P^{-1} \begin{pmatrix} S_{11} & S_{12} & S_{13} \\ S_{21} & S_{22} & S_{23} \\ S_{31} & S_{32} & S_{33} \end{pmatrix} P = \begin{pmatrix} \alpha & 0 & 0 \\ 0 & \beta & 0 \\ 0 & 0 & \gamma \end{pmatrix} \quad (P = \alpha_i \text{ or } \beta_i \text{ or } \gamma_i)$$

Probability density functions for the cosine of the angle between the vorticity and the principal strain rate directions for $Re_\tau=180$ and 640



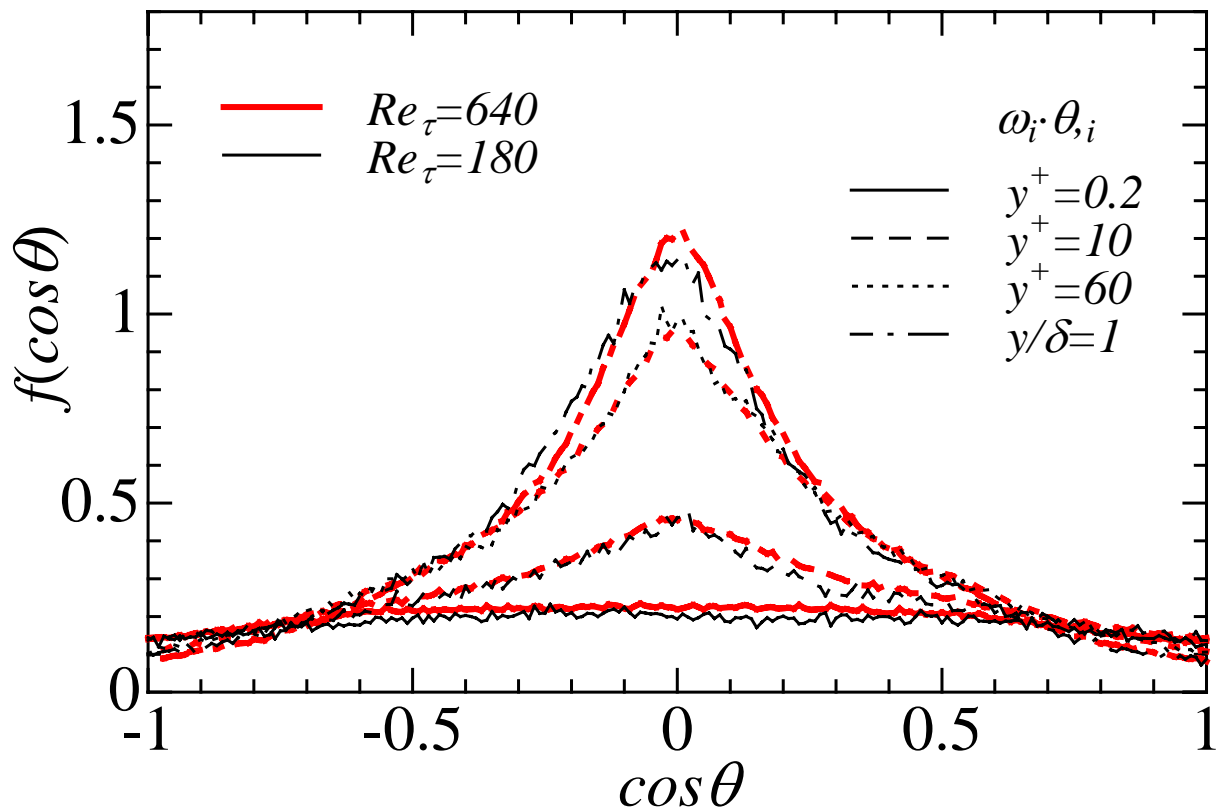
α_i : Extensive eigenvector; β_i : intermediate eigenvector
 γ_i : compressive eigenvector

Probability density functions for the cosine of the angle between the scalar gradient and the principal strain rate directions for $Re_\tau=180$ and 640



α_i : Extensive eigenvector; β_i : intermediate eigenvector
 γ_i : compressive eigenvector

Probability density functions for the cosine of the angle between the vorticity and the scalar gradient for $Re_\tau=180$ and 640



ω_i : vorticity; θ_{i*} : scalar gradient

Summary of the alignment issue

1. Vorticity vector

1) In the near-wall region

α_i, γ_i : 90 degree

β_i : 0 degree

2) Away from the wall

γ_i : 90 degree

β_i : 0 degree

Independent of y
Preferred direction is β_i .

2. Scalar gradient vector

1) In the near-wall region

β_i : 90 degree

α_i, γ_i : 45 degree

Mean gradients affect
the alignment significantly.

In the near-wall region

Preferred directions are
 α_i, γ_i .

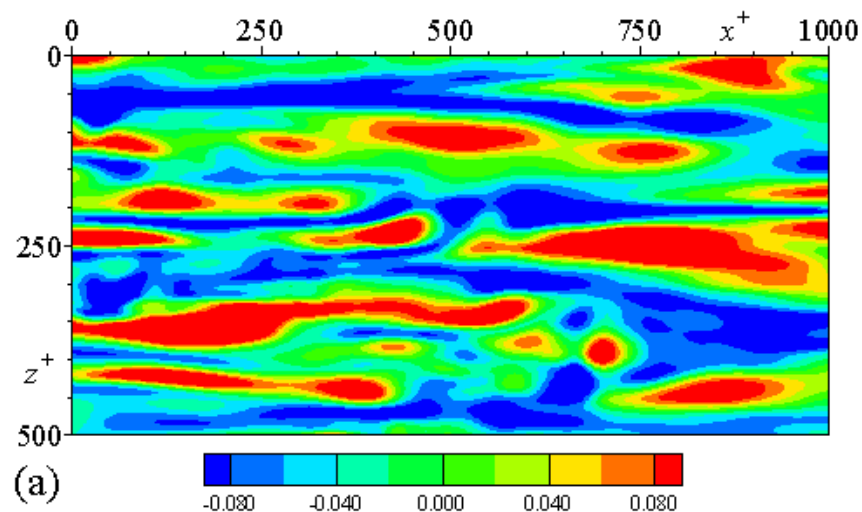
Away from the wall
Preferred direction is γ_i .

β_i : 90 degree
 γ_i : 0 degree

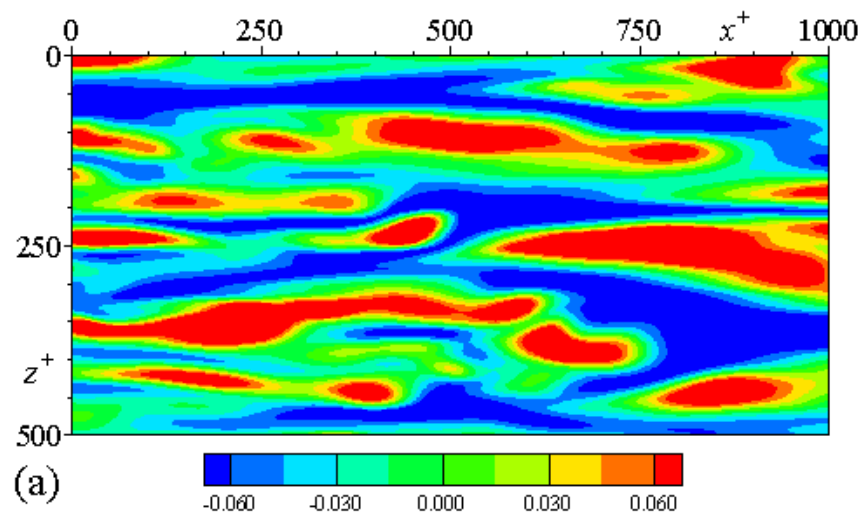
The near-wall similarity between u_1 and θ
is quite high,

but not perfect even at the wall.

Contours of u_1 and θ at $y^+ = 0.2$

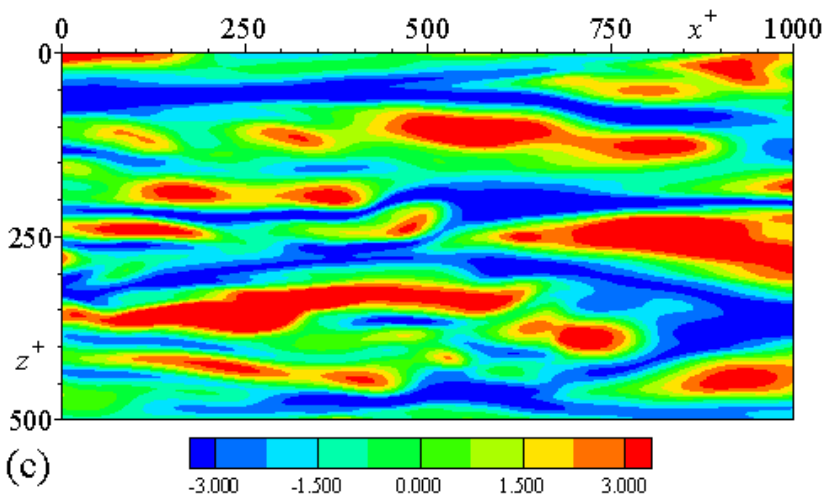


u_1

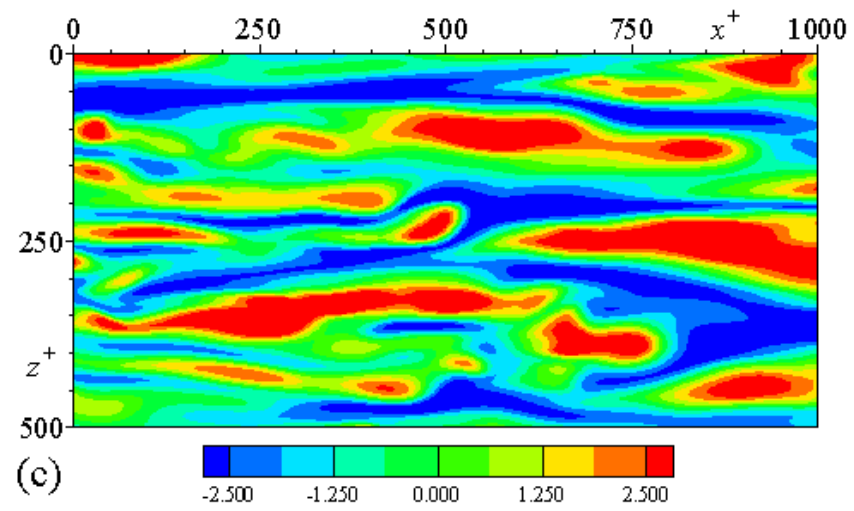


θ

Contours of u_1 and θ at $y^+ = 8$

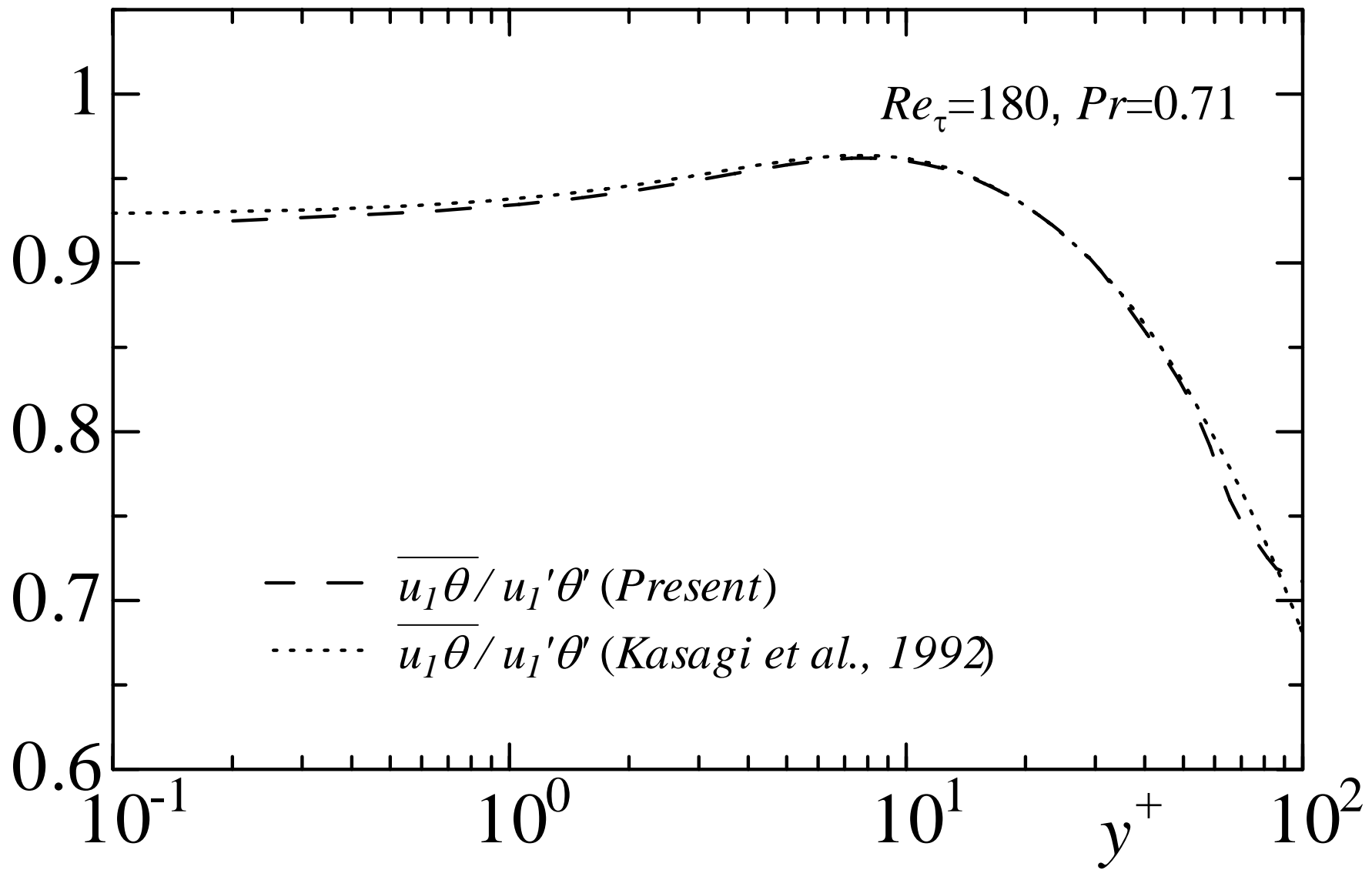


u_1

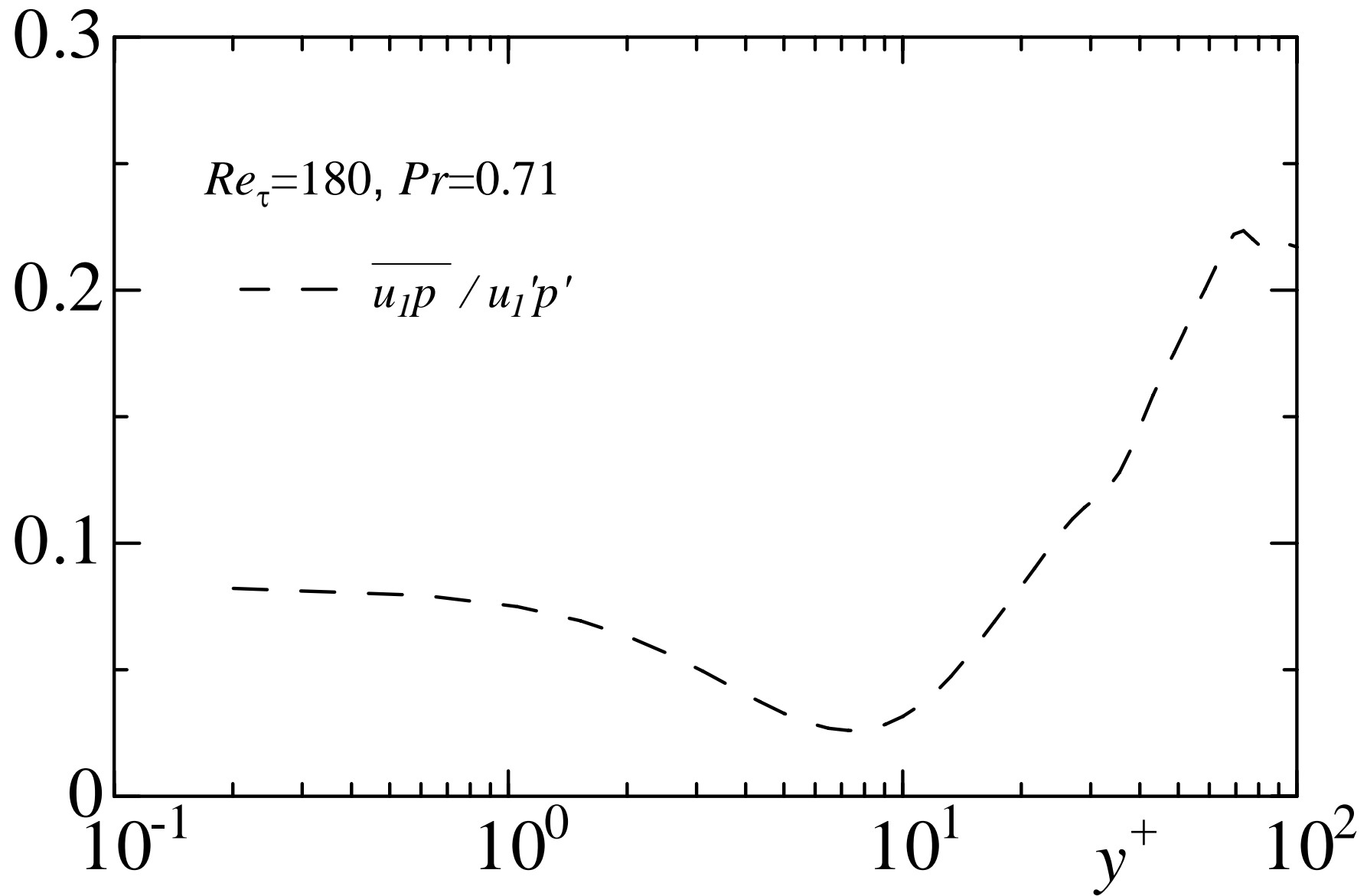


θ

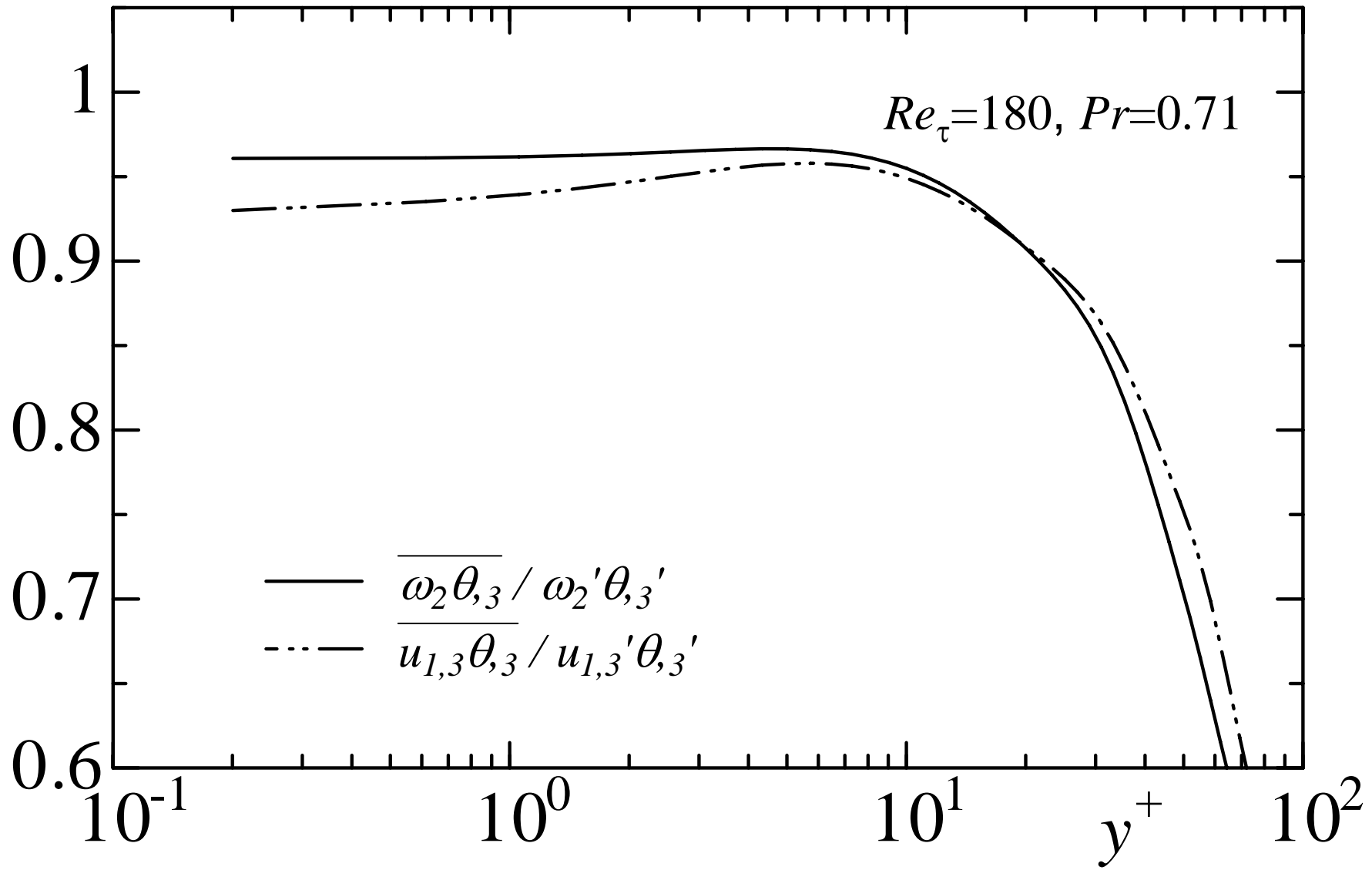
Correlation coefficient between u_1 and θ



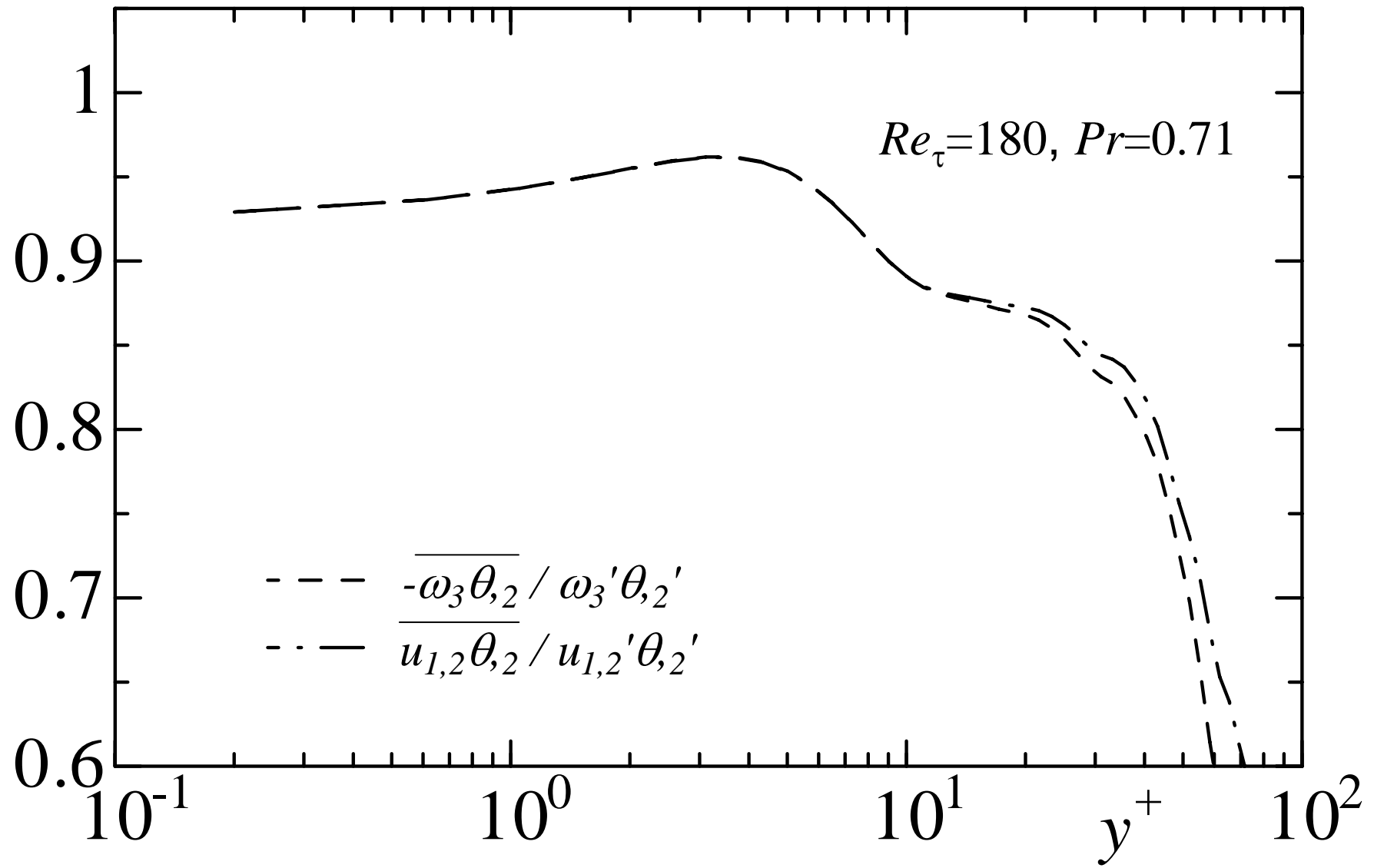
Correlation coefficient between u_1 and p



Correlation coefficients of $\overline{\omega_2 \theta_{,3}}$ and $\overline{u_{1,3} \theta_{,3}}$



Correlation coefficients of $-\overline{\omega_3 \theta_{,2}}$ and $\overline{u_{1,2} \theta_{,2}}$



What causes the imperfect similarity between u_1 and θ ?

Why is the correlation between ω_2 and $\theta_{,3}$
greater than that between u_1 and θ ?

Governing equations

$$\frac{Du_1}{Dt} = -\frac{\partial p}{\partial x_1} + \nu \left(\frac{\partial^2 u_1}{\partial x_i^2} \right)$$

$$\frac{D\theta}{Dt} = a \left(\frac{\partial^2 \theta}{\partial x_i^2} \right)$$

At the wall

$$\frac{\partial^2 u_1}{\partial x_2^2} = (1/\nu) \left(\frac{\partial p}{\partial x_1} \right)$$

$$\frac{\partial^2 \theta}{\partial x_2^2} = 0$$

Taylor series expansions u_1 and θ near the wall

$$u_1^+ = b_1 x_2^+ + c_1 x_2^{+2} + O(x_2^{+3})$$

$$\theta^+ = b_\theta x_2^+ + O(x_2^{+3})$$

$$c_1 x_2^{+2} = (1/2) \left(\partial^2 u_1 / \partial x_2^{+2} \right) x_2^{+2}$$

$$= (1/2\nu) \left(\partial p / \partial x_1 \right) x_2^{+2}$$

Taylor series expansions u_3 near the wall

$$u_3^+ = b_3 x_2^+ + c_3 x_2^{+2} + O(x_2^{+3})$$

$$\begin{aligned} c_3 x_2^{+2} &= \left(1/2\right) \left(\partial^2 u_3 / \partial x_2^{+2}\right) x_2^{+2} \\ &= \left(1/2\nu\right) \left(\partial p / \partial x_3\right) x_2^{+2} \end{aligned}$$

Taylor series expansions ω_2 near the wall

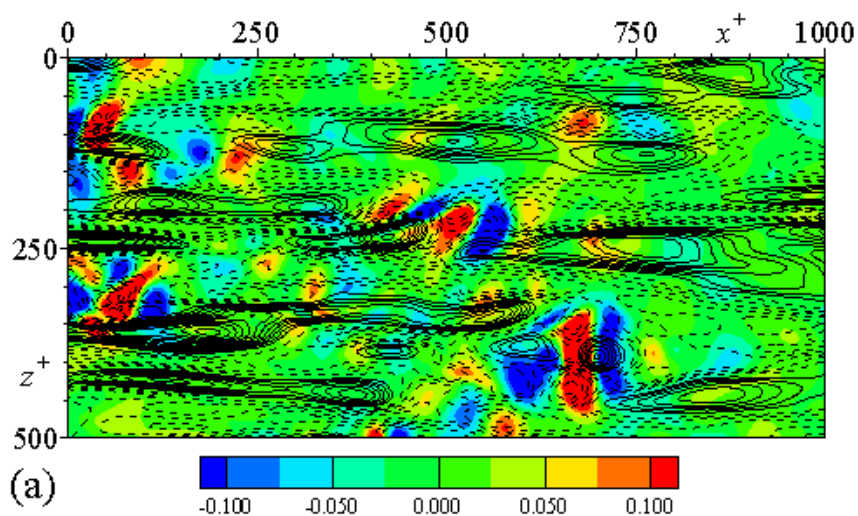
$$\omega_2^+ = u_{1,3}^+ - u_{3,1}^+ = (b_{1,3} - b_{3,1})x_2^+ + O(x_2^{+3})$$

i.e. the x_2^{+2} term has disappeared

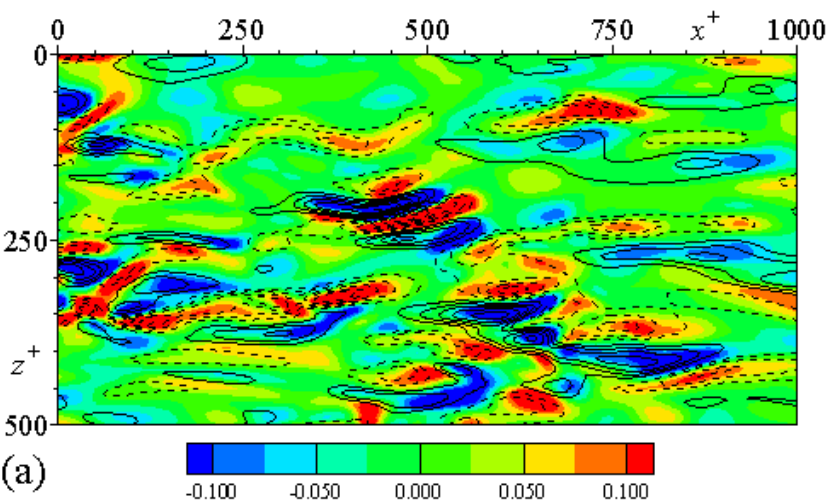
Contours of $p_{,1}$ and u_1

Contours of $p_{,3}$ and u_3

$y^+ = 0.2$

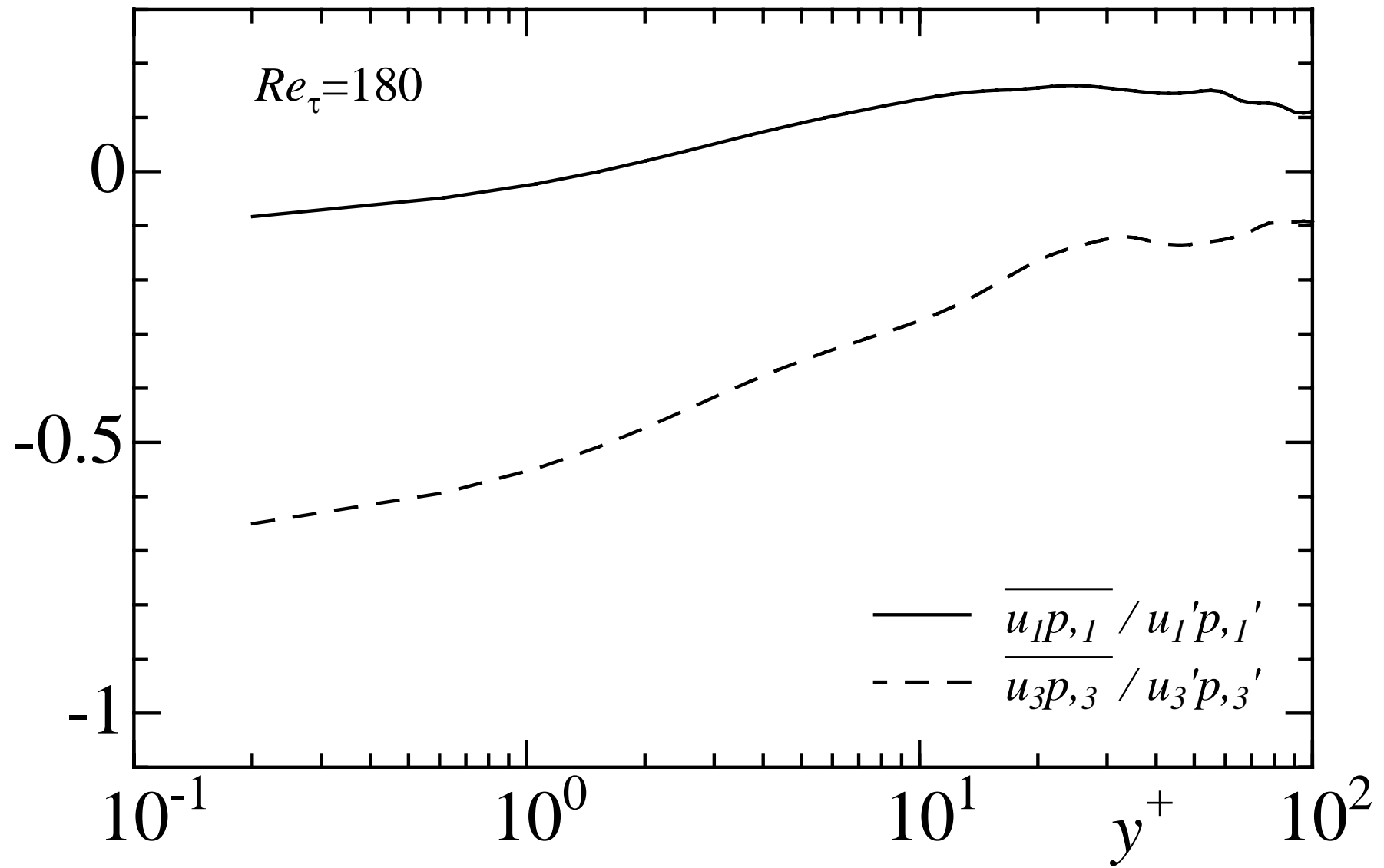


$p_{,1}$ (contour) with u_1 (lines)

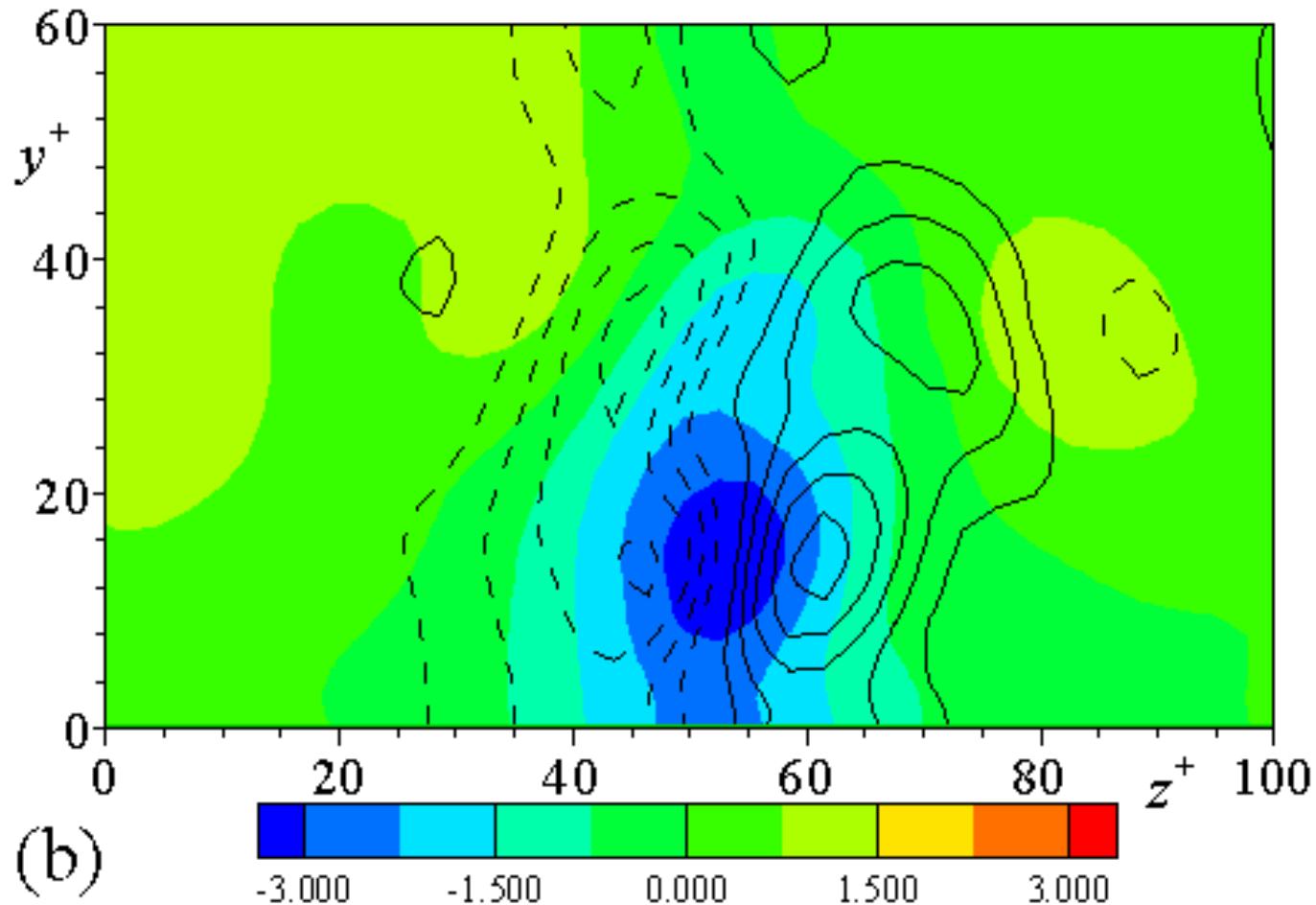


$p_{,3}$ (contour) with u_3 (lines)

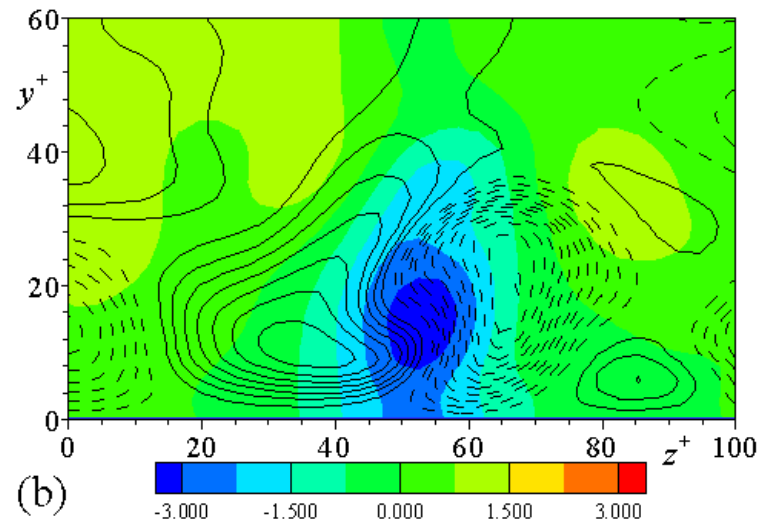
Correlation coefficients of $\overline{u_1 p_{,1}}$ and $\overline{u_3 p_{,3}}$



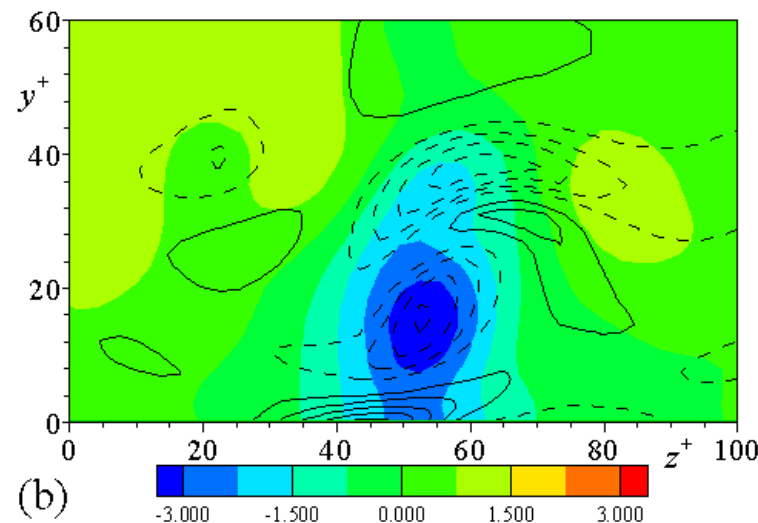
Contours of p (colour) and $p_{,3}$



Contours of p (colour)

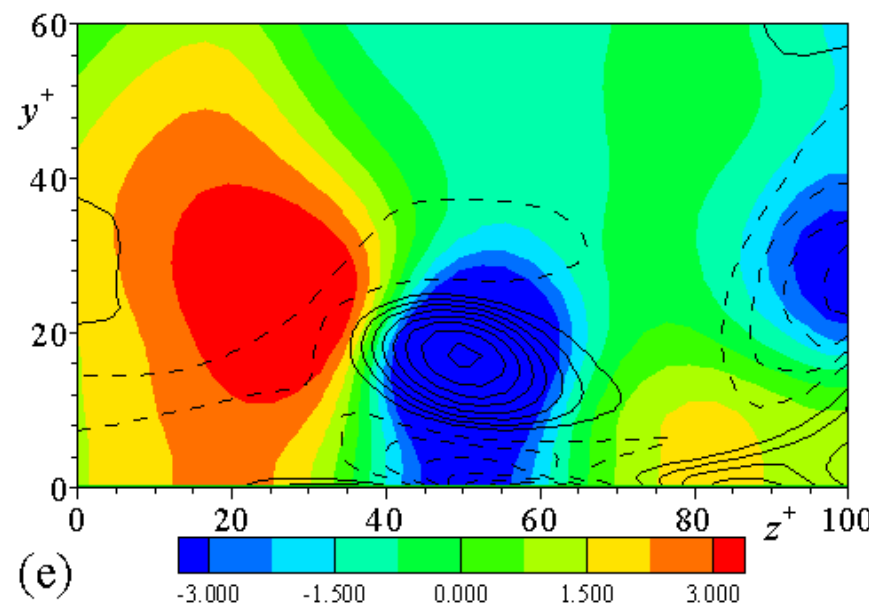
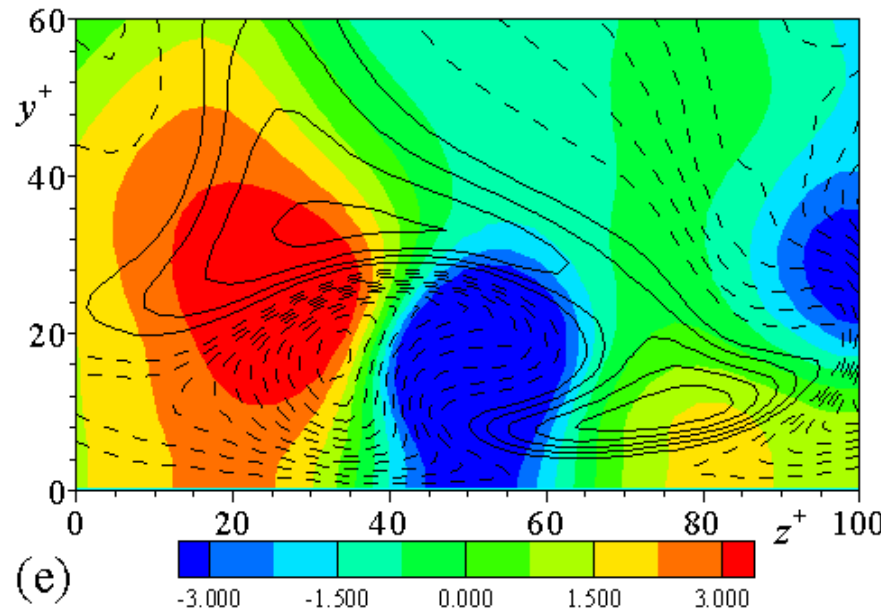


with u_1 (lines)



with ω_1 (lines)

Contours of p (colour) ...but at a larger x^+



Near-wall Taylor series expansion of the correlation coefficients

$$\frac{\overline{\omega_2 \theta_{,3}}}{\omega_2' \theta_{,3}'} = \frac{y^{+2} \left(\left(\overline{b_{1,3} b_{\theta,3}} - \overline{b_{3,1} b_{\theta,3}} \right) + O(y^{+2}) \right)}{y^{+2} \sqrt{(b_{1,3} - b_{3,1})^2} \sqrt{\overline{b_{\theta,3}^2}} \left(1 + O(y^{+2}) \right)} = \frac{\left(\overline{b_{1,3} b_{\theta,3}} - \overline{b_{3,1} b_{\theta,3}} \right)}{\sqrt{(b_{1,3} - b_{3,1})^2} \sqrt{\overline{b_{\theta,3}^2}}} + O(y^{+2})$$

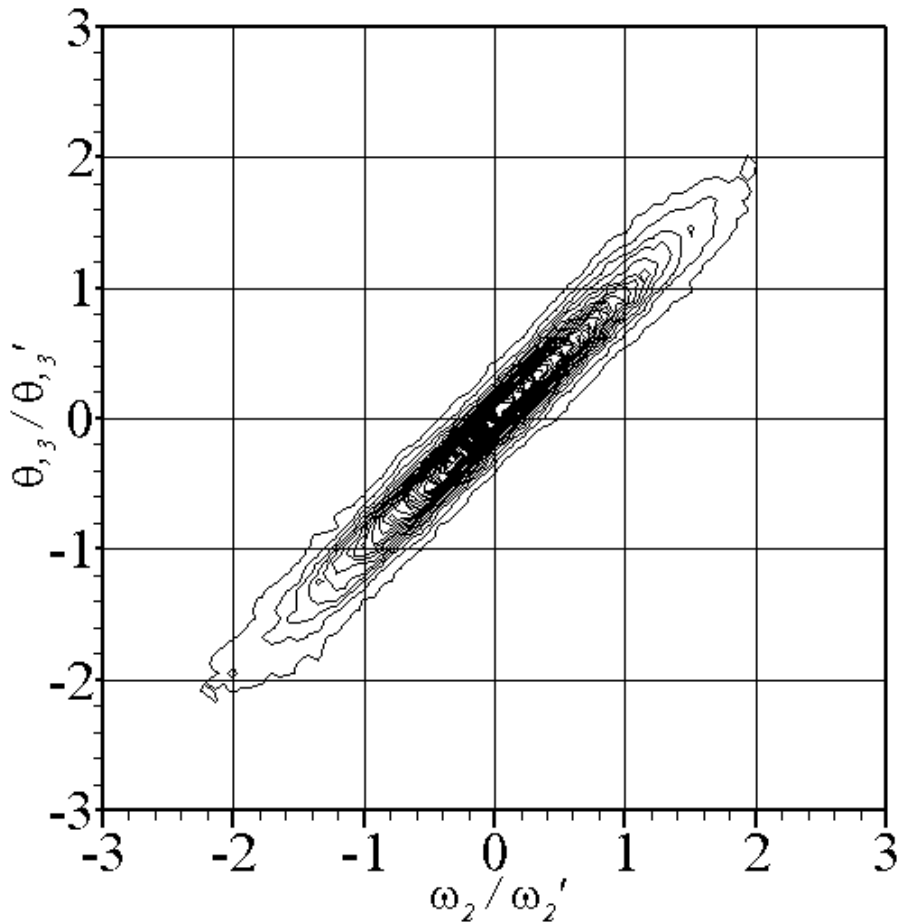
$$\begin{aligned} \frac{\overline{\omega_3 \theta_{,2}}}{\omega_3' \theta_{,2}'} &= \frac{- \left(\overline{b_1 b_\theta} + 2 \overline{c_1 b_\theta} y^+ + O(y^{+2}) \right)}{\sqrt{\overline{b_1^2}} \sqrt{\overline{b_\theta^2}} \left(1 + 2 \frac{\overline{b_1 c_1}}{\overline{b_1^2}} y^+ + O(y^{+2}) \right)} \\ &= \frac{-1}{\sqrt{\overline{b_1^2}} \sqrt{\overline{b_\theta^2}}} \left(\overline{b_1 b_\theta} + 2 \overline{c_1 b_\theta} y^+ + O(y^{+2}) \right) \cdot \left(1 - 2 \frac{\overline{b_1 c_1}}{\overline{b_1^2}} y^+ + O(y^{+2}) \right) \\ &= \frac{-1}{\sqrt{\overline{b_1^2}} \sqrt{\overline{b_\theta^2}}} \left(\overline{b_1 b_\theta} + 2 \left(\overline{c_1 b_\theta} - \frac{\overline{b_1 c_1}}{\overline{b_1^2}} \overline{b_1 b_\theta} \right) y^+ \right) + O(y^{+2}) \end{aligned}$$

Near-wall Taylor series expansion of the correlation coefficients

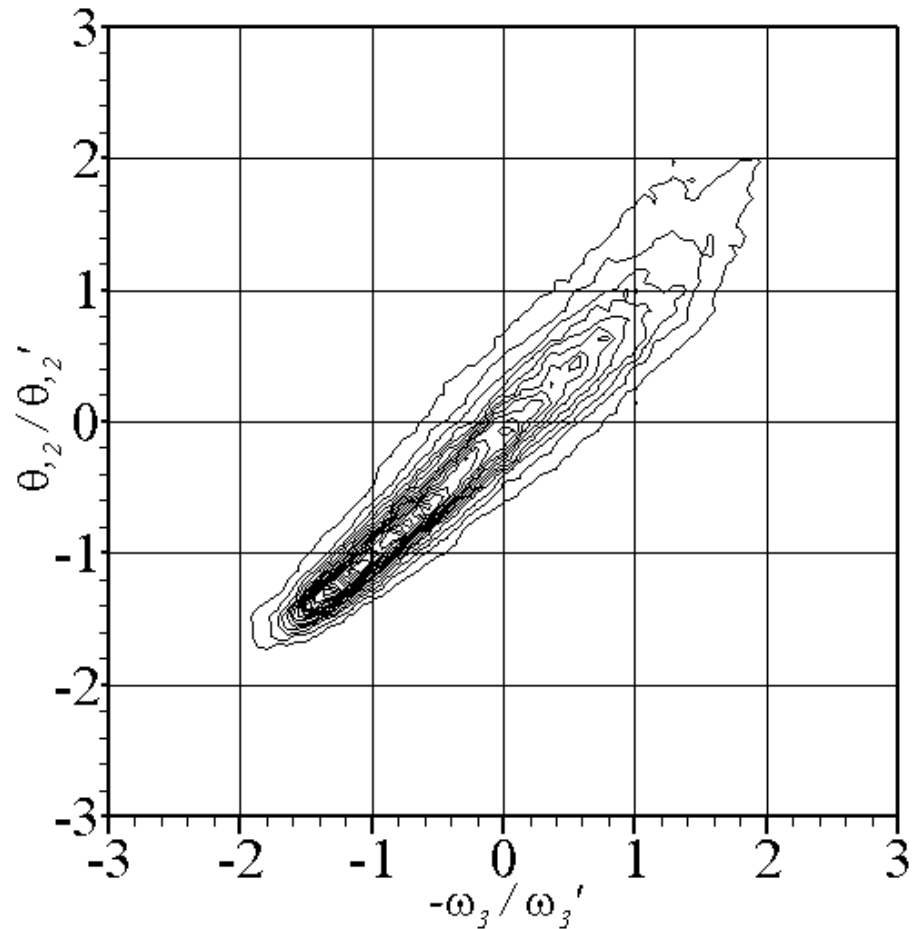
$$\begin{aligned}
 \frac{\overline{u_1\theta}}{u_1'\theta'} &= \frac{y^{+2} \left(\overline{b_1 b_\theta} + \overline{c_1 b_\theta} y^+ + O(y^{+2}) \right)}{y^{+2} \sqrt{\overline{b_1^2}} \sqrt{\overline{b_\theta^2}} \left(1 + \frac{\overline{b_1 c_1}}{\overline{b_1^2}} y^+ + O(y^{+2}) \right)} \\
 &= \frac{1}{\sqrt{\overline{b_1^2}} \sqrt{\overline{b_\theta^2}}} \left(\overline{b_1 b_\theta} + \overline{c_1 b_\theta} y^+ + O(y^{+2}) \right) \cdot \left(1 - \frac{\overline{b_1 c_1}}{\overline{b_1^2}} y^+ + O(y^{+2}) \right) \\
 &= \frac{1}{\sqrt{\overline{b_1^2}} \sqrt{\overline{b_\theta^2}}} \left(\overline{b_1 b_\theta} + \left(\overline{c_1 b_\theta} - \frac{\overline{b_1 c_1}}{\overline{b_1^2}} \overline{b_1 b_\theta} \right) y^+ \right) + O(y^{+2})
 \end{aligned}$$

Joint pdfs between ω_i and $\theta_{,j}$ at $y^+ = 8$

$i = 2 \quad j = 3$

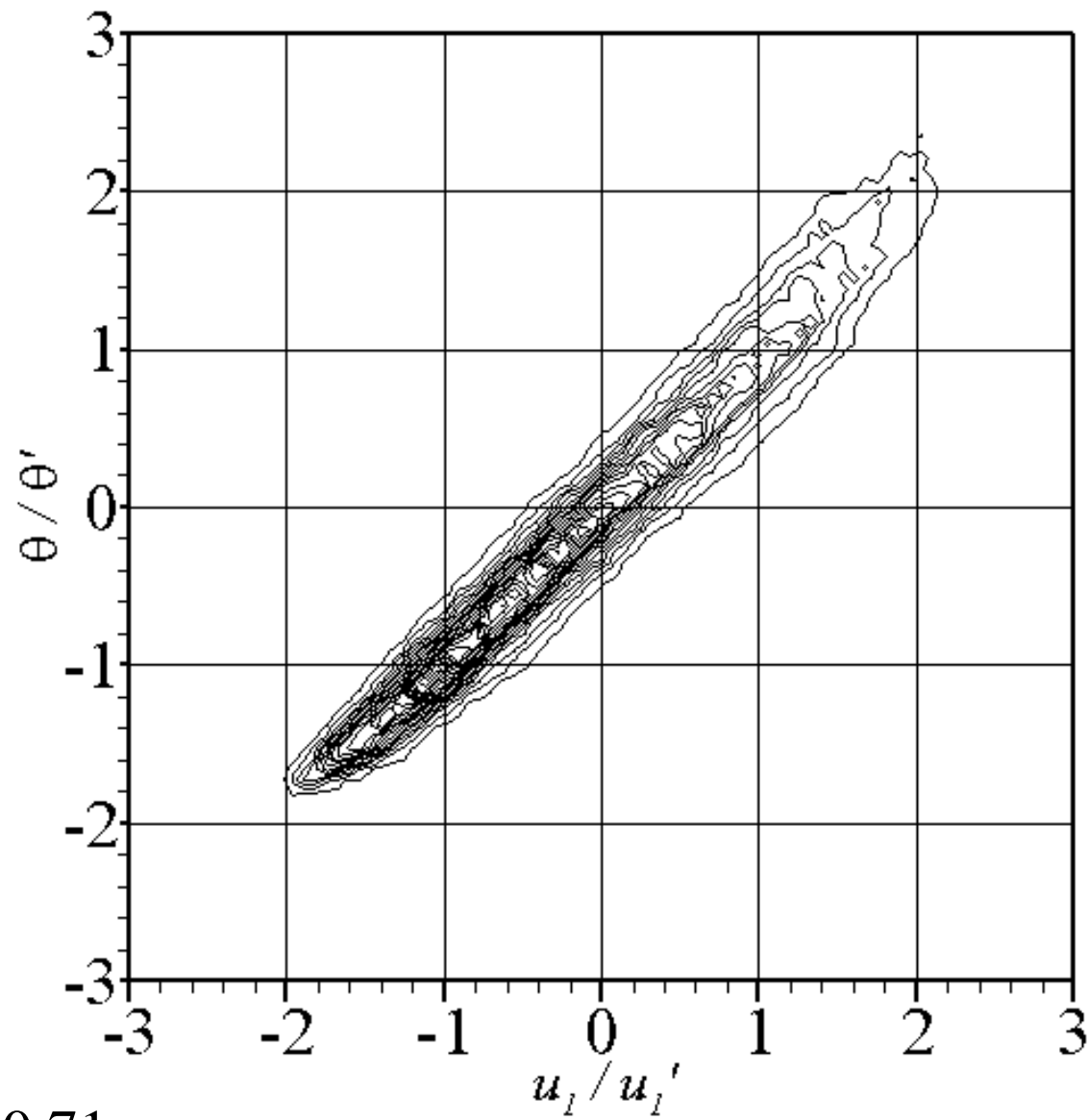


$i = 3 \quad j = 2$



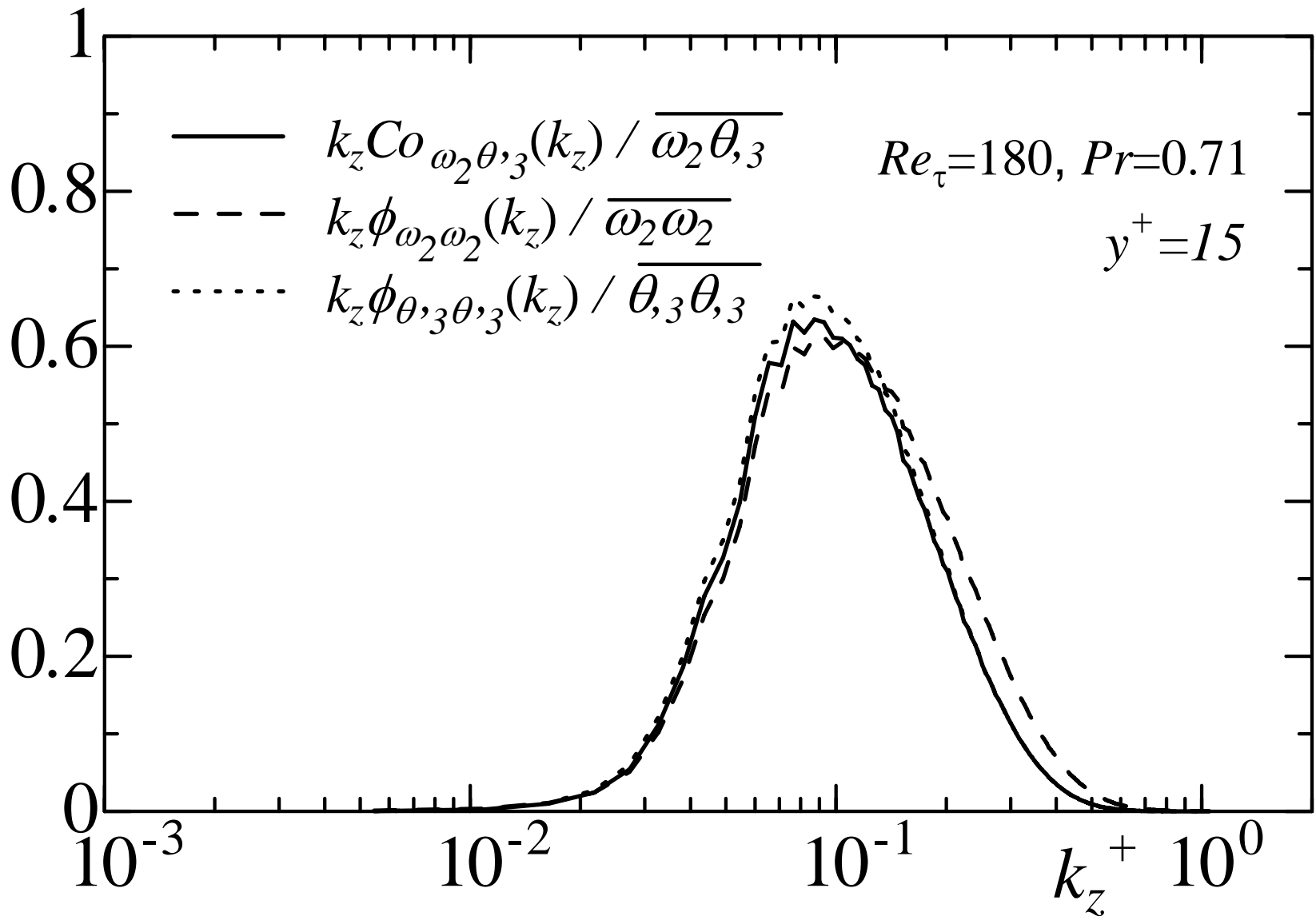
$Re_\tau = 180, Pr = 0.71$

Joint pdf of u_1 and θ at $y^+ = 8$

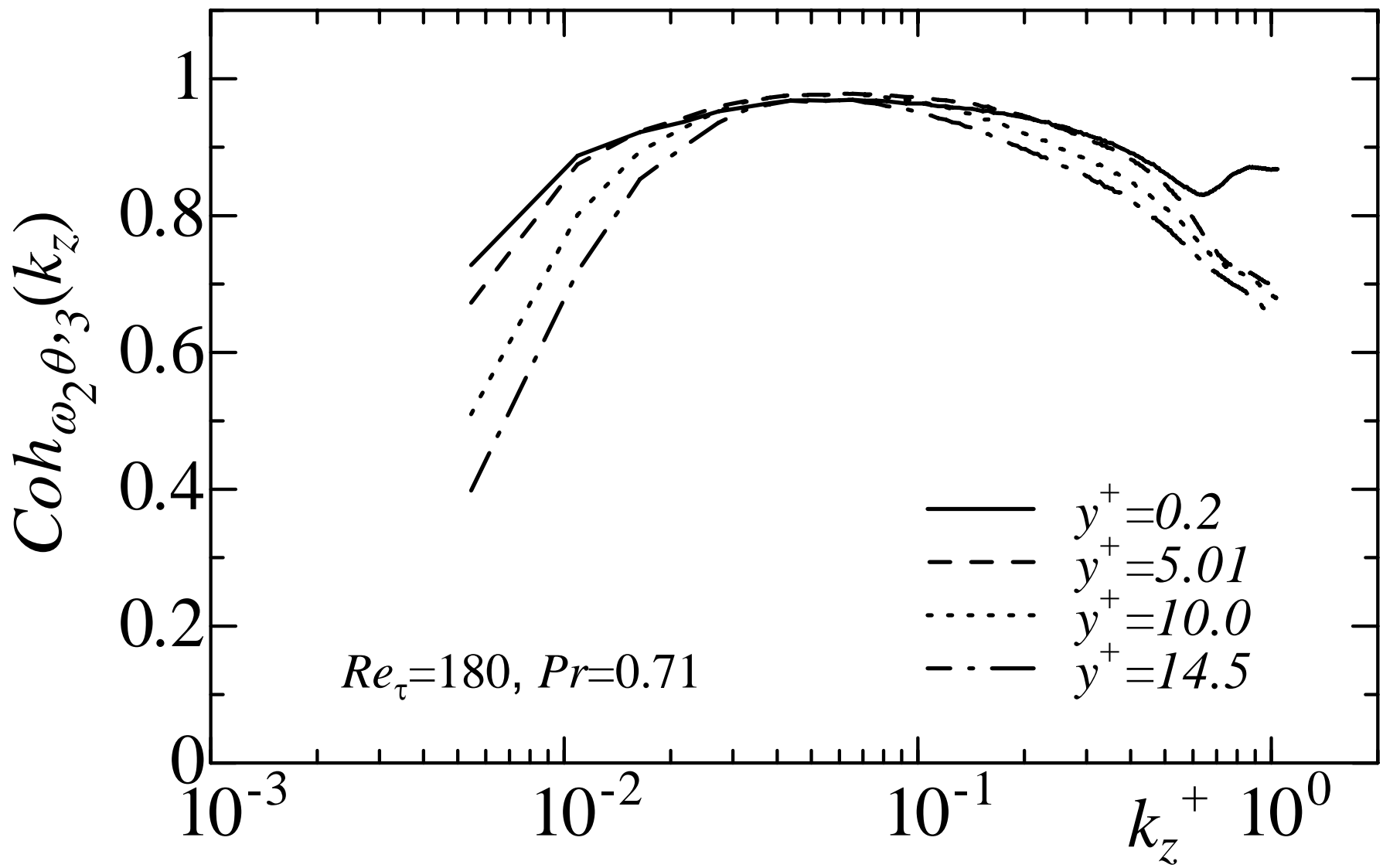


$Re_\tau = 180, Pr = 0.71$

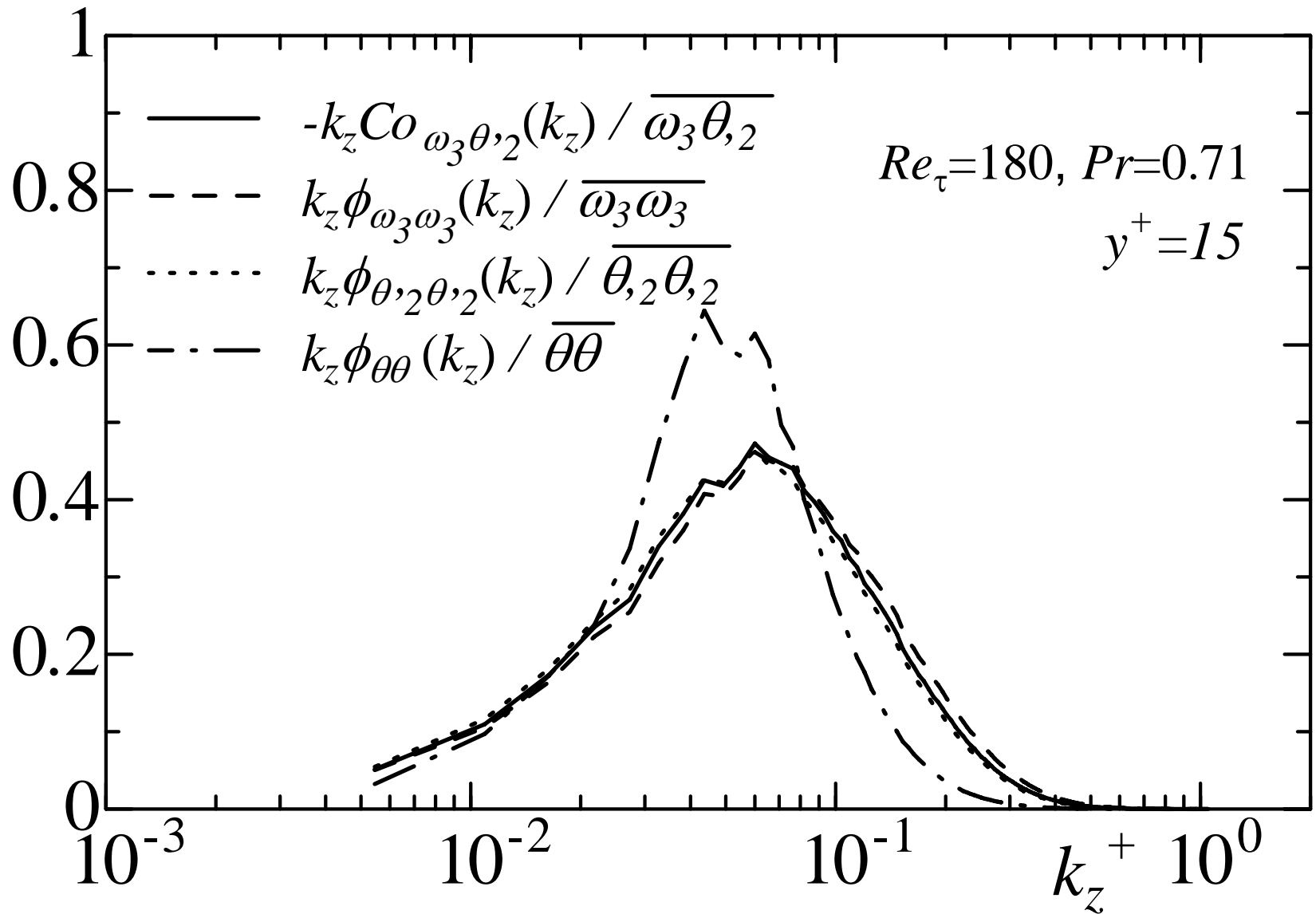
Spanwise co-spectra of ω_2 and $\theta_{,3}$ compared with spanwise spectra of ω_2 and $\theta_{,3}$



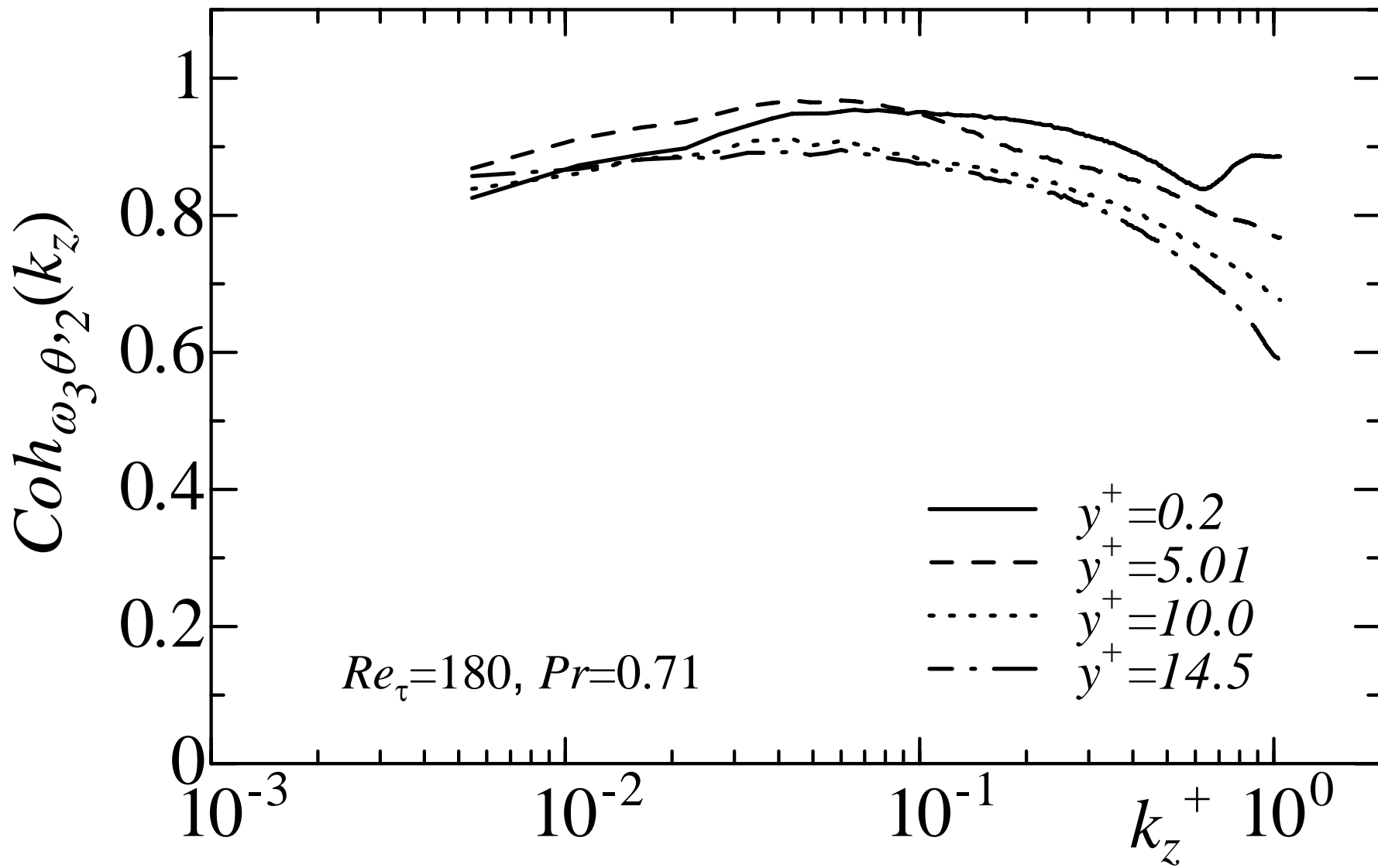
Spanwise spectral coherence of ω_2 and $\theta_{,3}$

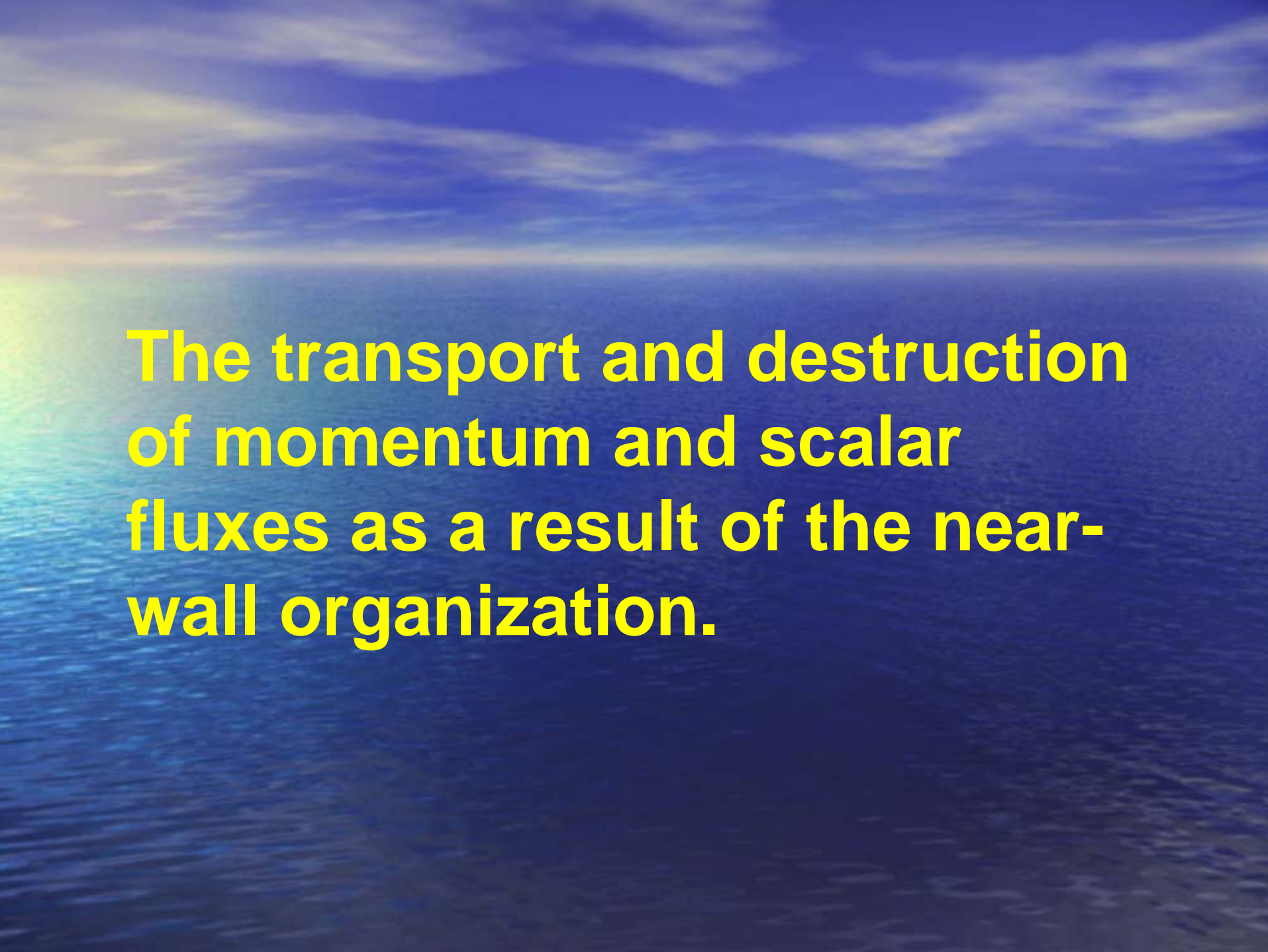


Spanwise co-spectra of ω_3 and $\theta_{,2}$ compared with spanwise spectra of ω_3 and $\theta_{,2}$



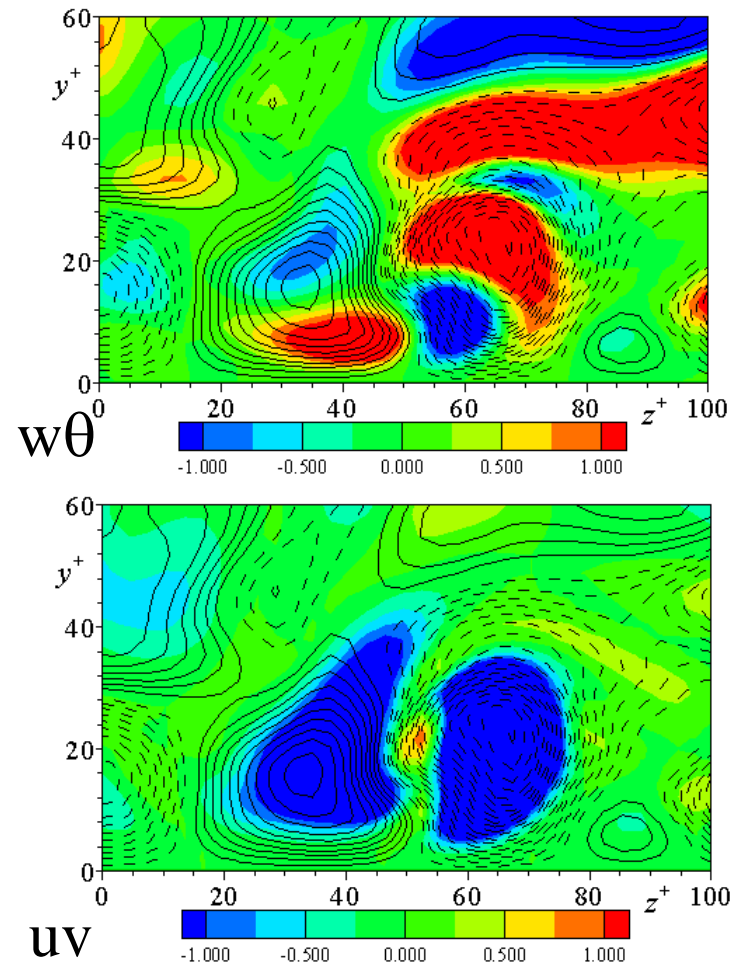
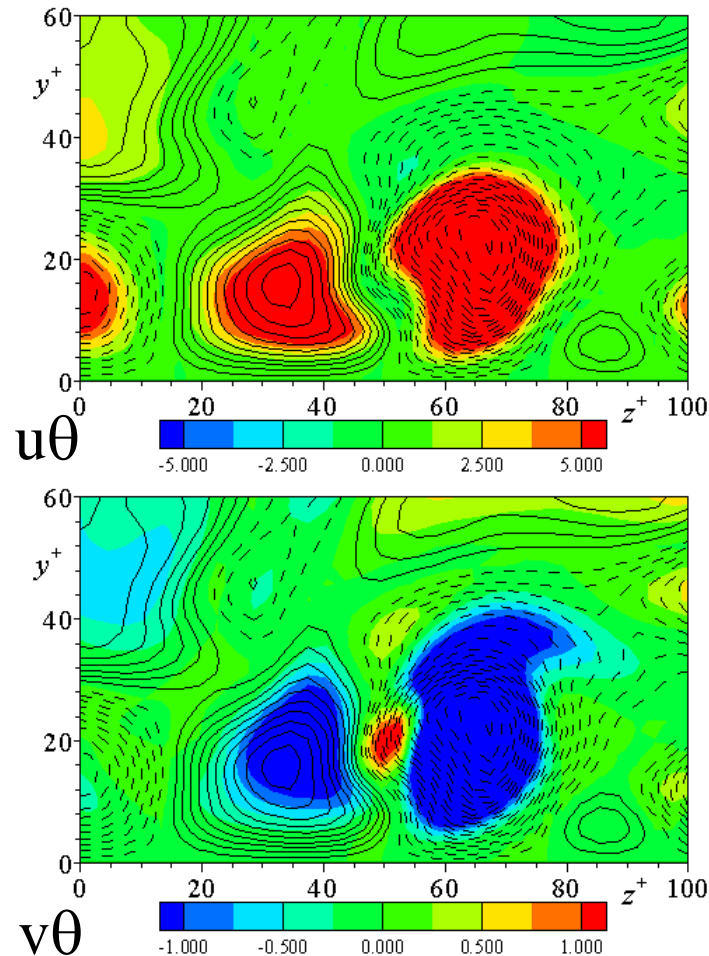
Spanwise spectral coherence of ω_3 and θ_2



The background of the slide features a wide-angle photograph of a calm sea meeting a blue sky filled with wispy, white clouds. The horizon line is visible in the distance.

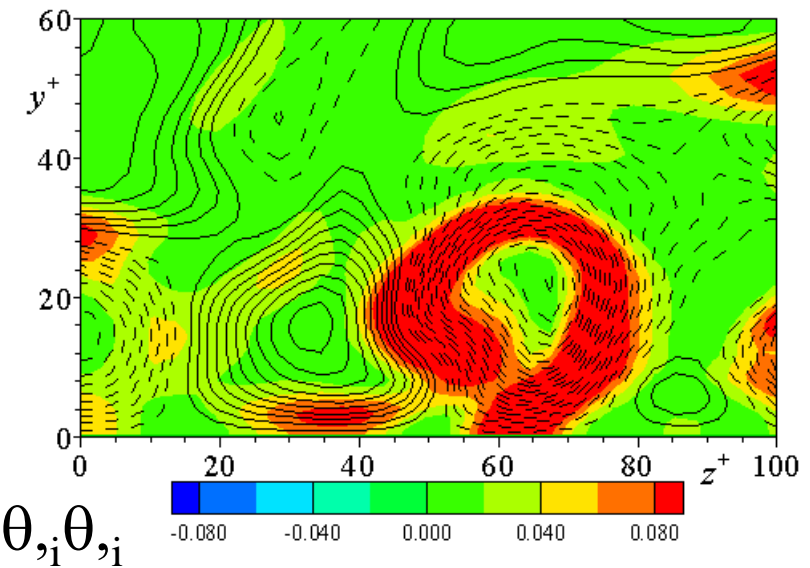
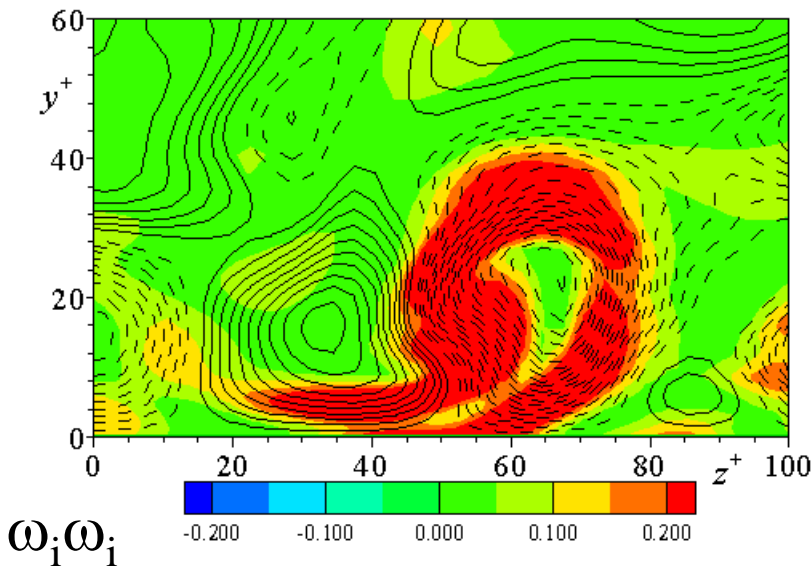
**The transport and destruction
of momentum and scalar
fluxes as a result of the near-
wall organization.**

Contours of instantaneous turbulent heat-fluxes for $\text{Re}_\tau=180$ and $\text{Pr}=0.71$



Color contours are the instantaneous $u_i\theta$ or uv , while lines are the instantaneous θ .
Solid and dashed lines are positive and negative values.

Contours of instantaneous enstrophy and scalar enstrophy for $\text{Re}_\tau=180$ and $\text{Pr}=0.71$



Colour contours are the instantaneous $\omega_i \omega_i$ or $\theta_i \theta_i$, while lines are the instantaneous θ . Solid and dashed lines are positive and negative values.

$$\mathcal{E}/\nu \equiv u_{i,j}u_{j,i} + \omega_i\omega_i$$

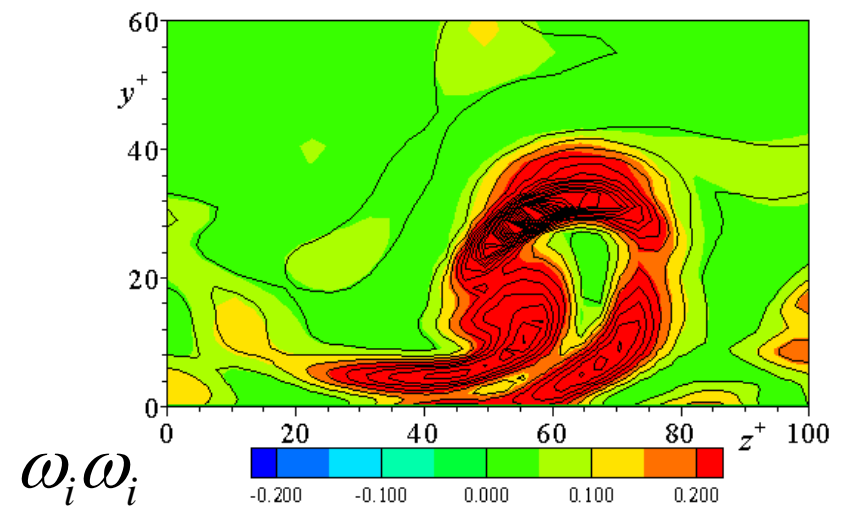
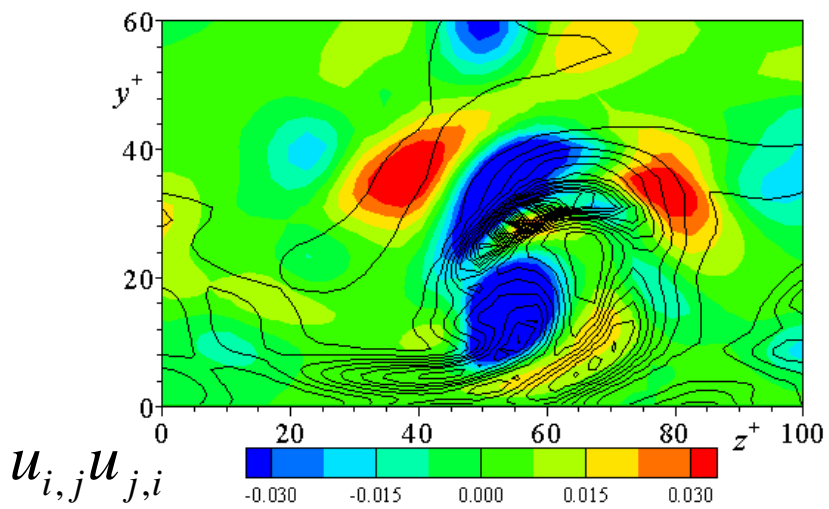
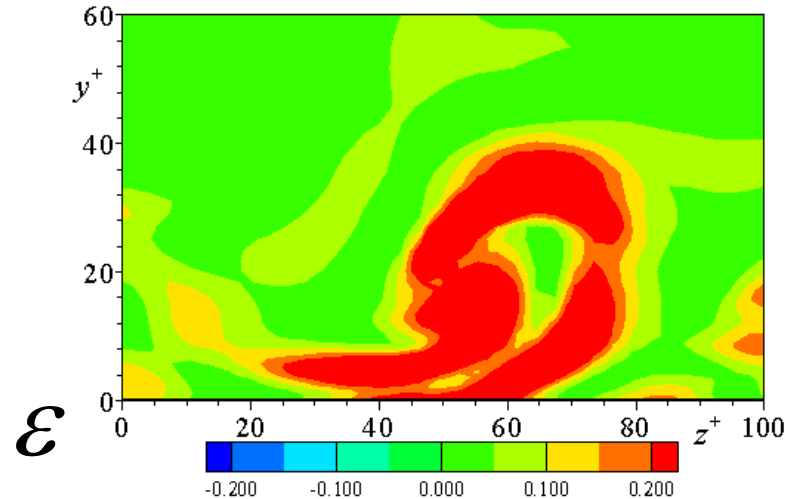
\mathcal{E} : Dissipation

$u_{i,j}$: Deformation tensor

$u_{i,j}u_{j,i}$: Second invariant of the tensor

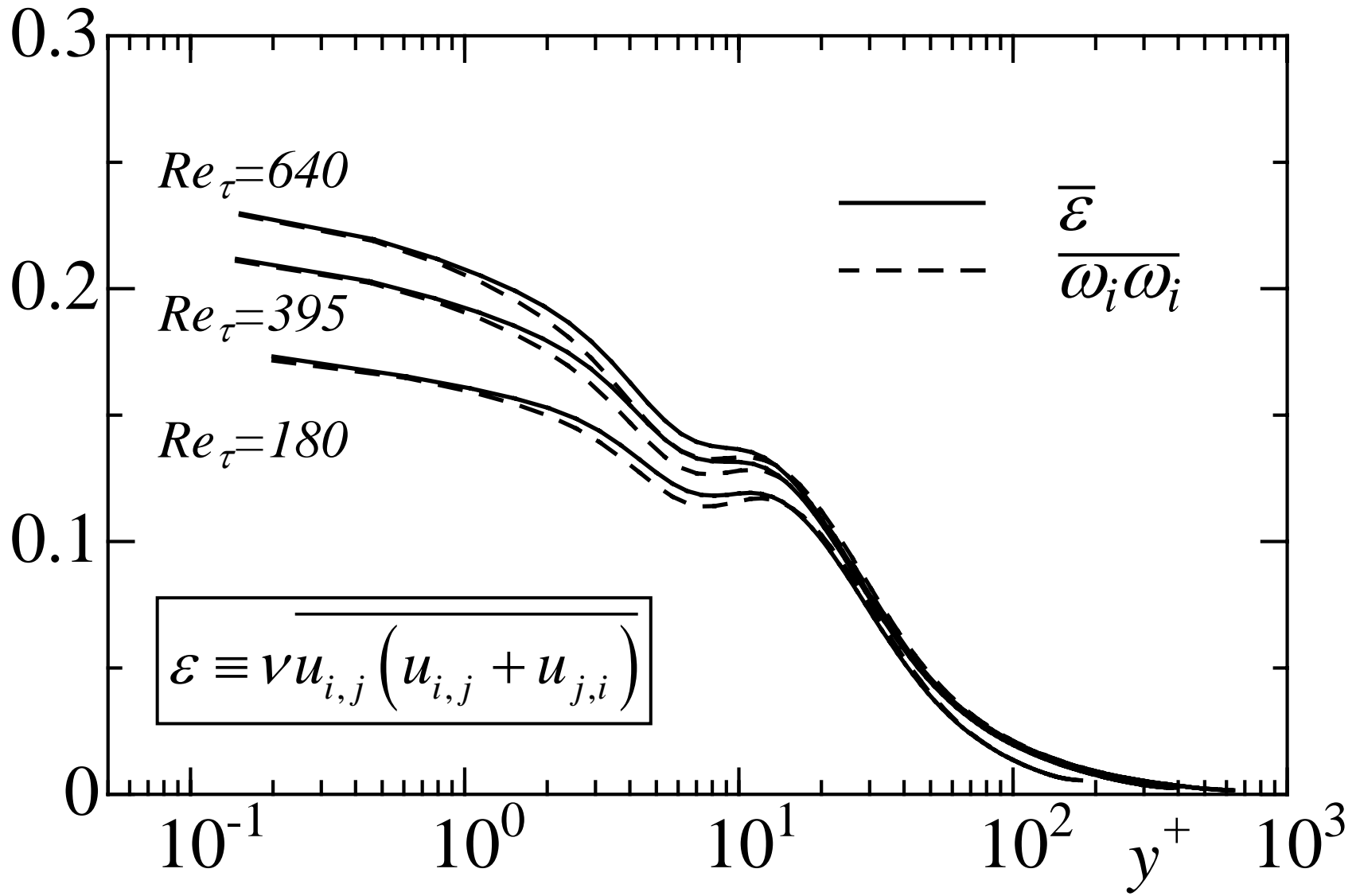
$\omega_i\omega_i$: Enstrophy

Instantaneous \mathcal{E} , $u_{i,j}u_{j,i}$, $\omega_i\omega_i$ for $\text{Re}_\tau=180$

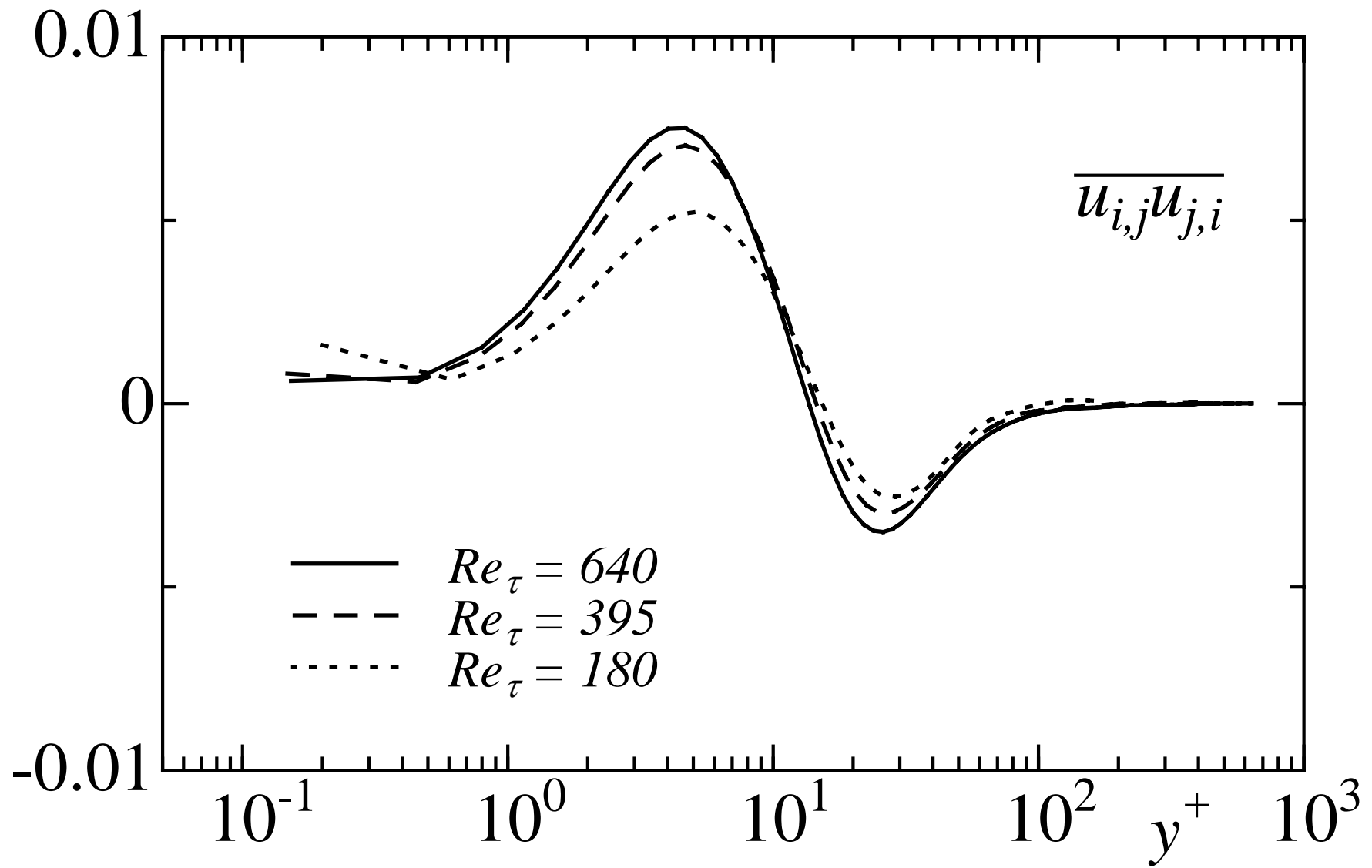


Lines are the instantaneous ε .

$\bar{\varepsilon}$ and $\overline{\omega_i \omega_i}$ normalized by wall units



$\overline{u_{i,j}u_{j,i}}$ normalized by wall units



$$\nabla^2 p \equiv -u_{i,j}u_{j,i}$$

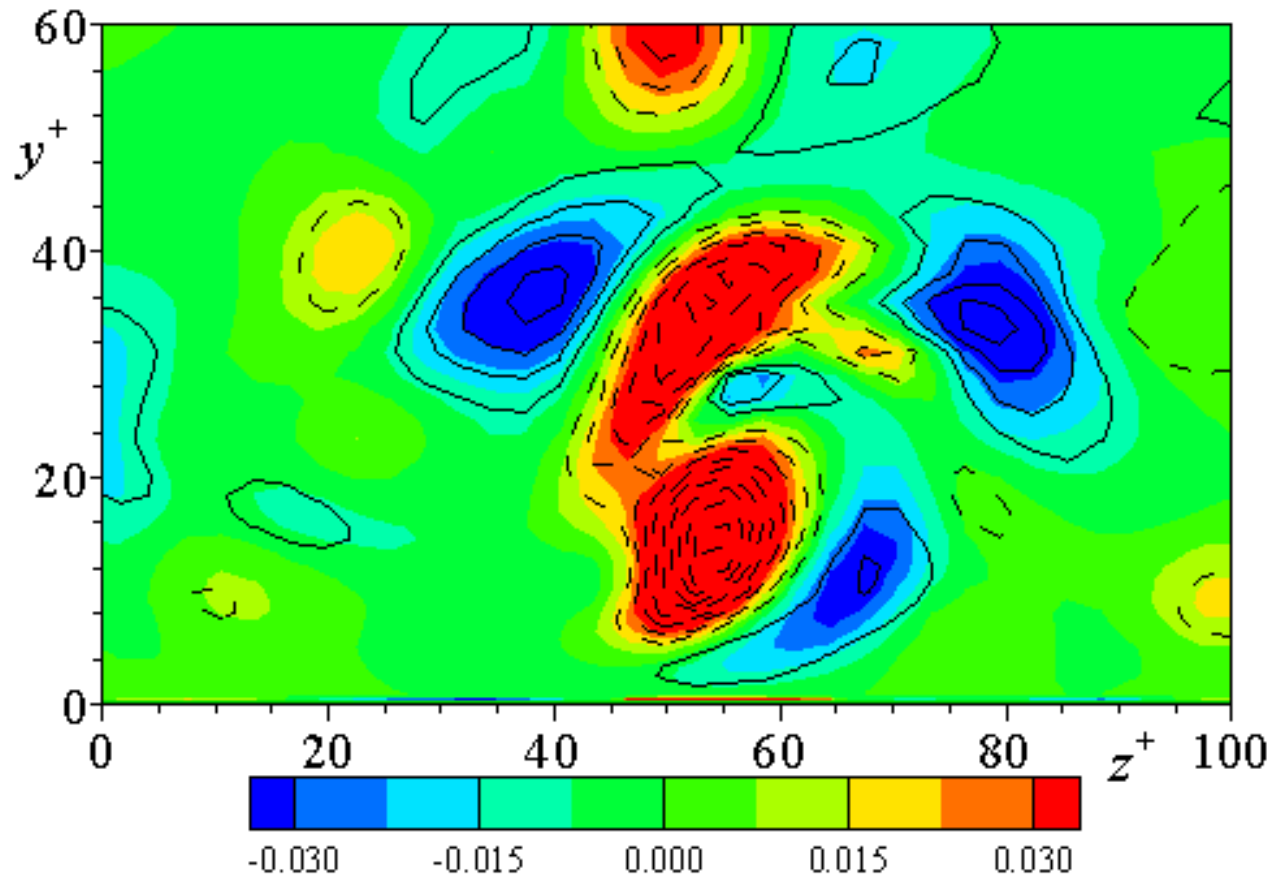
∇^2 : $(\partial^2 / \partial x_i^2)$

p : pressure fluctuation

$u_{i,j}$: Deformation tensor

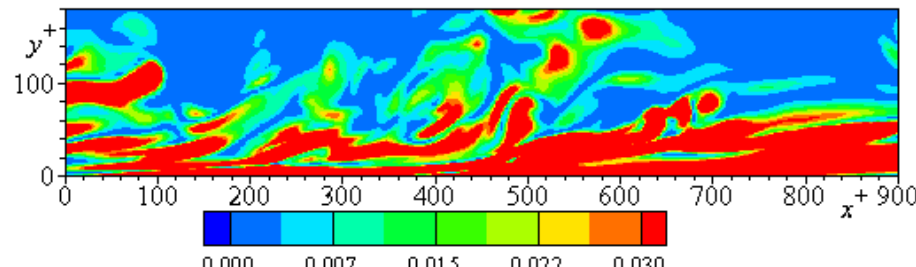
$u_{i,j}u_{j,i}$: Second invariant of the tensor

Instantaneous $\nabla^2 p$, $u_{i,j}u_{j,i}$ for $\text{Re}_\tau=180$

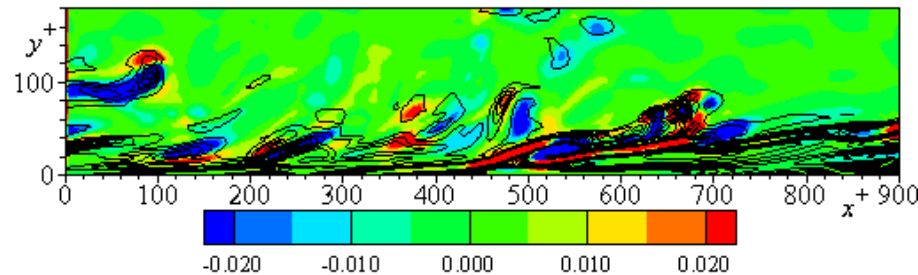


Color contours are the instantaneous $\nabla^2 p$,
while lines are the instantaneous $u_{i,j}u_{j,i}$.
Solid and dashed lines are positive and negative values.

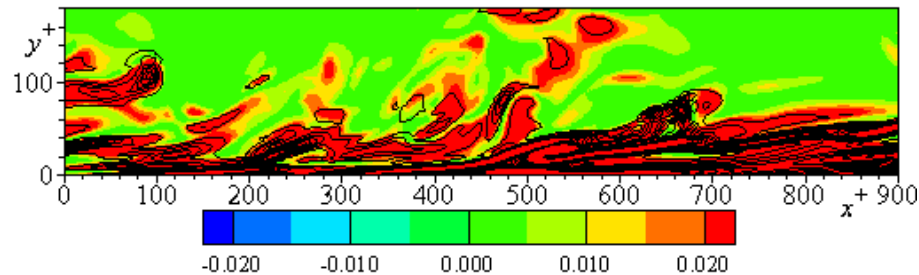
Instantaneous \mathcal{E} , $u_{i,j}u_{j,i}$, $\omega_i\omega_i$ for $\text{Re}_\tau=180$



\mathcal{E}



$u_{i,j}u_{j,i}$



$\omega_i\omega_i$

Lines are the instantaneous ε .

Conclusions

Near the wall, $\theta_{,i}$ is closely associated with ω_i ,

reflecting the **near-wall organization** (quasi-streamwise vortices, streaks and internal shear layers)

the **largest correlation** is between ω_2 and $\theta_{,3}$
reflecting the reduced role of pressure on ω_2

but the correlation between ω_3 and $\theta_{,2}$, which is identical to that between u_1 and θ , is also high

Away from the wall, $\theta_{,i}$ is less well correlated with ω_i , reflecting the presence of less well correlated large-scale motions of u_1 and θ

But there is concentrated enstrophy in the outer region

often in the form of sheet-like structures

at the so-called ‘fronts’ or ‘backs’...

Work in progress....

- effect of Pr (or Sc)
- different boundary conditions e.g. wall roughness

